1975

A Study Of The Influence Of Spandrel Beams On The Behavior Of Reinforced Concrete Slabs

Mukund Martand Moharir

76-11,775

MOHARIR, Mukund Martand, 1941-
A STUDY OF THE INFLUENCE OF SPANDREL BEAMS ON THE BEHAVIOR OF REINFORCED CONCRETE SLABS.

West Virginia University, Ph.D., 1975
Engineering, civil

Xerox University Microfilms, Ann Arbor, Michigan 48106

A STUDY OF THE INFLUENCE OF SPANDREL BEAMS ON THE BEHAVIOR OF REINFORCED CONCRETE SLABS

by

MUKUND MARTAND MOHARIR

A dissertation submitted to the Graduate School
of West Virginia University at Morgantown
in partial fulfillment of the requirements
for the Degree of Doctor of Philosophy

DEPARTMENT OF CIVIL ENGINEERING

MORGANTOWN

1 9 7 5

ACKNOWLEDGEMENTS

The writer wishes to express his special thanks to Dr. E. L. Kemp and Dr. W. J. Wilhelm for their able guidance and constant encouragement which has made this work a reality.

Thanks are also extended to Dr. S. Dowdy for her valuable guidance for the statistical part of the work incorporated in this dissertation.

Thanks are also due the other members of the writer's advisory committee, Dr. S. H. Advani and Dr. R. K. Seals for their constructive criticism and suggestions.

The National Science Foundation and the Engineering Experiment Station of W.V.U. are gratefully acknowledged for providing the necessary funds for this study.

Thanks are also extended to Dr. J. W. Saunders, Jr. for providing the data of the prototype testing.

Assistance of P. Frum and F. Culler during the experimental phase of this research is highly appreciated.

Finally, the writer thanks his wife, Vasanti, for her cooperative spirit and never-ending faith.

TABLE OF CONTENTS

TABLE OF CONTENTS (continued)

TABLE OF CONTENTS (continued)

TABLE OF CONTENTS (continued)

TABLE OF CONTENTS (continued)

LIST OF TABLES

LIST OF FIGURES

LIST OF FIGURES (continued)

Page

LIST OF SYMBOLS

a or L	=	center-to-center distance between adjacent columns
a_c	=	clear span between columns
A_l	=	total area of longitudinal reinforcement to resist torsion, sq. in.
A_n, C_n	=	theoretical summation constants of deflection function 'w'
A_s	=	area of nonprestressed tension reinforcement, sq. in.
A_t	=	area of a closed stirrup resisting torsion within a distance s, sq. in.
A_n', C_n'	=	semitheoretical summation constants of deflection function 'w'
b	=	width of the edge beam
C	=	torsional stiffness of the edge beam
d	=	distance from extreme compression fiber to centroid of tension reinforcement in the edge beam
d_o	=	overall depth of the edge beam
D	=	flexural rigidity of the slab
E	=	modulus of elasticity of material
E_m	=	modulus of elasticity of model (micro-concrete) mix
E_p	=	modulus of elasticity of prototype mix
f_r	=	modulus of rupture of concrete, psi
f_{sf}	=	factor of safety against flexure
f_{sts}	=	factor of safety against the combined torsion and shear interaction effect
f_y	=	specified yield strength of nonprestressed reinforcement, psi
f_c'	=	specified compressive strength of concrete, psi

h = thickness of the slab

i = dimensionless ratio or dummy variable

im = ultimate yield moment per unit length along negative yield line

I = moment of inertia of the edge beam section

j = dimensionless ratio or dummy variable

K = ratio of ultimate to cracking torque (T_u/T_c) for the edge beam

K_1 = load factor for the edge beam (Table 7.1)

L or a = center-to-center distance between adjacent columns

m = ultimate yield moment per unit length along positive yield line

mi = ultimate yield moment per unit length along nega- yield line

M = moment section will carry under combined stresses

M_{cr} = cracking moment of a section

M_u = ultimate balanced moment

N = number of simultaneous equations to be solved

q = uniform load intensity on the slab

q_{cr} = intensity of cracking load on the slab

q' = $A_s f_y/bdf_c'$

R = vertical reactive force on the column

s = shear or torsion reinforcement spacing in a direction parallel to the longitudinal reinforcement

T = torsion the section will carry under combined stresses

T_c = cracking torque of the edge beam

T_o = torsion the section will carry under torsion only

T_u = ultimate torsional capacity of the edge beam

T_1 = Torque constant = Torque per unit length/qa^2 (Figure 7.1)

v_c = allowable shear stress

v_{tc} = allowable torsional stress

v_{tu} = nominal total design torsional stress

v_u = nominal total design shear stress

V = shear the section will carry under combined stresses

V_B = total vertical reaction at the end of the edge beam

V_o = shear the section will carry under shear only

w = deflection function

w_{expt} = experimental slab central deflection

W = total load on the slab including self-weight

x = shorter overall dimension of a rectangular part of of a cross section

x_1 = longer center-to-center dimension of a closed rectangular stirrup, in.

y = longer overall dimension of a rectangular part of a cross section, in.

y_1 = longer center-to-center dimension of a closed rectangular stirrup, in.

z = section modulus

α = aspect ratio

β = dimensionless ratio locating yield line position

θ = torsional rotation of the edge beam

μ = Poisson's ratio of concrete

Z_u = nominal total design torsional stress

ϕ = capacity reduction factor

1 INTRODUCTION

1.1 General Remarks about Reinforced Concrete Beam-Slab Systems

Reinforced concrete slabs terminating at edge beams are often used for the floors of public and commercial buildings, multistory housing, bridge decks, etc. Concrete is used for these structures because no other material possesses a comparable combination of low cost with high strength, ductility and resistance to abrasion, corrosion and fire. Concrete slabs also provide adequate sound insulation between stories in buildings and can develop sufficient resistance in shear, torsion and bending.

1.1.1 Existing Design and Analysis Procedures

The present practice for the design of reinforced concrete beams and columns in the United States is to proportion the members with respect to the ultimate strength of the section and to use modified elastic methods to calculate the deformations. The 1971 ACI Building Code allows both two way and flat slabs to be designed by the same methods utilizing a section of the slab and an integral spandrel beam between adjacent exterior columns as a shallow beam. Although the slab and the spandrel beams proportioned by this method are usually satisfactory, there is a possibility that the spandrel beams may fail in torsion. Also, the method cannot account for the influence of spandrel beam torsion on the load carrying capacity of the slab. The conventional yield line theory may be used when torsional hinges are not formed in the edge beams. Influence of the spandrel beam torsion on slab capacity can be evaluated by using the yield line analysis modified by Kemp and Wilhelm [21].

Most codes of practice including the 1971 ACI Building Code give permissible span/depth ratios as a rough guide for deflection control [18]. Thus, in the absence of an 'exact' elastic solution, the designer is forced to rely on this rough guidance for deflection control and to make moment calculations based on either the Direct Design Method or Equivalent Frame Analysis. As a result, the designer does not know the factor of safety against flexural cracking for the slab and for the edge beams nor against the combined effect of torsion and shear interaction for the edge beams. If the designer uses the Conventional Yield Line Theory, he may provide excessive amount of slab reinforcement which may not be of much use once torsional hinges are formed in the edge beams.

Considering these difficulties, an improved design method would make a significant contribution to the analysis and design of floor slabs by providing the designer with (a) an elastic deflection for the slab central section, (b) the flexural cracking load for the slab, (c) proportions for the spandrels to provide an adequate and economic factor of safety against flexure, torsion and shear and (d) economic and reasonable amounts of slab reinforcement by using the Modified Yield Line Theory which can account for the influence of the spandrel beam torsion on the load carrying capacity of the slab. Since this modified theory has been verified by experimental data for square slabs only, additional data are necessary before such a method can be established as a design method.

Once it is accepted that the torsional stiffness of the edge beam is also one of the fundamental factors influencing the behavior of slab-spandrel structures, then several questions arise:

1. What is the magnitude of this influence in the elastic and inelastic zones?
2. Is it possible to use statistical methods to separate torsional stiffness effects from the effects of other parameters?

These questions must be resolved before any significant improvements can be made in design procedure for slabs.

In light of this discussion along with the brief review of various forces and displacements of the beam-slab structural system and the review of feasibility of using micro-concrete models for experimental work, the object and scope of this investigation is planned accordingly as discussed in the subsequent sections.

1.1.2 Generalized Forces and Displacements of the System

Casting beams, columns and slabs monolithically leads to considerable interaction between the individual components of the structural system. This interaction induces various combinations of bending, torsion and shear. The nature of these forces is primarily governed by the three loading zones; e.g., elastic, cracking and plastic zones which can be distinctly shown on a load versus displacement diagram. When the structure enters the cracked zone from the uncracked elastic zone, its sectional properties change, also the internal resisting mechanism developed by the structure to sustain the external forces changes considerably. Even though these external forces may be classified as the usual in-plane and normal bending, torsion and shear types, the internal resisting mechanism generated by the structure is a complex one that is not fully understood. In addition, the magnitudes of the forces and displacements induced in the system are significantly governed by the amount of fixity provided at the joints and the geometry of the loading diagram.

Slab deflections and spandrel beam torsional rotations as indicators of structural behavior should be of concern to the designer. These displacements depend on the load stages. First, there is a range of maximum stiffness associated with small displacements before the slab cracks; second, an increase of displacements during cracking but before yield of the steel; third, a range of loading where moment redistribution takes place because of plasticity and the displacements increase rapidly just before collapse. While in-plane strains caused by tensile membrane action generally occur in the slab, they are normally neglected in the formulation of energy equations defining collapse modes for the yield line theory. This leads to a conservative prediction of ultimate load, particularly when the spandrel beams do not fail [19].

1.1.3 Applicability of Micro-Concrete Modeling Technique

Whether consideration of a slab system is related to design or research, the working (service) load behavior, cracking load and ultimate (failure) load for the structure are of primary concern. It is now generally believed that structural models can be used effectively for studying a wide range of parameters related to each of these load stages, with some reservation regarding cracking similitude [4]. In the latter case reasonable simulation has been established for scale reductions down to the order of 1/4.

As indicated by several case studies [16,25,28], micro-concrete models predict reasonably well the deflections, modes of failure and failure loads for beams, columns and slabs. These indepth studies of materials, elastic behavior, cracking simulation, inelastic behavior, etc., pertaining to this modeling technique have resulted in a clearer understanding of its practical applications. Thus, it is proposed to use the modeling technique in the current investigation, as outlined in the following section of object and scope of the present study.

1.2 Object and Scope of the Investigation

From the introduction it is clear that before new design procedures for slabs can be established the influence of spandrel beams, particularly their torsional characteristics, must be understood. Previous work by Saunders [33] and Kemp and Wilhelm [21] have established a new yield procedure which has been verified by a limited number of tests on square slabs with varying edge beam dimensions. Both the modified yield line method and the experimental work need to be extended to the case of rectangular slabs with spandrel beams. This extension of previous theoretical and experimental work to the study of rectangular slab-spandrel systems is the principal objective of the present work. The results are expected to provide a clearer insight into the behavior of such systems and lay the foundation for design procedures in which the role of the spandrel beams will be recognized.

In order to achieve this objective, the scope of the investigation includes both an analytical and an experimental phase. The experimental work is intended to provide an understanding of the behavior for a full range of loading of slab-spandrel structures proportioned so that torsional hinges would form in the spandrel beams. Equally important, the experimental results are used to confirm the theoretical solutions.

The scope of the project is outlined below:

1. Three micro-concrete slab models were tested to failure to observe the influence of spandrel beams on the behavior of rectangular slabs. The primary variables were the slab aspect ratio and the depth of the edge beams. The aspect ratios (i.e., breadth to length) were 1:1, 1:1.5 and 1:2. In the three models the spans of the short side beams were 36 inches, 24 inches and 12 inches and the depths were 4-1/2 inches, 3 inches and 4-1/2 inches, respectively. The long edge beams were all 36 inches. The amount of steel, columns

dimensions, concrete strength and other parameters were held constant.

The square slab model was a scaled down version of a slab tested by Saunders [33] and was used as a control specimen.

A statistical design procedure (for a reason explained in Section 1.1) was developed for: (a) trend analysis to see if the data were in an elastic or plastic zone, (b) detection of sourcewise variation to check if the deflections and rotations were significantly the same for the prototypes and the models, (c) studying the effects of independent variables (e.g., EI/aD ratio, torsional stiffness of the edge beam, etc.) on the dependent variables (slab central deflection, beam rotation, etc.) in the experimental data.

2. The mathematical inequalities and the governing equilibrium equation were developed to enable the use of the modified yield line theory for predicting the moment capacity of rectangular slabs. These mathematical inequalities could determine the failure mode associated with the development of torsional hinges in the spandrel beams or the development of negative yield lines at the edges of the slab.

3. An elastic solution was developed for doubly symmetric (i.e., square) slabs which can account for the special boundary conditions imposed by slab edges being integral with spandrel beams as well as more traditional boundary conditions. This theoretical approach was intended primarily to predict and interpret the service load stress resultants and deformations as well as to predict the

cracking load of slab-spandrel systems. The experimental results of this study and others were used to verify the theoretical method.

4. For the design purposes, limit state load factors for flexural cracking of the edge beams, and the combined effect of torsion and shear on spandrel beams were derived for square and rectangular slabs under service loads. Also, the formulas for width and depth of edge beams for square and rectangular slabs were derived for design purposes. The results of a specific example were compared with the results obtained by Kemp and Wilhelm [21].

A new design method for slab-spandrel systems was originated which combined an elastic solution and the experimental work with the modified yield line method. Different parameters were studied to obtain an economical design for slab reinforcement.

2. LITERATURE REVIEW

2.1 Behavior of Reinforced Concrete Members Subjected to the Generalized Forces

2.1.1 Factors Influencing the Behavior of the Edge Beams

Shape of the loading diagram for the edge beam and the amount of fixity provided at its ends are the two important factors influencing its behavior as a member of the beam-slab structural system. These factors govern the location of a critical section in flexure and the magnitude of load on the slab which causes flexural cracking in the edge beam. The present state of knowledge of the load distribution diagrams, for various aspect ratios of the slab in an elastic zone, is somewhat limited. In considering lower bound solutions to rectangular slabs, Prager (29) developed expressions for the shear on a simply supported edge. Wood (39) shows that this is of constant intensity and not a triangular or trapezoidal distribution for the edge beam loads. He recommended a load intensity of qa/3 per unit length of the beam. His work is for the lower bound solution for collapse of a simply supported beam and the load intensity qa/3 may be close but not exactly the same as the one occurring at the end of elastic zone. Kromm's work (37) has shown that for a square plate this load intensity is nearly uniform (i.e. the loading diagram on the edge beam is approximately rectangular), for higher values of a/h ratio. Thus, the cosine load harmonics transmitted to the beam can be approximated to a single rectangular loop. In his work the a/h ratio was 20, a value which is generally exceeded in practice. But this work has the limitation of neglecting the transverse contration 'ϵ_z' making it inadequate to use as it is for a wide range of rectangular slabs terminating in edge beams. (See Section 4.4.2).

The second important factor influencing the behavior of the edge beam is the amount of fixity provided at its ends. The amount of fixity depends on condition of the joints between beams and columns, the dimensions of the columns, their prestressing forces, etc. The ACI Code [2] gives different moment distribution factors in the analysis of continuous beams because of the variable fixity effect. Corley, Jirsa et al. [10] have considered this effect in the method of 'equivalent frame analysis of slabs'. When the slab is continuous on the beams, the presence of adjacent panels increases the fixity. Kemp and Wilhelm [21] used ACI moment coefficients to calculate the negative moments developed at the column faces. In the present investigation, enough prestressing force was used on the columns to balance the vertical reactive forces at the corners. This could improve the fixity effect on the edge beams and also simulate the effect of the load induced by the super-structure (See Section 3.6.1).

2.1.2 Shear and Torsion Interaction

In the design of reinforced concrete members subjected to combined torsion and shear, it was a common practice to add the conventional shear stress to the torsional stress, whether calculated by elastic or plastic theory, and then to compare the total with the specified allowable stress. Many investigators have found this procedure unsatisfactory. Eroy and Ferguson [13] tested beams under torsion and shear. Their test results seem to fit well into the circular interaction curve given by

$$\left(\frac{T}{T_o}\right)^2 + \left(\frac{V}{V_o}\right)^2 = 1.0$$

Nylander's work [13] confirmed this interaction equation. The Australian Code adopted a more conservative approach given by a straight line equation

$$\left(\frac{T}{T_o}\right) + \left(\frac{V}{V_o}\right) = 1.0$$

Saunders, et.al., [33] have stated that, since both torsion and shear basically induced in-plane stresses, there is more interaction between torsion and shear than between torsion and bending. This fact is taken into consideration while deriving the design formulas for width and depth of the edge beam of a square panel, as shown in Sections 4.4.3 and 4.4.4.

2.2 Yield Line Theory

Johansen is the acknowledged pioneer in this field. In the year 1931 he provided the introductory theory and also an immense number of practical examples to explain it. His original work includes important features like the 'energy or work method', the 'equilibrium method' and detailed analysis of the existing test data. He discovered the presence of nodal forces and their use in the formulation of equilibrium equations. Until about 1950 there still remained one important question unanswered. This was that, although either the work or the equilibrium method could be used to find the most critical layout of a particular shape of pattern, it always seemed possible to discover another shape of pattern, whose critical layout gave an even lower failure load. The difficulty was resolved by the concepts of upper and lower bound solutions of limit analysis.

Mansfield (1957) used the calculus of variations to find the worst (critical) layout for a system of yield lines. His results were the same as those obtained by Johansen using the nodal force concepts. His 'equilibrium method' gives conservative results of the failure loads when membrane action is also predominant along with the flexural one [39]. In the same way, the conventional 'energy or work method' fails to account for the work done by the membrane forces.

Kemp and Wilhelm [21] have suggested the modified yield line approach for a failure mode in which torsional hinges are formed in the edge beams along with the positive yield lines in the slab. They illustrated the practical use of the approach by applying it to the slab test of the University of Illinois. Their method is generally applicable to a wide range of slab configurations and is not restricted to square and rectangular slabs. Their theory is confirmed for square panels, but the present state of knowledge is inadequate to predict the failure mode of a rectangular slab-spandrel structural system.

2.3 Elastic Solutions

Timoshenko, [37] et.al. prescribed elastic solutions for rectangular slabs and plates with edge conditions such as fixed edges, simply supported edges, free edges and their different combinations. A solution is also available for some EI/aD values in the case of a doubly symmetric slab and plate elastically supported without torsion. But there is no elastic theory derived for the composite beam-slab structure with torsional effects. Wood [39] has stated the importance of this analytical work in the following words:

"For several years it has been doubtful whether it was worthwhile to program computers for elastic behavior of composite action. It now appears that this should definitely be undertaken, alongside a study of plastic composite action."

Considering the importance of this elastic solution, it may prove very useful to develop a general theory for doubly symmetric and also for rectangular slabs having any of the following five possible edge conditions (i) free edges, (ii) simply supported edges, (iii) edges elastically supported without torsion, (iv) edges elastically supported with torsion, and (v) fixed edges. The detail analysis of the doubly symmetric case is given in Sections 4.2 and 4.3, whereas the service load requirements of the rectangular panels are discussed in Section 7.2 and 7.3.

2.4 Micro-Concrete Model Studies

2.4.1 Materials

Small scale models are becoming increasingly important in research on structural concrete. They are very appropriate for studying slab-spandrel behavior because of the saving in time and money during their fabrication. While the majority of model studies have concerned themselves with the elastic and inelastic behavior of structures under static loads, small scale models have occasionally been used to study the response of structures for some unconventional fundamental variables existing in the specific circumstances. Rocha and Silveira [30] used them to determine thermal stresses in concrete dams. Litle, Forcier et al. [26] used them for shell-buckling studies. Barges and Pereira [6], also Dobbs and Cohen [11] tested small scale models to predict dynamic behavior of the prototype structures. All these studies and many more have shown a reasonable correlation between the prototype and the corresponding model behavior.

Micro-concrete models use type I or type III cement. Mirza, White and Roll [28] have reported the properties of micro-concrete model mixes using type III cement. Aldridge, et.al., [3] have successfully fabricated micro-concrete models from type I cement. These models may or may not have coarse aggregates, but the fine aggregates are invariably present. Sabnis and White [28] have used gympsum morters consisting of gypsum, sand and water. Their curing time is very short (one day or less) but the main disadvantage is the strong influence of moisture content on their mechanical properties. In the present investigation, type I cement was used to fabricate the models of the prototype structures made of type I cement.

Harris, Sabnis and White [16] conducted an in-depth study of reinforcement for small scale models of concrete structures. Their study involves a number of choices for model reinforcing steel including round steel wires, square steel rods, cold rolled threaded steel rods, plain rusted steel wires, custom deformed wires, etc. A careful choice of model reinforcing, combined with the proper annealing process will result in imparting suitable properties for each particular model study [16]. In the model studies of slabs terminating in edge beams, the main reinforcement in the beams should be of straight rods (and not of the wires available in circular rolls) to achieve higher order of the fabrication accuracy.

2.4.2 Elastic Behavior

Elastic models may be constructed of any material for which the stress-strain relationship is essentially linear to the point of anticipated maximum elastic strain of the prototype. Elstner [12] has tested elastic models of flat plate and flat slab floor systems. In micro-concrete, the compressive strength of the mix governs the extent of the elastic zone and can be controlled accordingly [28]. This is one of the reasons for using micro-concrete mixes in the behavioral studies of the slab-spandrel structural system. Harris, et.al., [16] have shown that the stress-strain curve of the reinforcement is generally linear to a sufficient strain limit and does not obstruct the elastic behavior of micro-concrete models. Therefore the slab-spandrel models may have reinforcement selected from the wide variety of locally availables steel wires and rods (See Section 3.3).

2.4.3 Cracking Simulation

A number of model tests [49,28] have been reported to simulate cracking behavior of the prototype structures. In general, model specimens when compared with prototypes, exhibit greater cracking strain and more plasticity in tension. Clark [9] reported that for small models crack spacing was greater than that scaled from the prototype, but the strains and crack-width could be predicted because the material properties of both the model and the prototype were known accurately.

Tests conducted by Elstner [12], Mirza [28] and others at different research centers indicate that although the total number of cracks decreases as the model size is reduced, the overall load deformation characteristics under any loading combination (load-deflection, moment-rotation, torque-twist, etc.) can be reproduced with reasonable accuracy in small-size models built from micro-concrete. Load-deflection characteristic is one of the prime concerns of the designer, making it appropriate to use small-size models during the experimental investigation of the slab-spandrel systems.

2.2.4 Inelastic Behavior

Inelastic or ultimate strength models have been increasingly used in design and research problems since the advent of the ultimate strength theory. A number of successful tests have been reported on the micro-concrete models constructed to simulate the inelastic behavior of prototype slabs [12]. Flat plates and slabs with quite complex behavior were studied at different scales and with different materials. At the Portland Cement Association a 3/4 scale reinforced concrete model was tested [12]. At the University of Illinois a 1/4 scale reinforced small aggregate concrete model and a 1/16 scale reinforced micro-concrete model were tested [28]. At M.I.T. three 1/28 scale reinforced micro-concrete models were studied. All these tests required the selection of materials which exhibited the same stress-strain characteristics as those of the prototype upto the yield point and also in the post yielding ductility zone. The tests have convincingly demonstrated the importance of micro-concrete models in predicting the behavior of prototype structures.

Thus, the small-size micro-concrete models fabricated with reasonable accuracy, coupled with good instrumentation, can be of much help to the experimental investigator in the field of slab-spandrel floor systems.

2.5 Previous Prototype Testing at W.V.U.

At the West Virginia University Concrete Research Laboratory, three single panel large scale specimens consisting of a slab supported by four edge beams and four columns were tested [33] to ultimate load to observe their behavior and to obtain data for the doubly symmetric case. These three specimens are referred to as prototype specimens 1, 2 and 3. The three concrete mixes used had compressive strengths of 3785, 4151 and 4892 psi respectively and the corresponding split tensile strengths were 380, 389 and 500 psi at the time of testing. The columns 1 x 1 foot square were 12 feet center to center. Each one was prestressed to an initial load of 80 kips, approximately 2 hours prior to testing. Relevant data pertaining to steel spacing and yield strengths, which will be referred to very often in this report, are summarized in Table 2.1. The slabs were loaded uniformly with an airbag loading system and extensive test data were recorded with the help of a digital strain indicator. Part of the data to be used in the subsequent research work are given in the print-outs of Appendices C and D.

This prototype work can be used in various ways such as verification of elastic analysis, to check instrumental and fabrication accuracies of the model structures, to originate a new design procedure for the design of the slab-spandrel floor structures, etc. as shown in the following chapters of this report.

Table 2.1 Steel spacing and yield strengths in prototype specimens

Item	Spec 1	Spec 2	Spec 3
Slab edge steel two layers			
#3 bar spacing	6"	6-3/4"	5-1/4"
effective depth	2-3/4"	2-7/8"	2-7/8"
yield strength	47,500 psi	53,605 psi	53,605 psi
#3 bar spacing	6-7/8"	7-3/4"	6"
effective depth	3-1/8"	3-1/4"	3-1/4"
yield strength	47,500 psi	53,605 psi	53,605 psi
Slab center steel two layers			
#3 bar spacing	6"	6-3/4"	6-3/4"
effective depth	2-5/8"	2-3/4"	2-3/4"
yield strength	47,500 psi	53,605 psi	53,605 psi
#3 bar spacing	6-7/8"	7-3/4"	7-3/4"
effective depth	3"	3-1/8"	3-1/8"
yield strength	47,500 psi	53,605 psi	53,605 psi
Beam steel			
#6 corner bars			
yield strength	46,400 psi	46,400 psi	46,400 psi
stirrups 5" x 16" outside			
bar size	#3	#2	#2
spacing	4-3/8"	4-3/4"	4"
yield strength	50,400 psi	49,830	40,100 psi

3. EXPERIMENTAL INVESTIGATION AND OBSERVED BEHAVIOR

3.1 Introduction

Experimental work was in the field of micro-concrete testing. Several trial mixes were made and their compressive and tensile strength properties observed. Locally available steel wires and rods were suitably annealed and used as a model reinforcing material. Typical problems such as prestressing of small columns, mounting of light weight electrical gages, making of small stirrups and cages of beams, etc., associated with the fabrication and testing of small scale models required special attention, care and technique.

Three models of slabs terminating in edge beams were tested to failure. They had aspect ratios of 1:1, 1:1.5 and 1:2. They were loaded uniformly with an airbag loading system. Their elastic and inelastic behavior was studied. Deflection and torsional rotation data was noted with the help of a digital strain indicator. Based on this observed data, various load-deformation curves were plotted. Using dimensional analysis, displacements of the prototype structure were calculated and compared with the existing test data [33] and also with the theoretical analysis results, details of which are given in Chapter 5.

3.2 Design of the Micro-Concrete Mix

3.2.1 Fine Aggregates

Locally available Ohio River Sand was used as a fine aggregate. It was carefully graded so as not to have an excessive amount of very fine material which would have reduced the workability of the mix. A typical gradation curve is shown in Figure 3.1. All the particles passed through a standard U.S. sieve #4. Casting of the slender columns whose "workable" cross sectional areas were further reduced because of the presence of different reinforcing cages, made it essential to use this type of gradation curve for the sand. The moisture content varied from season to season and was experimentally determined for each batch of sand before using it.

3.2.2 Compressive and Tensile Strengths of Trial Mixes

The compressive and tensile strengths of a micro-concrete mix depend on different variables such as, water/cement ratio, aggregate/cement ratio, specimen size, maximum size of aggregate, method and rate of loading, effect of differential curing, statistical volume effects etc. From this list, only the first two quantities (i.e. water/cement ratio and aggregate/cement ratio) were varied so as to make a meaningful and appropriate choice of the mix. Cylindrical molds 3 x 6 inch were used and the standard ASTM [5] procedure adopted in casting and testing the specimens.

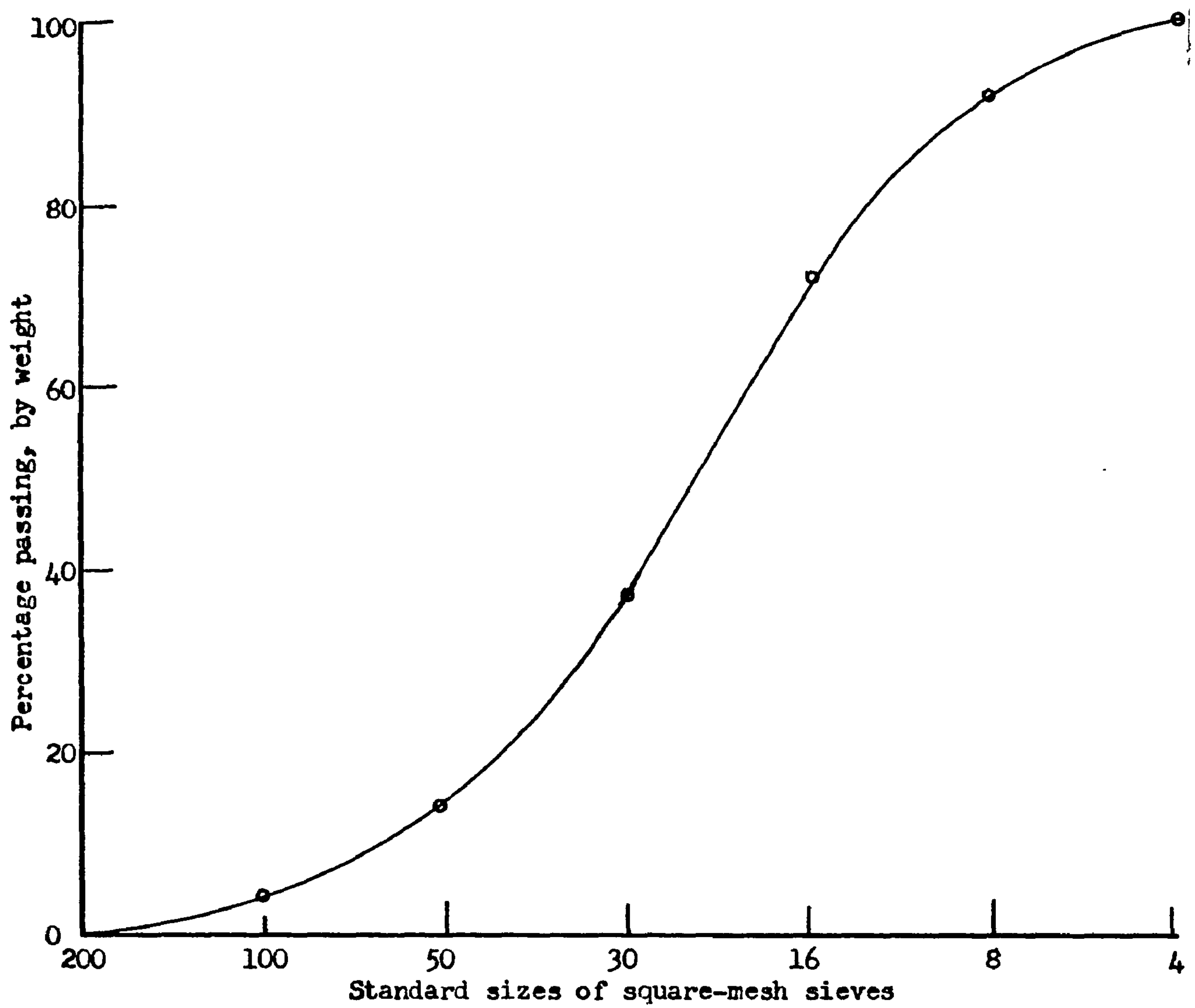

Figure 3.1 Typical gradation curve for the Ohio River Sand

Table 3.1 Compressive and tensile strengths of trial mixes

Mix Number	Proportion	Split Tensile Strength (psi)	Compressive Strength (psi)
M7	1:4:0.70	422	3602
M8	1:4:0.65	433	3841
M9	1:4:0.75	418	3309
M10	1:4:0.80	391	3090
M11	1:4.5:0.60	-	1580
M12	1:4.5:0.65	-	2108
M13	1:4.5:0.70	282	3156
M14	1:4.5:0.75	271	2740
M15	1:4.5:0.80	341	3333
M16	1:3.5:0.60	421	4823
M17	1:3.5:0.65	406	4242
M18	1:3.5:0.70	361	3652

Note: Each reported strength is an average of four cylinders tested after 28 days of curing.

Strengths of the trial mixes reported in Table 3.1 were obtained after 28 days of curing.

3.2.3 Elastic Properties of the Design Mix

The mix, M17, had a compressive strength of 4242 psi. Its tensile strength was 406 psi. These values are within 5 percent of the corresponding strengths of the prototype mix of specimen 2. Thus the M17 mix was selected as the design mix.

Poisson's ratio was determined for the mix from the uniaxial compression tests on 6 x 12 inch cylinders. Instrumentation consisted of two SR-4 wire strain gages mounted vertically in series and two other gages from the same lot mounted horizontally in series. In addition four dummy gages were fixed on the surface of an unloaded 6 x 12 inch cylinder of the same mix and identical to the test cylinder in all respects, for temperature compensation. The gages were fully protected from moisture with the help of duco-cement and a moisture-sealant. Each gage length was more than three times the maximum size of the aggregates. The Poisson's ratio determined was 0.179. The test results are summarized in Table 3.2.

The standard ASTM procedure is recommended to determine the modulus of elasticity of a normal weight concrete [5]. Exactly the same procedure was followed for the designed micro-concrete mix. The modulus of elasticity was found to be 2.60×10^6 psi.

Table 3.2 Determination of Poisson's ratio for the design mix M17

Serial Number	Circumferential Strain S.I. Box Reading	Circumferential Strain Strain ($\mu\epsilon$)	Longitudinal Strain S.I. Box Reading	Longitudinal Strain Strain ($\mu\epsilon$)	Poisson's[1] Ratio
Set I/1	2684	-	790	-	-
2	2704	20	680	110	0.181
3	2725	21	560	120	0.175
4	2748	23	450	130	0.177
Set II/1	2700	-	770	-	-
2	2720	20	650	120	0.167
3	2738	18	550	100	0.180
4	2757	19	450	100	0.190

1 Average value of Poisson's ratio = 0.1785

3.3 Reinforcement

The principal characteristic of the prototype steel which should be simulated in the reinforcement of micro-concrete models is the stress-strain relationship at all load stages. Reinforcement used in this investigation was chosen from a wide variety of wires purchased in small quantities from many sources. These wires were tested in a tension-testing machine. Table 3.3 was used to select their gage numbers. A small test program was planned to study the annealing effects on ductibility and yield strength of some of these wires. The results are given in Table 3.4. SR-4 wire strain gages were used to study the stress-strain relationship. Typical curves before and after annealing are given in Figure 3.2. A distinct yield plateau was observed for the annealed wires.

Wires purchased in the form of circular coils were straightened by pulling them in a tightening wrench. Care was taken not to exceed their elastic limits. On an average, the selected reinforcing material had a yield strength of 51.5 ksi with a well defined plateau at this stress level.

3.4 Formwork and Reinforcement Cages

Laminated 3/4 inch plywood was used in constructing the formwork. It met the usual requirements of rigidity and watertightness. The formwork was carefully designed to minimize errors in construction of the models. It could be assembled and dismantled

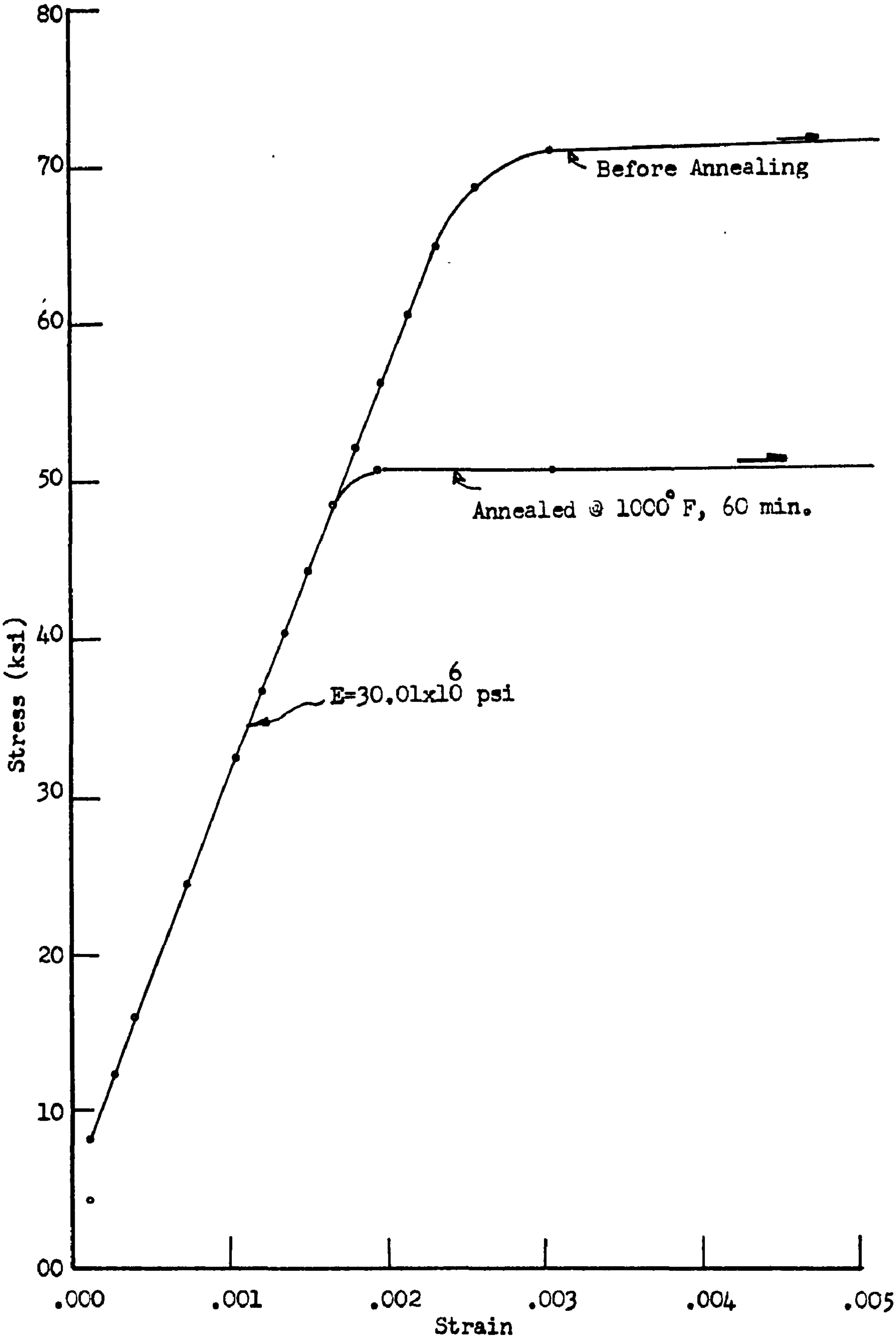

Figure 3.2 Typical stress-strain curve for steel

Table 3.3 Sizes for model reinforcement

Prototype Bar #	Diameter (inch)	Model Scale	Diameter for model steel (in.)	SWG1 for model steel
2	0.250	1:5	0.0500	17, 18
2	0.250	1:4	0.0625	16
3	0.375	1:5	0.0750	14, 15
3	0.375	1:4	0.0940	12, 13
6	0.750	1:5	0.1500	8, 9
6	0.750	1:4	0.1875	6, 7

1 SWG = Standard Wire Gage

easily. Each separable part was numbered so as to locate its position conveniently during reconstruction. The forms consisted of 3 basic parts; a center section, four column forms and four outside beam sections. Heavy diagonal bracings were used to add to the rigidity of the structure. To attach the rotational gages (see Section 3.6.3), 1/4 inch threaded rods were inserted in the beam sections. It was necessary to remove the forms at an early age of curing in order to prevent damaging shrinkage effects on the specimens.

Assembly of a reinforcement cage may be done by welding, brazing or soldering or by hand tying with fine wire. Heating involved in the first three methods would have caused local changes in the properties of the reinforcement, so the fourth method was used. It was somewhat time-consuming but produced cages with the desired rigidity. In a beam cage four corner bars were made of two SWG #6 and two SWG #7 rods (see Table 3.3). Stirrups consisted of SWG #16 wires, spaced 1.01 inch apart. They were made by bending the wires on an iron block of appropriate size with machined corners. Four holes of 1/2 inch depth for the four corner bars were drilled in a 6 x 10 x 3 inch wooden block. A central hole of 1/2 inch diameter going all along the width of the block was used to insert a long threaded rod. To the other end of the rod was an identical 6 x 10 x 3 inch wooden block. After placing the four corner bars and the calculated number of stirrups in between, these two end blocks could be fixed to the 1/2 inch

Table 3.4 Effect of Annealing on reinforcing wires

Treatment	SWG#9 Measured Diameter = 0.140 in. Area = 0.01539 in^2		SWG#11 Measured Diameter = 0.1205 in. Area = 0.1141 in^2		SWG#12 Measured Diameter = 0.100 in. Area = 0.00786 in^2	
	Yield Load Lb	Yield Stress ksi	Yield Load Lb	Yield Stress ksi	Yield Load Lb	Yield Stress ksi
As supplied by the manufacturer	1100	71.6	840	73.6	550	71.6
Annealed at 1000°F for 60 minutes	-	-	520	45.6	325	41.4
Annealed at 1000°F for 30 minutes	-	-	-	-	405	51.7

Note: Values in the table are average of five specimens. SWG#9 and SWG#12 are galvanized wires in the form of circular rolls. SWG#11 is a straight welding rod.

threaded rod by means of four nuts. Then the stirrups were tied to the corner bars. The ends of these bars were bent in the form of standard hooks which gave the required fixity effect between beams and columns.

A similar technique was used in assembling the column cages except that instead of rectangular stirrups spiral reinforcement was used. Mild steel #3 bars served as longitudinal reinforcement. Typical beam and column cages are shown in Figures 3.3 and 3.4.

3.5 Test Specimens

Three single panel micro-concrete specimens consisting of a slab supported by four edge beams and four columns were tested to failure. The specimens were identical in all respects with the exceptions of span and depth of the short beams. This could help to generalize the behavior of a slab-spandrel system having the aspect ratio as a fundamental variable. The prestressing force on the columns was also a variable, but it did not change the behavior of the structure. In each specimen the magnitude of the prestressing force was large enough to counter-balance the lifting effect at the corners, which would have otherwise existed because of the presence of vertical reactive forces.

For all the specimens the slab steel consisted of two layers of center span steel and two layers of edge steel. The center span steel was terminated before entering the beam. The edge

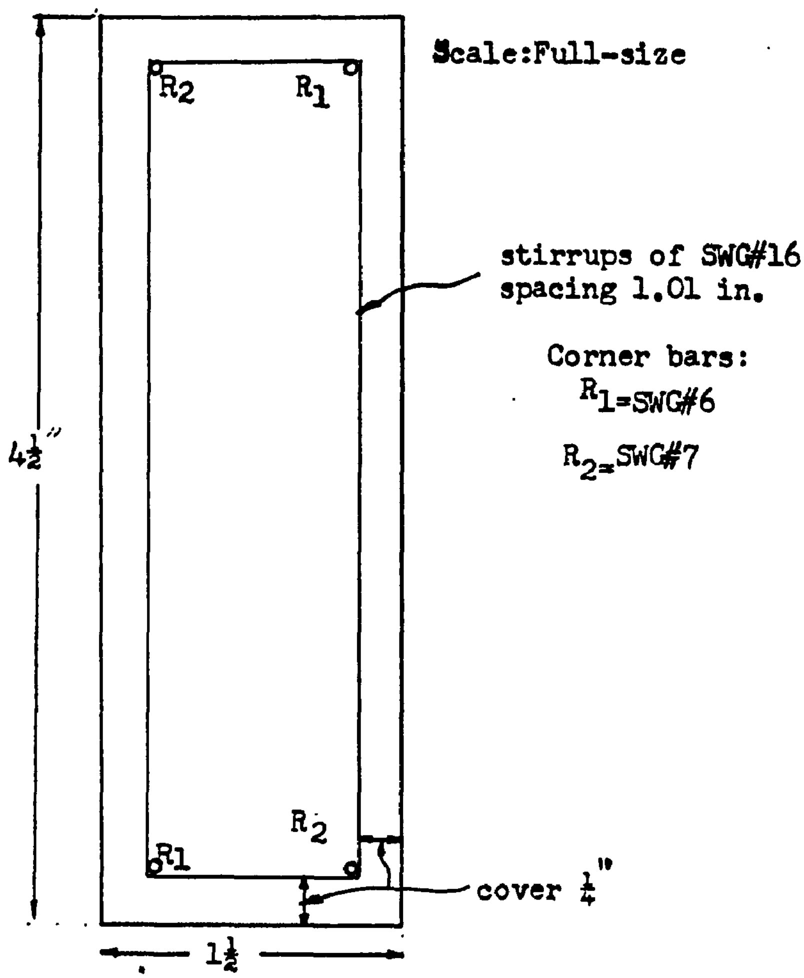

Figure 3.3 Typical beam section with reinforcement

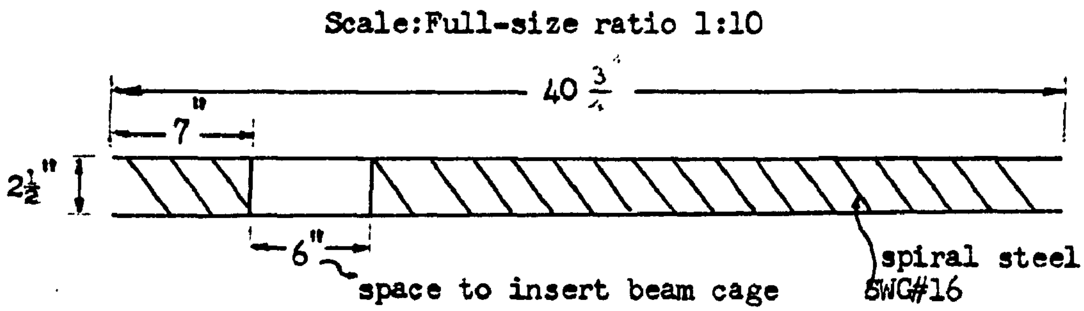

Figure 3.4 Typical column cage

steel was bent into the beam cage to achieve the required anchorage effect at the junction. Half of the bars were of the length determined by the bond length plus span/8, for the reason that the negative moments near the slab central sections are smaller compared to those at the edges. The bars were arranged alternately as shown in Figure 3.5. The size and spacing of the stirrups was adjusted to obtain an ultimate torque T_u approximately equal to the cracking torgue T_c in the long beams of the specimens. The reinforcement spacing is given in Table 3.5. A drawing of a typical beam section is shown in Figure 3.3.

The first specimen tested was a model of prototype specimen 2 [33], with a scale ratio of 1:4. A plan and section with dimensions are shown in Figure 3.7. The prestressing force on each column was 5 kips. This resulted in the same intensity in model and prototype columns. The results of the elastic theory, prototype testing[33] and the test of this model specimen 1 were compared (see Sections 5.3 and 5.4). This helped verify the dependability of the modeling technique. It also served to check fabrication accuracy and reliability of instrumentation.

The second specimen was a rectangular one (Figure 3.8) with an aspect ratio of 1:2. The prestressing force on each column was 2.5 kips. Both long and short beams had 1-1/2 x 4-1/2 inch cross sections. After observing the behavior of the short beams it was decided to reduce their depth in the third specimen which was also a rectangular type having an aspect ratio of 1:1.5, with a

Scale 3/2" = 1'

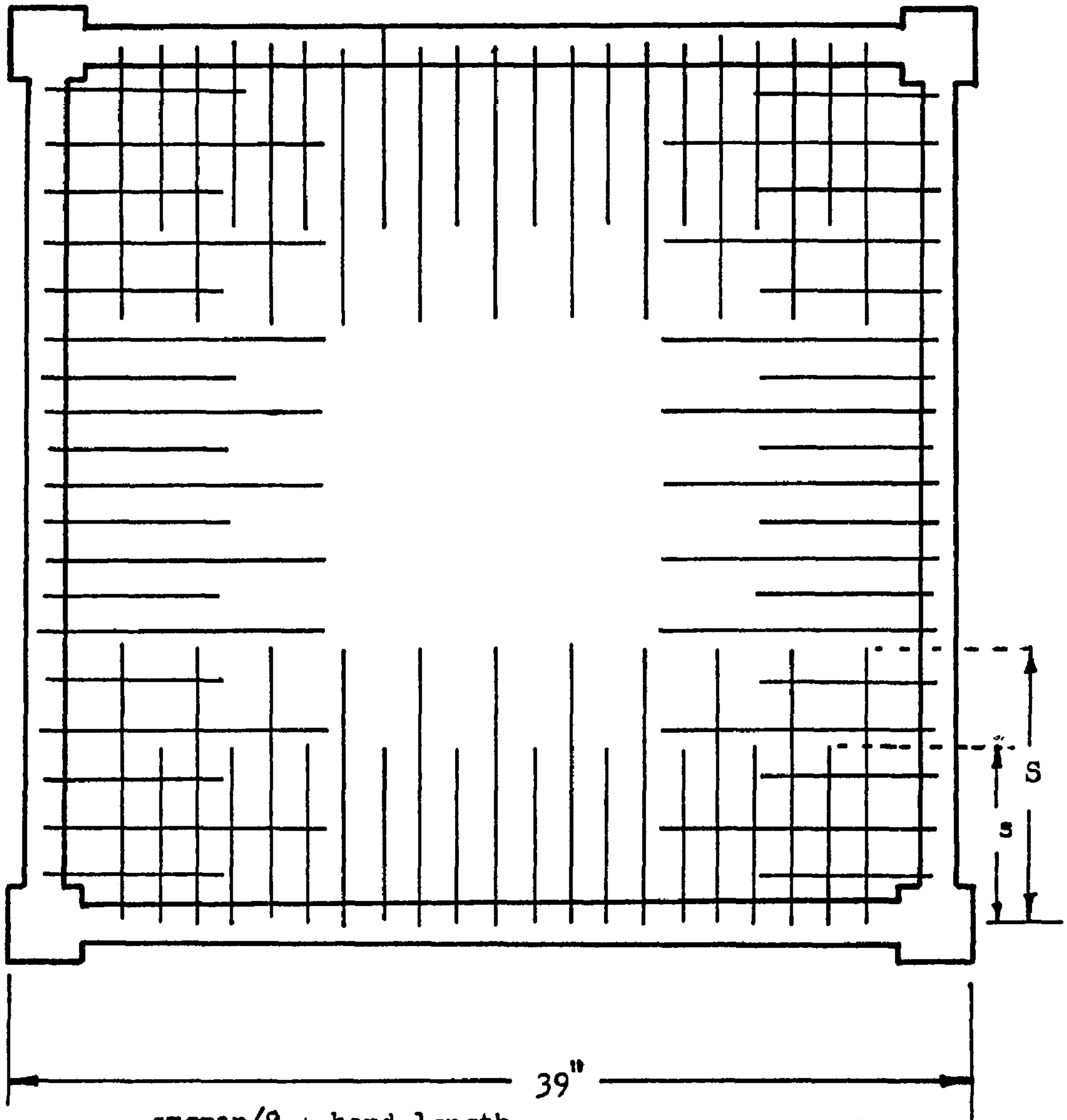

s=span/8 + bond length
S=span/4 + bond length

Figure 3.5 Typical slab edge steel

Table 3.5 Fabrication data of model specimens

Item	Spec 1	Spec 2	Spec 3
Long Beams			
span	36"	36"	36"
depth	4-1/2"	4-1/2"	4-1/2"
width	1-1/2"	1-1/2"	1-1/2"
Short Beams			
span	36"	18"	24"
depth	4-1/2"	4-1/2"	3"
width	1-1/2"	1-1/2"	1-1/2"
Slab Steel, 2 Layers[1]			
SWG #12 spacing	2.01"/2.26"	2.00"/2.25"	2.02"/2.27"
effective depth	3/4" avg. of 2 layers	3/4" avg. of 2 layers	3/4" avg. of 2 layers
yield strength	51.7 ksi	50.1 ksi	52.7 ksi
Beam Steel[2]			
corner rods, 2 Of SWG #6, 2 of SWG #7	47.3 ksi	47.3 ksi	47.3 ksi
stirrups	SWG #16	SWG #16	SWG #16
spacing	1.01"	1.01"	1.01"
yield strength	51.5 ksi	51.5 ksi	51.5 ksi

1 Data for both positive and negative steels (each in two layers)

2 Effective cover for the stirrups was 1/4".

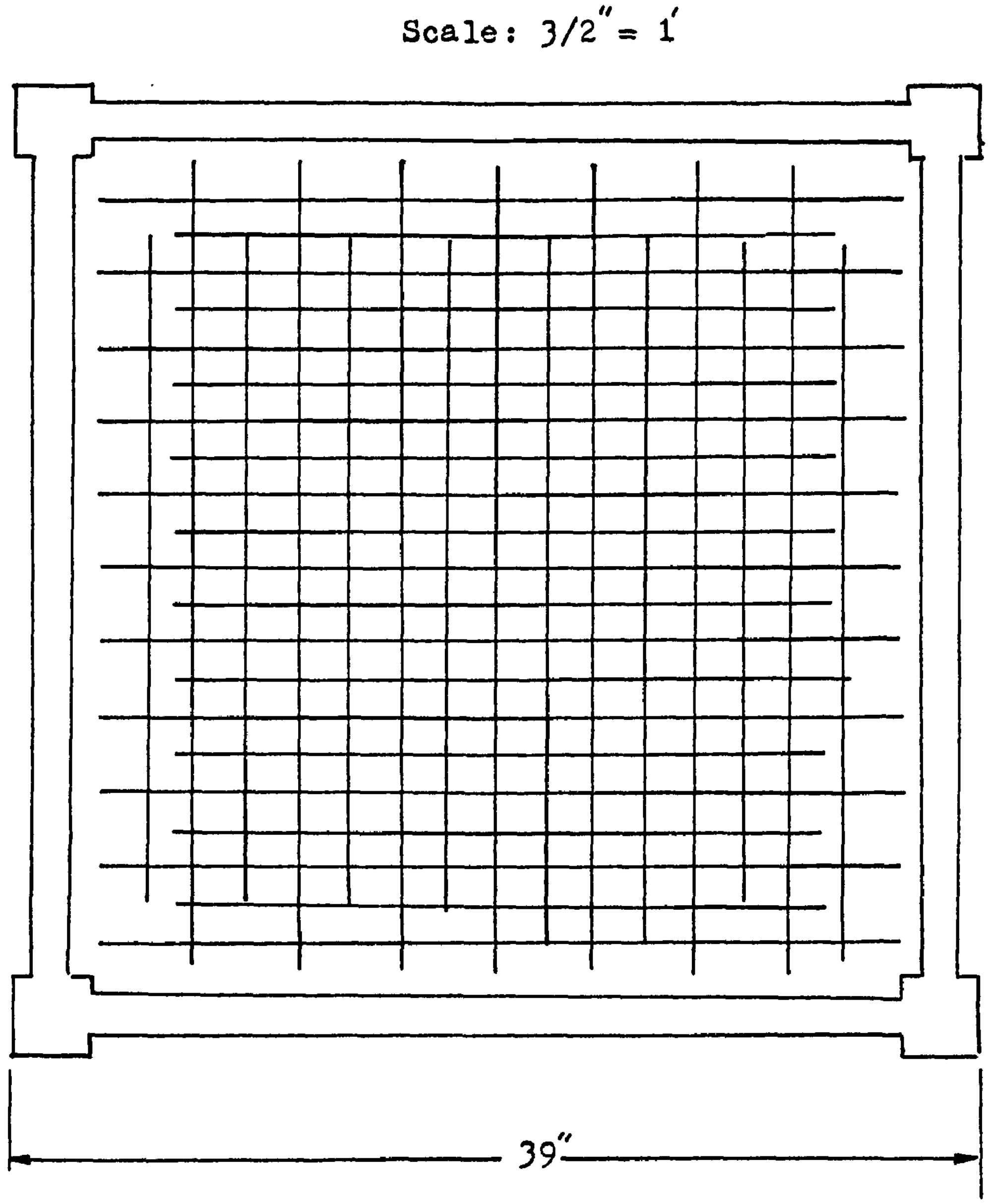

Figure 3.6 Typical slab center span steel of model specimen 1

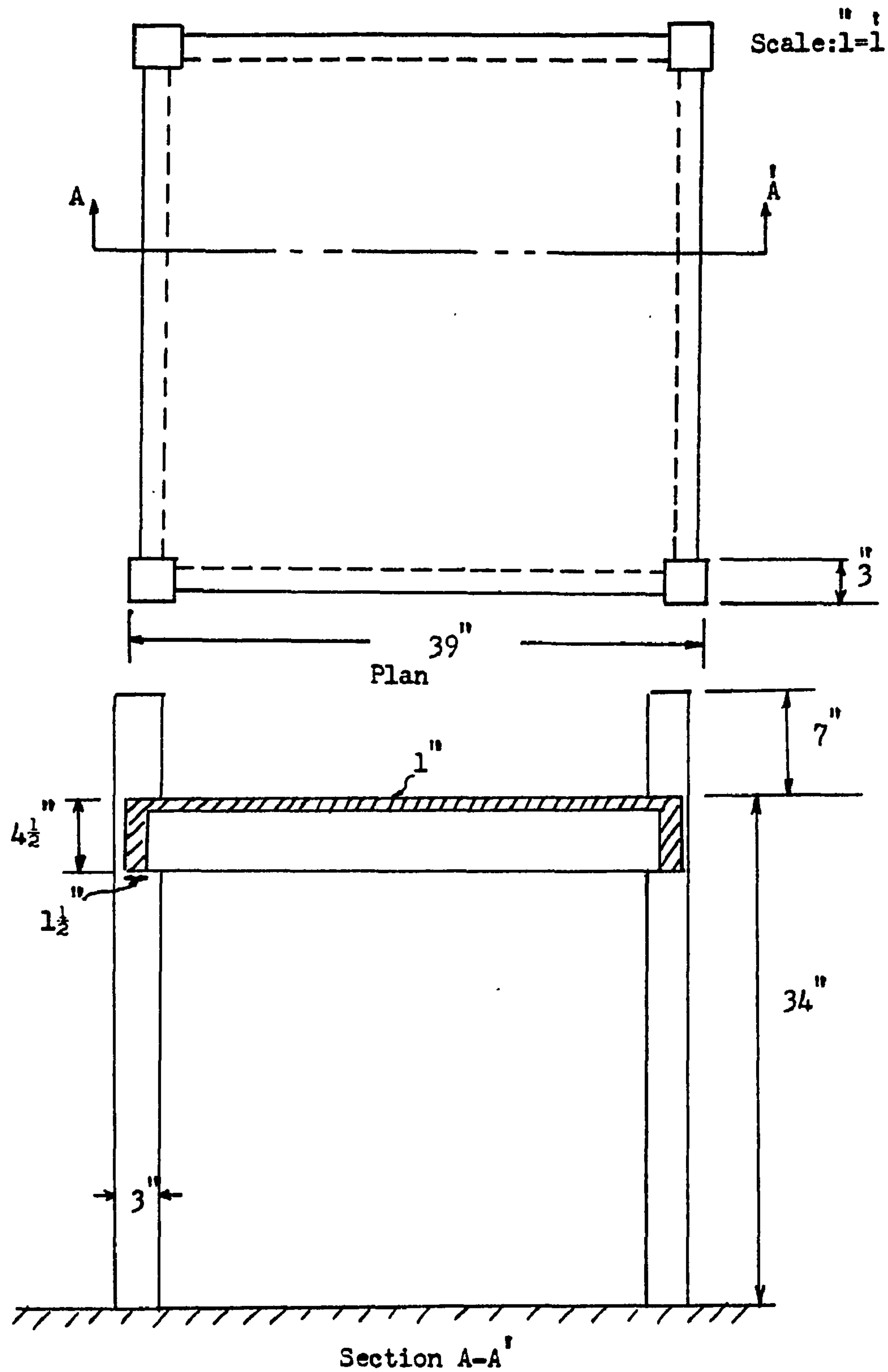

Figure 3.7 Dimensions of model specimen 1

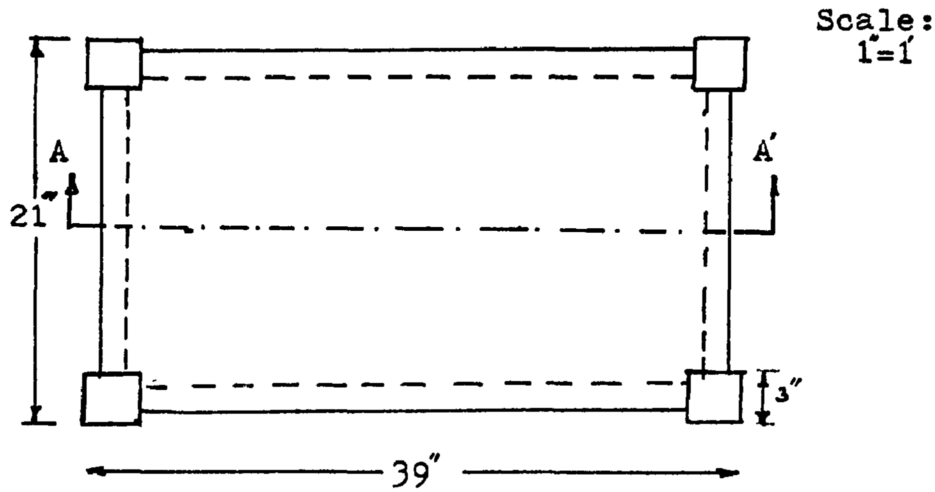

Plan

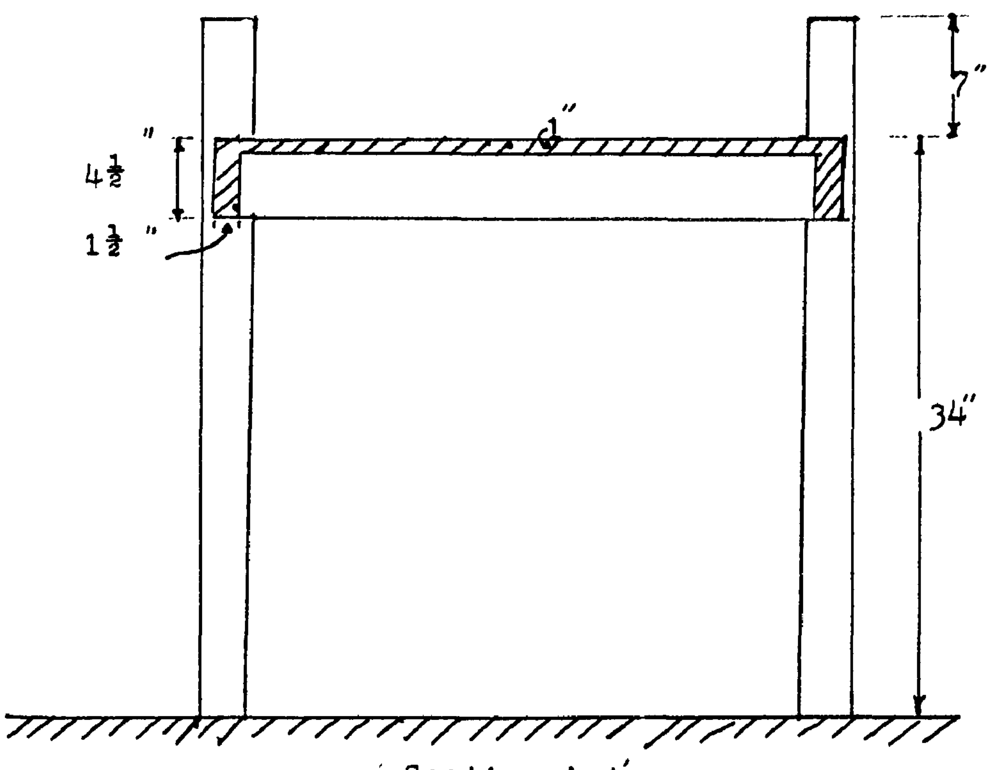

Section A-A'

Figure 3.8 Dimensions of model specimen 2 prestressing force of 3.33 kips on each column. The long beams had 1-1/2 x 4-1/2 inch cross sections and the short ones had 1-1/2 x 3 inch cross sections. The reduction in the depth was to obtain the same span to depth ratio for both the long and short beams. The geometric dimensions and structural properties involved in fabrication of these models are summarized in Table 3.5.

3.6 Test Procedures

3.6.1 Prestressing of the Columns

All the columns were prestressed to simulate the loads of a building above and also to counter-balance the vertical reactive forces at the corners caused by the slab. It also served to reduce the rotation of the columns. In each case, the prestressing force was applied approximately 2 hours prior to testing. During the casting of each column 5/8 inch diameter steel tubes 40.75 inches long were embedded concentrically all along its length of 41 inches, except the top 1/4 inch portion. The four columns of the specimen were placed on a rectangular steel frame made of four 41 x 4 x 3/4 inch plates attached to the Laboratory floor. Four 1/2 inch diameter fully threaded rods passing through the steel tubes were used to connect the specimen to the base plates. In each case, the prestressing force was transferred to the column through a load cell and the threaded rod by means of a hand-tightened nut. Figure 3.9 gives a schematic of this prestressing setup.

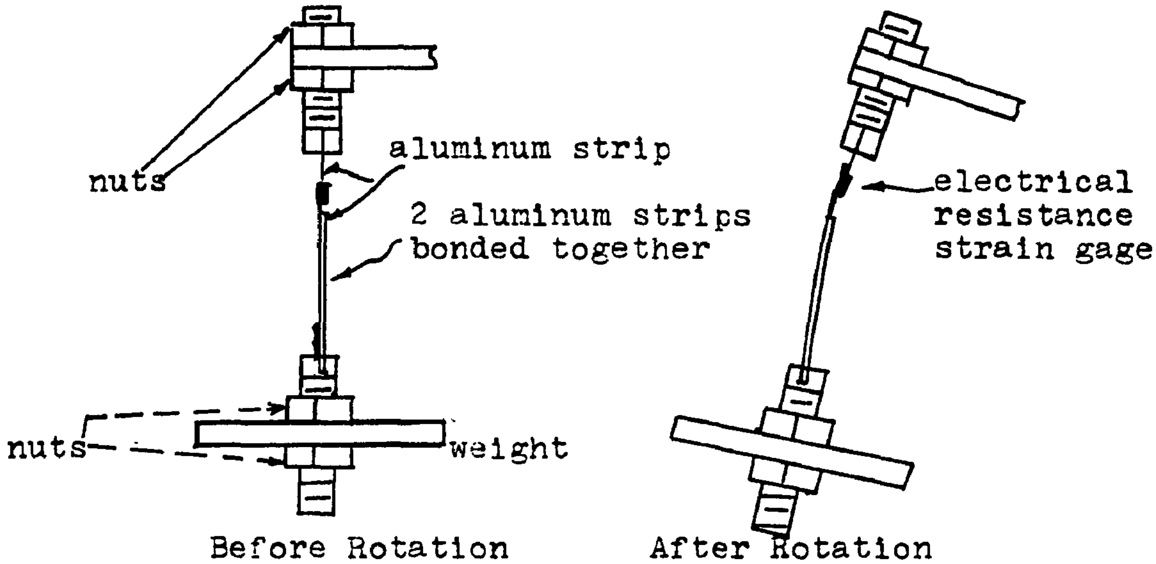

Rotation Transducer

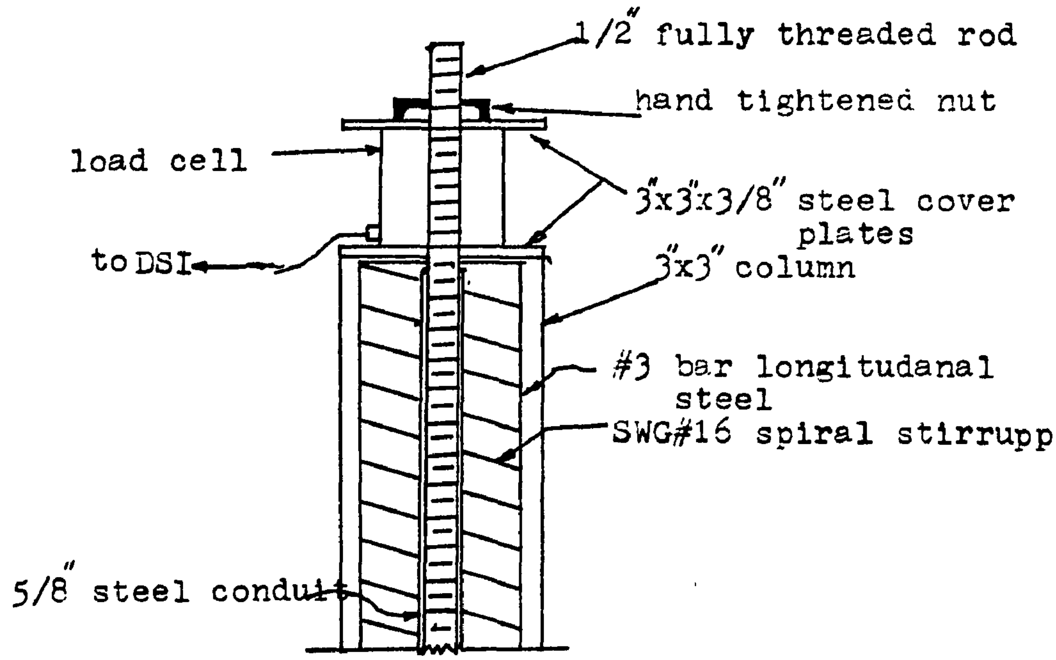

Prestressed Column

Figure 3.9. Sketches of rotation transducer and
pressed column

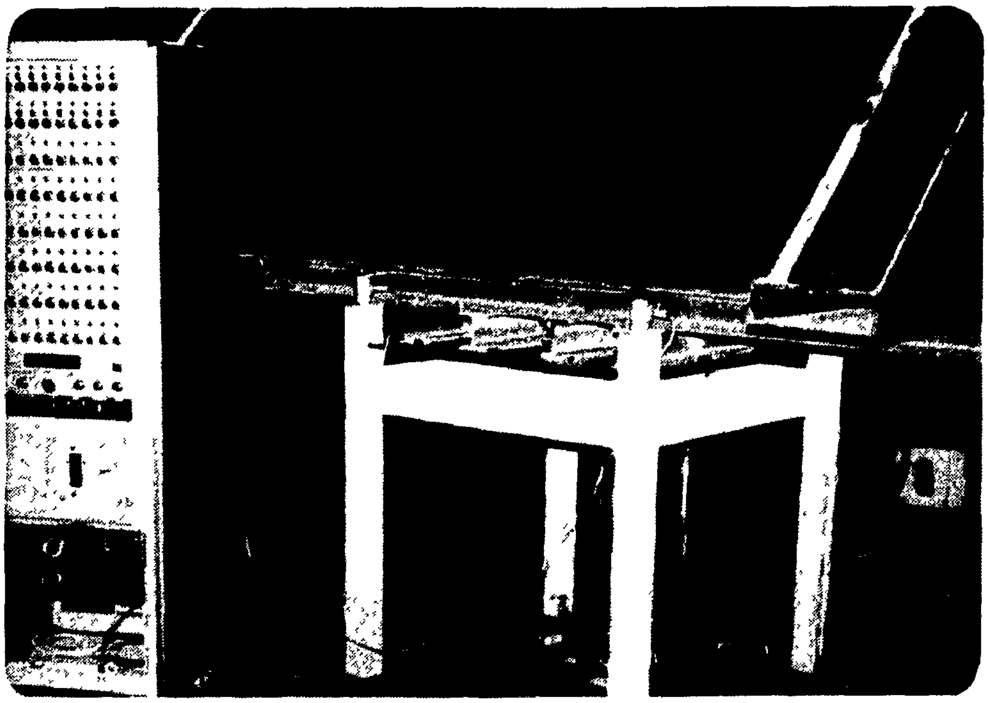

Figure 3.10 General test setup

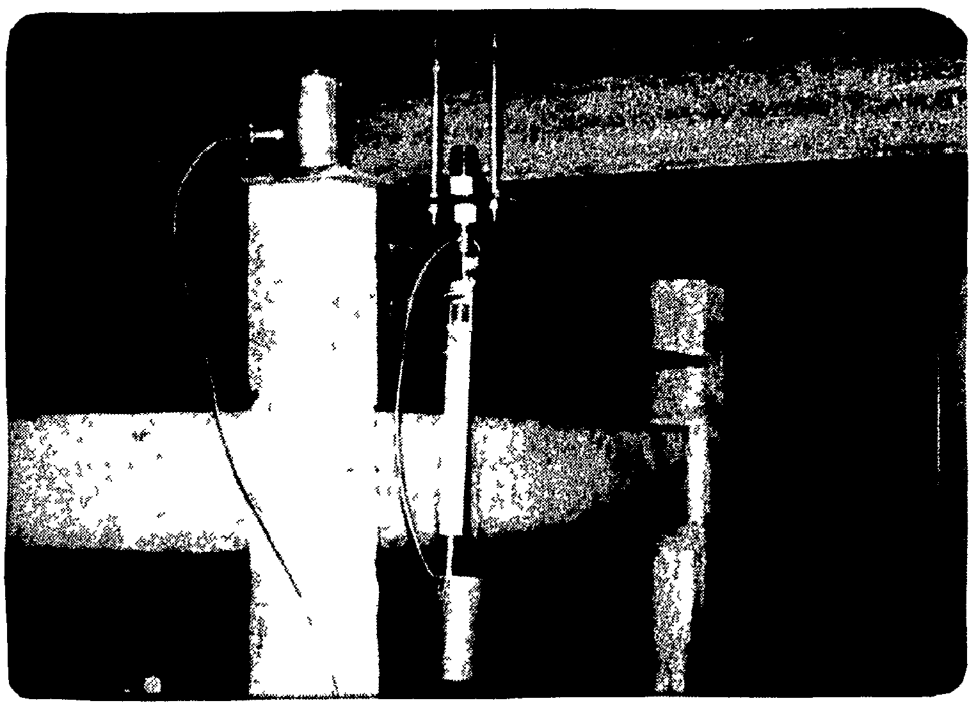

Figure 3.11 General test setup

3.6.2 Loading of the Test Specimen

The test specimens were loaded with a uniform load by means of an airbag loading system. The airbag was restrained by a reaction frame which was erected over the specimen. The frame consisted of a 39 x 39 x 1/4 inch plate attached to the steel columns through I-sections. The photographs of the test setup, which illustrate the reaction frame are shown in Figures 3.10 and 3.11.

The airbag was connected to the airline through a regulator. The pressure was supplied from the available air pressure pipe-lines. An additional air line connected the airbag to a pressure test chamber so that the actual air pressure at the airbag could be measured. The airbag was folded in such a way that its surface, connected to the inlet and outlet air lines, was always in contact of the slab. The load was measured by high and low load manometers. Loads less than 225 psf were measured by the low load manometer. Oil with a specific gravity of 0.827 was used in this manometer. High loads (above 225 psf) were measured by a manometer filled with mercury. The manometers were graduated in an increment of 1 psf. They were connected to the pressure test chamber with a control valve which could regulate pressure in the airbag at the desired load intensity.

3.6.3 Recording the Beam Rotations and the Slab Deflections

For specimen 1 the edge beam torsional rotations were measured along one of the edge beams at the center line and at distances of 6 inches and 12 inches from the center line. For specimens 2 and 3 torsional rotations were measured at the center lines of the short and long beams and also at the quarter points of the long beams. These rotations were measured by a specially designed lightweight pendulum type rotation transducers [38] using bonded strain gages as the sensing elements (see Figure 3.9). The gages used in the prototype testing [33] were heavier in weight compared to those used in the model testing program. This decrease in weight was necessary because of the smaller cross sections of the beams in the models. Reduction in bending stress of the lightweight g ages was partially compensated by a longer lever arm provided by a longer aluminum strip compared to that of the heavier gage used in the prototype work.[33] A large amount of strain could be induced in the vicinity of the bonded strain gages by using a thinner cross section at that portion of the aluminum strip. This arrangement increased the sensitivity of the gages. A typical gage was tuned for an output of 28,000$\mu\epsilon$ per radian of rotation, resulting in an accuracy of about 1 percent in the angular measurement.

Deflections of the slab were measured at several locations shown in Appendix B. They were measured by deflection transducers described by Onysko [38] and using bonded strain gages as the sensing elements. They were tuned for an output of 2000 $\mu\epsilon$ per inch of deflection.

These sensitivities of 1 in 28,000 and 1 in 2000 for the typical rotation and deflection gages respectively, were found satisfactory for this experimental investigation. Condensed tables of deflections and rotations are given in the Appendix B. These tables were prepared from the data recorded by the automatic print-out of the digital strain indicator of the Budd Instrument Company.

3.7 Test Results

Extensive test data were recorded during the course of this investigation. They are summarized in Appendix B. An important portion, which will be referred to frequently in the subsequent discussion and for which different graphs (Figures 3.12 thru 3.16) are plotted, is presented in Table 3.6 and Table 3.7.

3.8 Observed Behavior of the Test Specimens

The test specimens exhibited a particular trend in behavior which was influenced mainly by the span and depth of the short beams, the two fundamental variables in this experimental investigation. The observed behavior of these specimens could help to confirm some of the structural concepts. For example, in accordance with the elastic theory, specimen 1 which had the highest aspect ratio (1:1) showed minimum cracking strength in flexure but had a maximum slope of the elastic portion of load versus deflection curve. On the other hand, specimen 2 which had the lowest aspect ratio (1:2) exhibited the maximum cracking strength and the minimum slope.

The model specimen 1 reproduced the load-deflection and load-rotation characteristics of prototype [33] with reasonable

Table 3.6 Slab central deflections and beam central torsional rotations for specimen 1

Applied load (psf)	Deflection (in x 10^{-3})	Predicted[1] Prototype Deflection (in x 10^{-3})	Rotation (rad x 10^{-4})	Predicted[1] Prototype Rotation (rad x 10^{-4})
15	-	-	0.66	.466
30	5.5	15.54	1.20	.847
50	9	25.41	2.00	1.412
70	14	39.6	2.00	1.412
90	15.5	43.8	4.00	2.824
110	19	53.7	5.33	3.76
130	22	60.8	6.42	4.54
150	26	73.5	7.54	5.334
170	29	82.0	8.66	6.12
190	32	90.5	-	-
210	33.5	93.6	-	-
245	45.5	128.8	-	-
290	54	152.6	-	-

1 See Section 5.2 for explanation of these predicted values

Table 3.7 Slab central deflection and beam central torsional rotation for model specimens 2 and 3

Model Specimen 2

Load Stage (psf)	Deflection (in x 10^{-3})	Rotation (rad x 10^{-4})	Load Stage (psf)	Deflection (in x 10^{-3})	Rotation (rad x 10^{-4})
100	4.00	1.787	1200	57.5	11.62
210	8.00	2.235	1400	74.5	18.78
400	16.0	2.680	1500	80.0	19.66
620	26.0	5.361	1600	89.0	25.02
800	33.5	6.705	1700	104	33.52
1000	45.5	10.72	1800	126	46.47

Model Specimen 3

Load Stage (psf)	Deflection (in x 10^{-3})	Rotation (rad x 10^{-4})	Load Stage (psf)	Deflection (in x 10^{-3})	Rotation (rad x 10^{-4})
50	5.00	2.238	600	57.5	-
100	8.50	4.467	620	60.0	22.34
132	11.0	-	680	69.0	26.40
170	14.0	-	730	79.0	30.00
200	15.0	8.500	800	85.0	31.30
270	21.5	-	880	104.5	44.31
300	29.0	-	940	122.0	46.50
350	32.5	-	1000	141.0	61.20
420	39.0	11.63	1100	165.0	76.00
470	44.0	12.97	1170	234.0	165.0
500	46.5	-	1230	291.0	330.0
570	53.0	21.95	-	-	-

accuracy. Though the model beams had a smaller total number of cracks, the overall cracking patterns displayed by the model and the prototype had a striking resemblance. A typical behavior associated with specimen 2 was an early occurrence of flexural cracks at the centers of the long beams. The specimen had the lowest aspect ratio of 1:2 resulting in the predominance of one-way action more in this specimen than the other two. This was perhaps the reason for this early crack formation. Or, it might have occurred because of a typical distribution of load transmitted to the beams by the slab. This behavior of the long beams is somewhat difficult to explain at this stage, in the absence of results from the elastic theory. In specimen 3, reduction in the depth of the short beams gave the desired results. Severe cracks caused by torsion and shear were visible in the beams at sections near the columns. Also, bending and torsion cracks were formed all along the length of the beams indicating a maximum utilization of the material and adequate bond of the reinforcement.

In all the test specimens positive yield lines originated at the center of the slab and started propagating along the paths prescribed by the yield line theory. It was possible to observe this propagation phenomenon as it happened during the loading process. Spandrel sections near the columns were heavily cracked, tending to form torsional hinges at these locations. After removing the airbag, it was possible to observe flexural cracks caused by negative moments in the slab. These cracks were formed on the top surface of the slab all along its junction with the edge beams. The ultimate deflections of the specimens were very large (approximately twice the depth of the slab). Thus, they exhibited the ductile type of failure recommended by the ACI Building Code.

3.9 Observed Load-Deformation Curves

Based on the experimental data different load-deflection and load-rotation curves are plotted for model specimens 2 and 3 (see Figures 3.12 thru 3.16). Characteristics of similar curves for model specimen 1 can be seen in Figures 5.3 and 5.5 which give model prediction values obtained after multiplying the observed model reading (deflection or rotation) by an appropriate dimensionless constant. The detail discussion along with the statistical analysis of this model specimen 1 test data is given in Appendix A. Figure 3.12 of the observed slab central deflection of model specimen 2 shows clearly the elastic portion of straight line up to 1125 psf. The same elastic limit is shown in all the three graphs (Figures 3.12, 3.13 and 3.14) of this model specimen. After the load of 1125 psf the transition zone shown by the dotted line starts in these load-deformation curves. The inelastic zone starts at about 1325 psf. This zone continued until the final collapse which took place at about 2200 psf after which the slab could sustain no more load. The theoretical calculations based on the yield line theory are given in Section 4.5.4. For specimen 2 the theoretical ultimate load is 1850 psf, a value nearly 25%

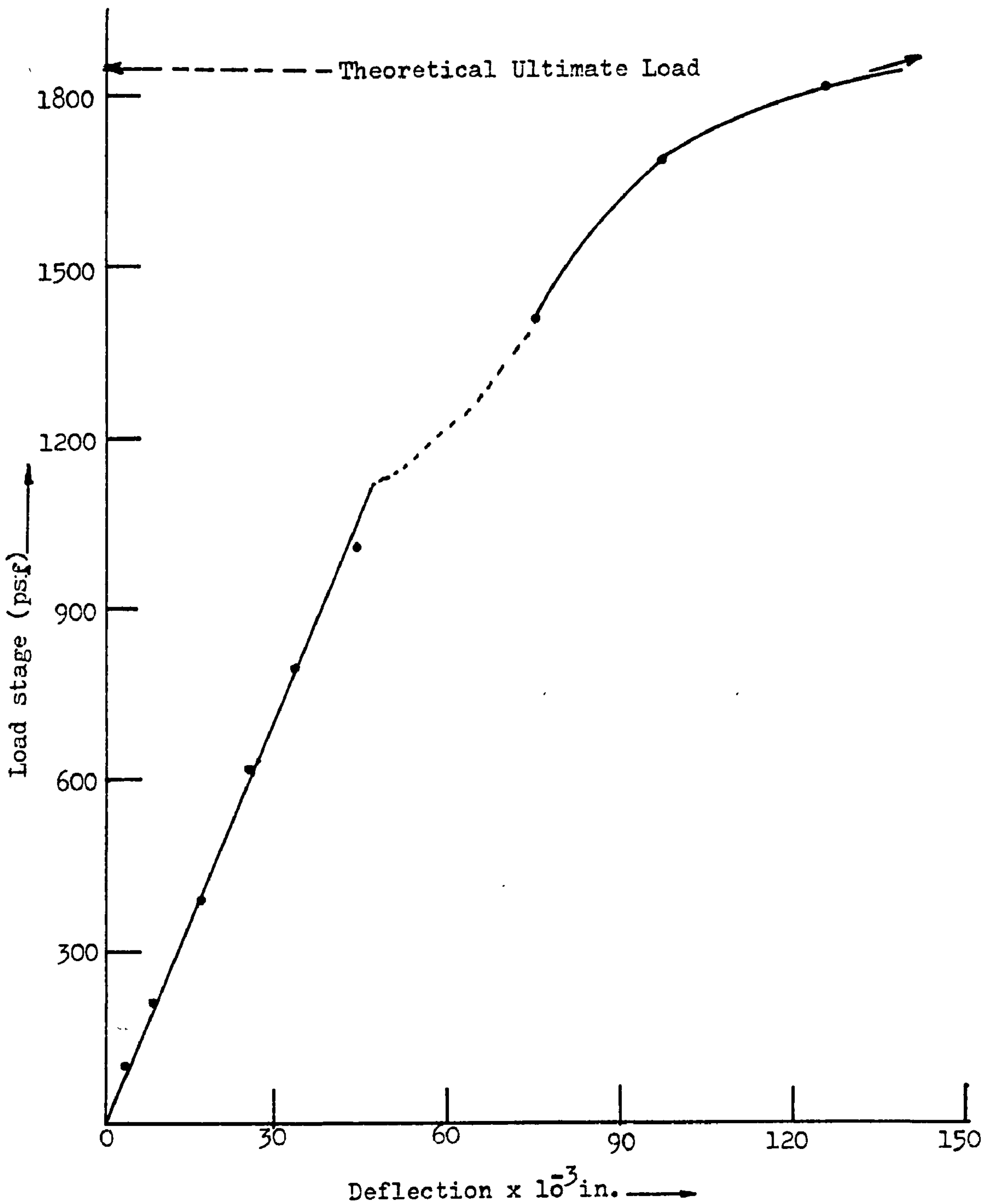

Figure 3.12 Slab central deflection, model specimen 2

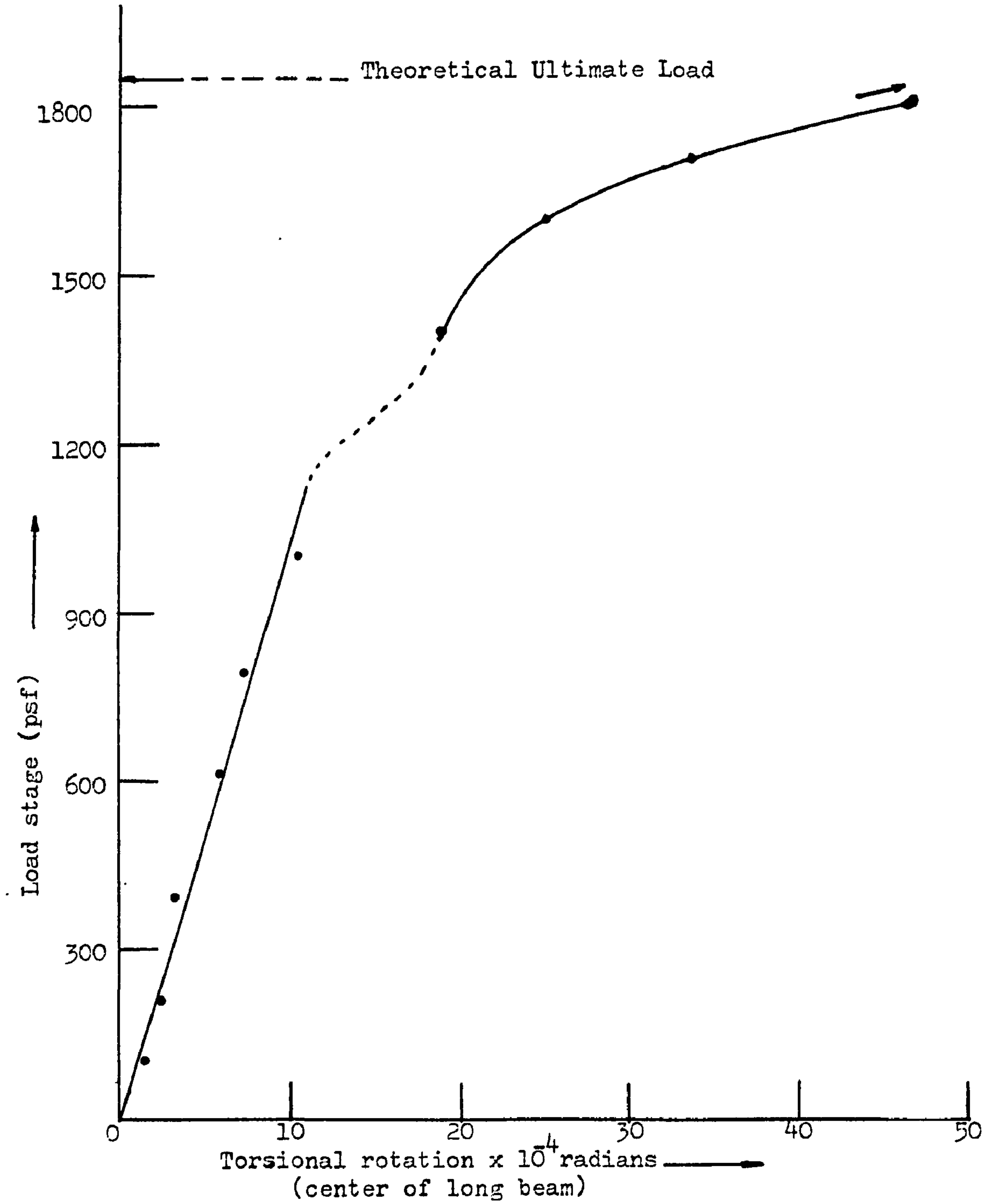

Figure 3.13 Torsional rotation, model specimen 2

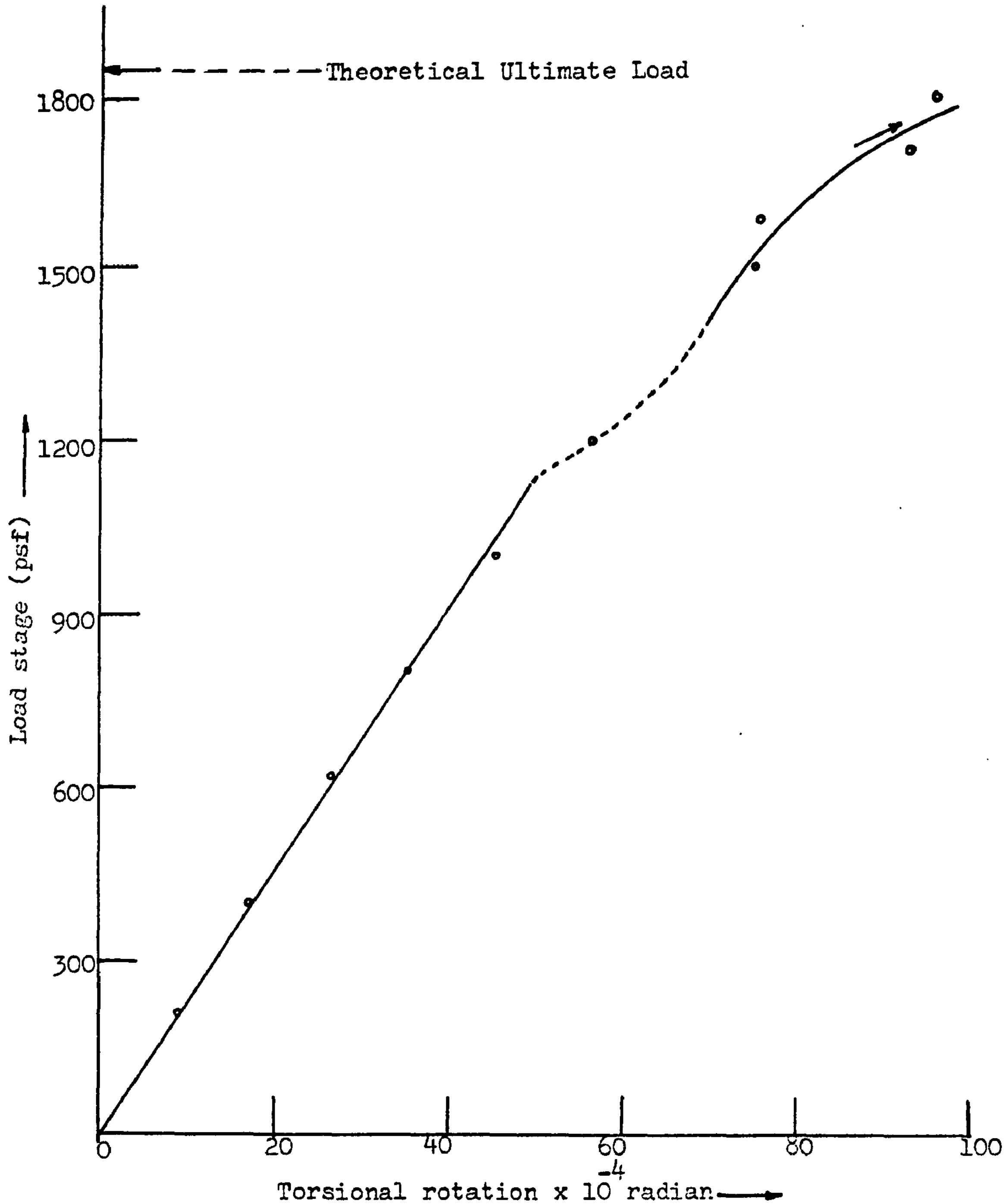

Figure 3.14 Torsional rotation, model specimen 2

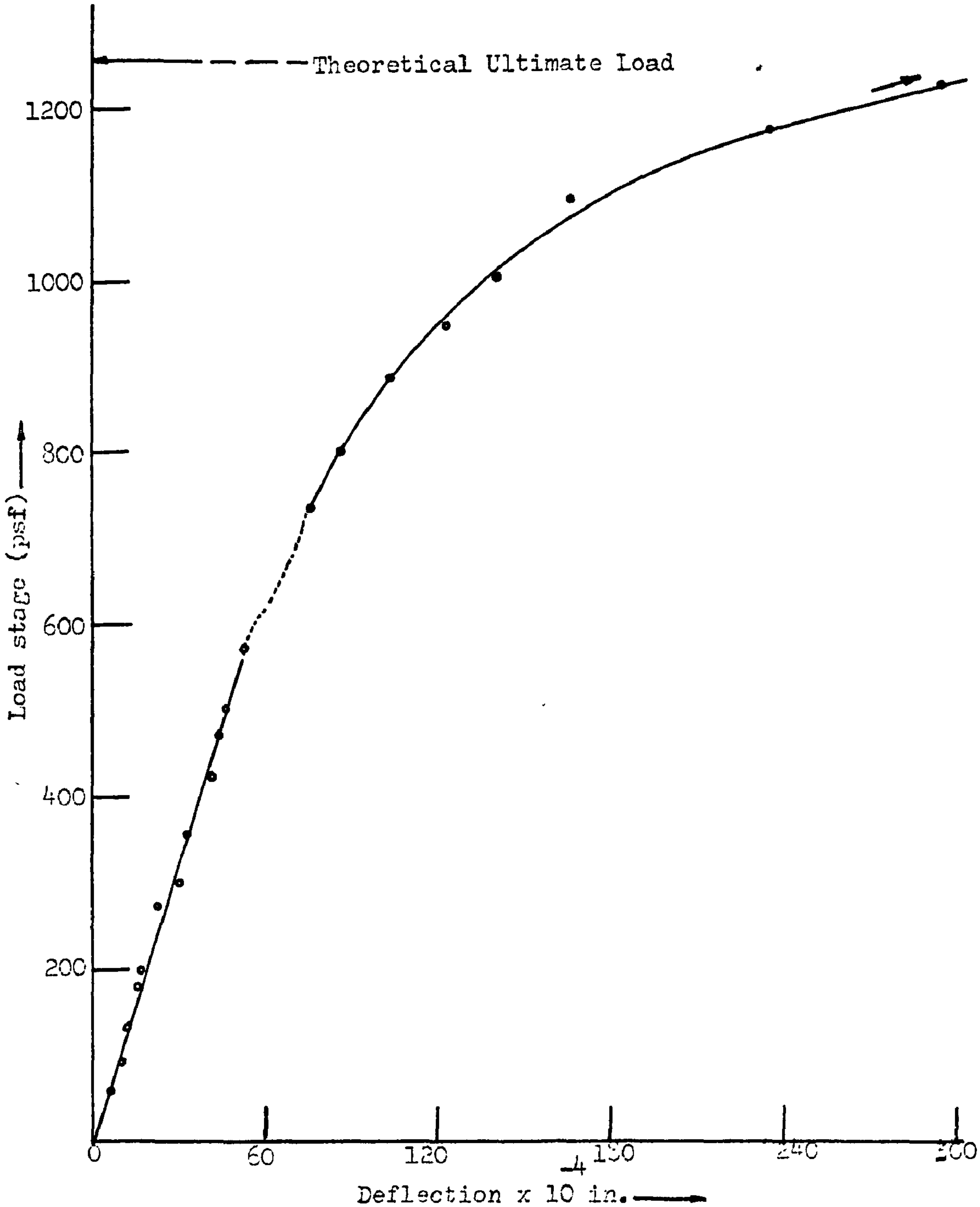

Figure 3.15 Slab central deflection, model specimen 3

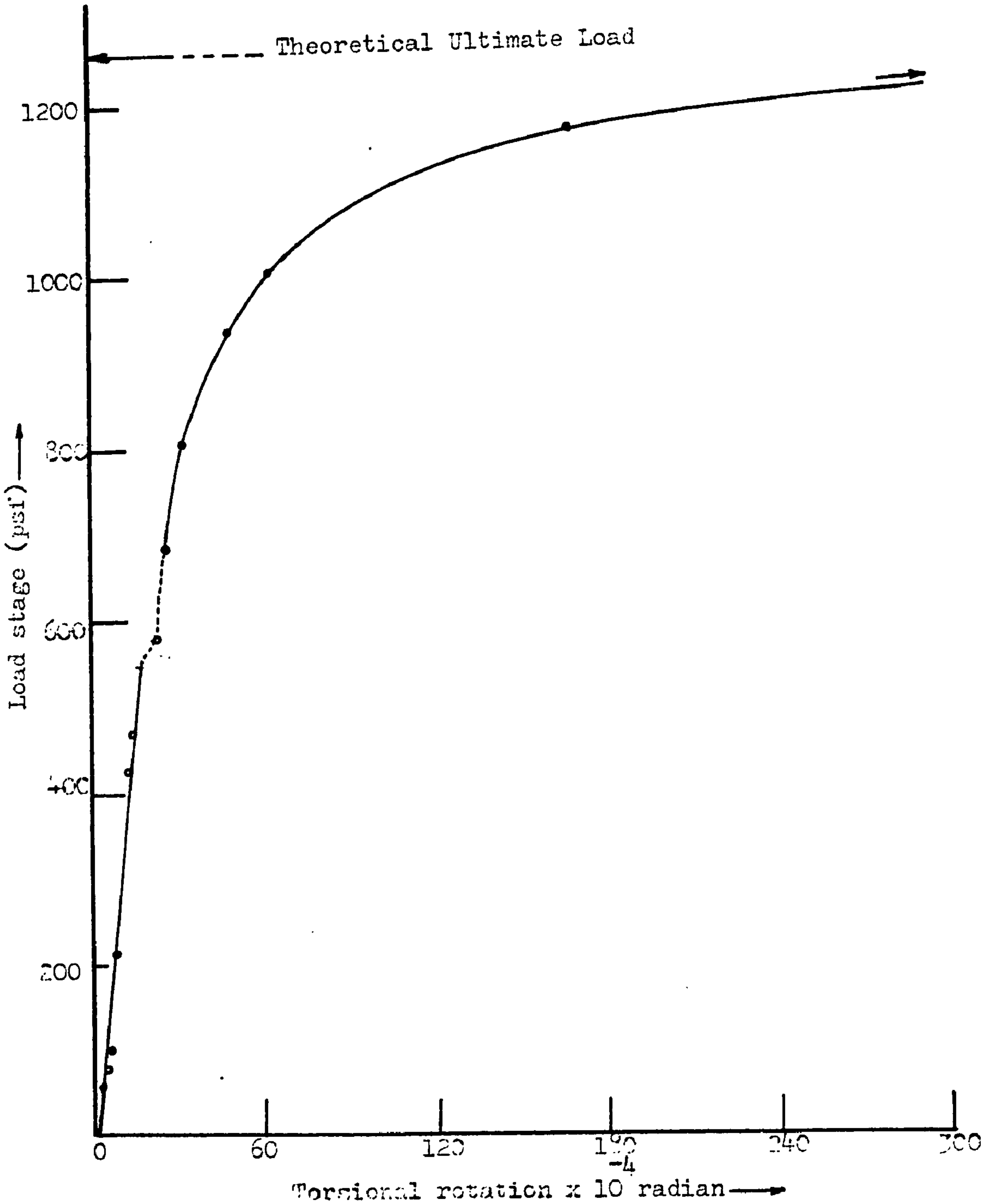

Figure 3.16 Torsional rotation, model specimen 3

smaller than the observed one because of the excessive membrane action, as pointed out by Wood [18].

Similar curves are observed (see Figure 3.15 and 3.16) for the load-deflection and load-rotation data of model specimen 3. As indicated by these curves the elastic limit ended at about 575 psf after which the transition zone (dotted portion) started. The inelastic zone was from about 700 psf onwards. The total collapse occurred at 1600 psf. The yield line theory gives this ultimate load value as 1260 psf (see Section 4.5.4), indicating the presence of a significant membrane action as expected from this structural system.

Recalling that model specimen 2 had dimensions of 36 x 18 inches whereas specimen 3 had 36 x 24 inches, one can expect larger magnitudes of elastic and ultimate loads in specimen 2 compared to the corresponding values of specimen 3, as shown by these curves. Also, specimen 2 showed higher flexural cracking strength compared to the specimen 3.

4. THEORETICAL ANALYSIS

4.1 Introduction

Theoretical work undertaken for this investigation can be divided into three major sections and their sub-sections as follows:

1. Elastic solution of doubly symmetric (i.e. square) case of flat plates and slabs,
   - (a) elastically supported edges without torsion,
   - (b) elastically supported edges with torsion and development into free edges, simply supported edges, fixed edges and elastically supported edges without torsion.
2. Service load requirements of doubly symmetric case,
   - (a) flexural cracking of slab,
   - (b) flexural cracking of edge beams,
   - (c) torsion and shear requirements of edge beams,
   - (d) design formulas for edge beams.
3. Inelastic analysis of rectangular and square panels
   - (a) conventional yield line theory,
   - (b) modified yield line theory,
   - (c) combination of above (a) and (b).

The analytical work given in 1.(b), 2.(a), 2.(b), 2.(c), 2.(d) and 3.(c) is not available in the literature and therefore will be discussed in detail. The tested specimens of model and prototype structures will be analyzed in the light of this theoretical work.

4.2 Elastically Supported Doubly Symmetric Flat Plates and Slabs Without Torsion

4.2.1 Assumed Solution

The assumed solution is based on the theory of small deflections of laterally loaded flat plates. Accordingly, the deflections are assumed to be small in comparison with the thickness of the slab. At the boundary it is assumed that the edges of the slab are completely free for in-plane movements; thus the reactive forces at the edges are normal to the slab. A general differential equation for the deflected surface of the slab can be written as:

$$\frac{\partial^4 w}{\partial x^4} + \frac{\partial^4 w}{\partial x^2 \partial y^2} + \frac{\partial^4 w}{\partial y^4} = \frac{q}{D} \tag{4.1}$$

To satisfy this differential equation and also the conditions of symmetry, the following deflection function is assumed:

$$w = \frac{q}{768D} \left[(16x^4 - 24a^2x^2 + 5a^4) + (16y^4 - 24a^2y^2 + 5a^4)\right]$$

$$+ \sum_{n=1,3,5}^{\infty} A_n \left(\cosh \frac{n\pi y}{a} \cos \frac{n\pi x}{a} + \cosh \frac{n\pi x}{a} \cos \frac{n\pi y}{a}\right)$$

$$+ \sum_{n=1,3,5}^{\infty} C_n \left(y \sinh \frac{n\pi y}{a} \cos \frac{n\pi x}{a} + x \sinh \frac{n\pi x}{a} \cos \frac{n\pi y}{a}\right) \tag{4.2}$$

It consists of two parts i.e. a particular integral and a complimentary function. Each one has interchangeable terms in x and y to satisfy the requirement of the doubly symmetric structure. The complimentary function is a solution of the homogeneous equation, whereas, the particular integral satisfies the governing equation

4.1 . The summation constants A_n and C_n are to be chosen to suit the boundary conditions under study.

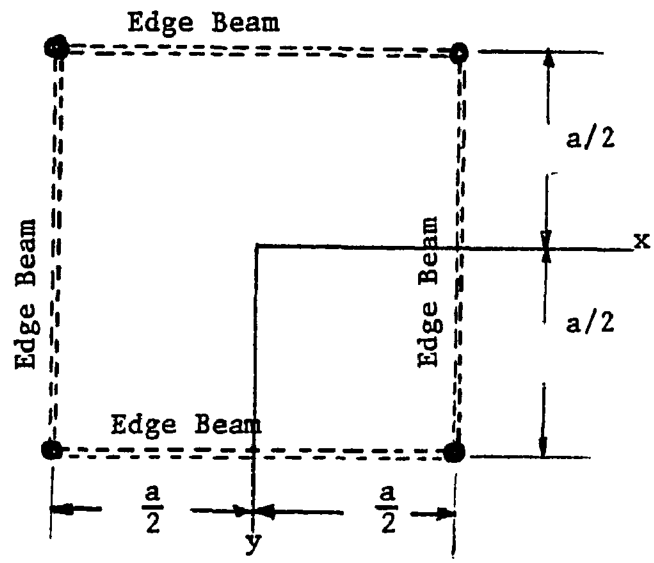

Figure 4.1 Slab with elastically supported edges

The co-ordinate axes are chosen along the center lines of the slab as shown in Figure 4.1. Loading is symmetric of uniform intensity q. The beams are identical in all respects. In this part of the solution, the slab is just resting on the beams with the edges free to rotate in any plane. The construction is not assumed to be monolithic, that is the slab and the beams are separately cast without any torsional effect at their junction.

4.2.2 Boundary Conditions

The slab is simply supported on the beams. Edges are free to rotate and there is no bending moment M_x along the edges x = a/2. Also the bending moment M_y along the edges y = a/2 is zero. The analytical expression for this boundary condition is

$$\left[\frac{\partial^2 w}{\partial y^2} + \mu \frac{\partial^2 w}{\partial x^2}\right]_{y = \frac{a}{2}} = 0 \qquad (4.3)$$

The deflection of the slab along the edge is equal to the deflection of the beam. The shear in the z direction transmitted from the slab to the supporting beam is given by

$$-V_y = D\left[\frac{\partial^3 w}{\partial y^3} + (2 - \mu)\frac{\partial^3 w}{\partial x^2 \partial y}\right]_{y = a/2}$$

So, the differential equation of the deflection curve of the beam will be

$$D\left[\frac{\partial^3 w}{\partial y^3} + (2-\mu)\frac{\partial^3 w}{\partial x^2 \partial y}\right]_{y = a/2} = EI\left[\left(\frac{\partial^4 w}{\partial x^4}\right)\right]_{y = \frac{a}{2}} \qquad (4.4)$$

This equation represents the second boundary condition. The algebraic and the hyperbolic functions contained in expression of Equation 4.2 are developed in cosine series by using a Fourier expansion. Then, using the two boundary conditions of Equations 4.3 and 4.4 we arrive at a set of equations for the constants A_n and C_n as shown in the next section.

4.2.3 Formation of the Simultaneous Summation Equations

The boundary condition of Equation 4.3 is satisfied by partially differentiating the deflection function of Equation 4.2 .

$$\frac{\partial^2 w}{\partial y^2} + \mu \frac{\partial^2 w}{\partial x^2}$$

$$= \frac{q}{768D} (192y^2 - 48a^2)$$

$$+ \Sigma A_n \left[(\frac{n\pi}{a})^2 \cosh \frac{n\pi y}{a} \cos \frac{n\pi x}{a} - (\frac{n\pi}{a})^2 \cosh \frac{n\pi x}{a} \cos \frac{n\pi y}{a}\right]$$

$$+ \Sigma C_n \left\{-x (\frac{n\pi}{a})^2 \sinh \frac{n\pi x}{a} \cos \frac{n\pi y}{a} + \cos \frac{n\pi x}{a} \left[\frac{2n\pi}{a} \cosh \frac{n\pi y}{a}\right.\right.$$

$$\left.\left. + y (\frac{n\pi}{a})^2 \sinh \frac{n\pi y}{a}\right]\right\}$$

$$+ \frac{\mu q}{768D} (192 x^2 - 48 a^2)$$

$$+ \mu \Sigma C_n \left\{-y (\frac{n\pi}{a})^2 \sinh \frac{n\pi y}{a} \cos \frac{n\pi x}{a} + \cos \frac{n\pi y}{a} \left[\frac{2n\pi}{a} \cosh \frac{n\pi x}{a}\right.\right.$$

$$\left.\left. + x (\frac{n\pi}{a})^2 \sinh \frac{n\pi x}{a}\right]\right\}$$

$$+ \mu \Sigma A_n \left[- (\frac{n\pi}{a})^2 \cosh \frac{n\pi y}{a} + (\frac{n\pi}{a})^2 \cosh \frac{n\pi x}{a} \cos \frac{n\pi y}{a}\right]$$

Using $\frac{n\pi}{2} = \alpha_n$ and $y = a/2$, boundary condition of Equation 4.3 yields:

$$\Sigma A_n (\frac{n\pi}{a})^2 \cosh \alpha_n \cos \frac{n\pi x}{a} + \Sigma C_n \cos \frac{n\pi x}{a} \left[+ \frac{2n\pi}{a} \cosh \alpha_n\right.$$

$$\left. + \frac{a}{2} (\frac{n\pi}{a})^2 \sinh \alpha_n \right]$$

$$+ \frac{\mu q}{768D} (192 x^2 - 48 a^2) + \mu \Sigma C_n \left[- \frac{a}{2} (\frac{n\pi}{a})^2 \sinh \alpha_n \cos \frac{n\pi x}{a}\right]$$

$$+ \mu \Sigma A_n \left[- (\frac{n\pi}{a})^2 \cosh \alpha_n \cos \frac{n\pi x}{a}\right] = 0 \qquad (4.5)$$

Expressing $\frac{\mu q}{768D}$ $(192x^2 - 48a^2)$ in a Fourier series as

$\frac{2\mu q a^2}{^3D}$ $\Sigma (-1)^{\frac{n+1}{2}}$ $\frac{1}{n^3}$ $\cos \frac{n\pi x}{a}$, Equation (5) leads to:

$$A_n \left\{ \left(\frac{n\pi}{a}\right)^2 (1 - \mu) \cosh \alpha_n \right\}$$

$$+ C_n \left\{ \frac{2n\pi}{a} \cosh \alpha_n + \frac{a}{2} \left(\frac{n\pi}{a}\right)^2 \sinh \alpha_n (1 - \mu) \right\}$$

$$= (-1)^{\frac{n-1}{2}} \frac{2\mu q a^2}{\pi^3 n^3 D} \tag{4.6}$$

$$A_n (1 - \mu) \cosh \alpha_n + C_n \left[\frac{2a}{n\pi} \cosh \alpha_n + (1 - \mu) \frac{a}{2} \sinh \alpha_n \right]$$

$$= \frac{2\mu q a^4 (-1)}{n^5 \pi^5 D}^{\frac{n-1}{2}} \tag{4.7}$$

In the same way, by using the appropriate derivatives of the deflection function of Equation 4.2, boundary condition of Equation 4.4 gives:

$$\frac{qa}{4} + D \Sigma A_n \left\{ \left(\frac{n\pi}{a}\right)^3 \sinh \alpha_n \cos \frac{n\pi x}{a} + \left(\frac{n\pi}{a}\right)^3 \cosh \frac{n\pi x}{a} \sin \alpha_n \right\}$$

$$+ D \Sigma C_n \left[\left(\frac{n\pi}{a}\right)^3 x \sinh \frac{n\pi x}{a} \sin \alpha_n \right.$$

$$\left. + \cos \frac{n\pi x}{a} \left\{ 2\left(\frac{n\pi}{a}\right)^2 \sinh \alpha_n + \left(\frac{n\pi}{a}\right)^2 \sinh \alpha_n + \frac{a}{2} \left(\frac{n\pi}{a}\right)^3 \cosh \alpha_n \right\} \right]$$

$$+ D(2 - \mu) \left[\Sigma A_n \left\{ - \left(\frac{n\pi}{a}\right)^3 \sinh \alpha_n \cos \frac{n\pi x}{a} - \left(\frac{n\pi}{a}\right)^3 \cosh \frac{n\pi x}{a} \sin \alpha_n \right\} \right.$$

$$+ \Sigma C_n \left\{ -\left(\frac{n\pi}{a}\right)^2 \sinh \alpha_n \cos \frac{n\pi x}{a} - \frac{a}{2} \left(\frac{n\pi}{a}\right)^3 \cosh \frac{n\pi x}{a} \sin \alpha_n \right.$$

$$\left. \left. - \left(\frac{n\pi}{a}\right) \sin \alpha_n \left\{ \frac{2n\pi}{a} \cosh \frac{n\pi x}{a} + \left(\frac{n\pi}{a}\right)^2 x \sinh \frac{n\pi x}{a} \right\} \right\} \right]$$

$$= EI \left\{ \frac{q}{2D} + \Sigma A_n \left[\left(\frac{n\pi}{a}\right)^4 \cosh \alpha_n \cos \frac{n\pi x}{a} \right] \right.$$

$$\left. + \Sigma C_n \left[\frac{a}{2} \left(\frac{n\pi}{a}\right)^4 \sinh \alpha_n \cos \frac{n\pi x}{a} \right] \right\} \tag{4.8}$$

Some of the terms of Equation 4.8 are expanded in half-range cosine, series, for example:

$$\cosh\frac{n\pi x}{a} = \sum_{i=1,3,5}\left[\frac{2}{a}\ \frac{2i\pi}{aK}\ \sin\frac{i\pi}{2}\ \cosh\frac{n\pi}{2}\right]\ \cos\frac{i\pi x}{a} \tag{4.9}$$

where $K = (\frac{n\pi}{a})^2 + (\frac{i\pi}{a})^2$

The Fourier expansion of any constant is

$$\text{Const} = \sum_{n=1,3,5} \frac{4\ \text{Const}}{n\pi}\ \sin\frac{n\pi}{2}\ \cos\frac{n\pi x}{a}$$

(a) Replacing the terms by their Fourier expansions,

(b) changing the dummy variable n to the variable i in the single summation terms, (c) grouping together the terms that contain same $\cos(i\pi x/a)$ as a factor and then (d) observing that Equation 4.8 is satisfied for any value of x, one can conclude that the coefficient by which $\cos(i\pi x/a)$ is multiplied must be equal to zero for each value of i. This procedure transforms Equation 4.8 into:

$$D(\frac{i\pi}{a})^3 A_i \left\{\sinh\alpha_i - (2-\mu)\sinh\alpha_i - \frac{EI}{D}(\frac{i\pi}{a})\cosh\alpha_i\right\}$$

$$+ D(\frac{i\pi}{a})^2 C_i \left\{3\sinh\alpha_i + (\frac{i\pi}{2})\cosh\alpha_i - (2-\mu)\sinh\alpha_i - (2-\mu)(\frac{i\pi}{2})\cosh\alpha_i - \frac{EI}{D}\frac{a}{2}(\frac{i\pi}{a})^2\sinh\alpha_i\right\}$$

$$+ \sum\left[\left\{DA_n(\frac{n\pi}{a})^3\sin\alpha_n - D(2-\mu)A_n(\frac{n\pi}{a})^3\sin\alpha_n - D(2-\mu)C_n\sin\alpha_n(\frac{n\pi}{a})(\frac{2n\pi}{a})\right\}(\frac{4i\pi}{a^2K}\ \sin\alpha_i\ \cosh\frac{n\pi}{2})\right]$$

$$+ \sum\left[\left\{DC_n(\frac{n\pi}{a})^3\sin\alpha_n - D(2-\mu)C_n(\frac{n\pi}{a})\sin\alpha_n(\frac{n\pi}{a})^2\right\}\left[\frac{2}{K}\ \frac{i\pi}{a}\ \sin\alpha_i\ \sinh\frac{n\pi}{2} - \frac{8}{aK^2}(\frac{n\pi}{a})(\frac{i\pi}{a})\ \sin\alpha_i\ \cosh\frac{n\pi}{2}\right]\right]$$

$$= \frac{4q}{i\pi}\ \sin\alpha_i\left[\frac{EI}{2D} - \frac{a}{4}\right] \tag{4.10}$$

This equation is based on the second boundary condition of Equation 4.4

4.2.4 Coupled Equation and Computer Solution

Equation 4.7 and Equation 4.10 are the two uncoupled equations having A_n and C_n as the only unknown quantities. The final coupled equation in terms of C_n can be obtained by eliminating A_n. Thus, this final equation will represent an infinite set of linear simultaneous equations in the unknown C_1, $C_3 \ldots . C_\infty$.

By Equation (4.7):

$$A_n = \left(\frac{1}{1-\mu}\right) \frac{1}{\cosh \alpha_n} \left\{ \frac{2\mu q}{n^5} \frac{a^4 (-1)^{\frac{n-1}{2}}}{\pi^5 D} - C_n \left[\frac{2a}{\pi} \cosh \alpha_n + (1-\mu) \frac{a}{2} \sinh \alpha_n\right]\right\} \qquad (4.11)$$

This value of A_n is substituted in Equation 4.10 .

After a few pages of simplification, the final coupled equation in terms of C_n becomes:

$$C_i D \beta_i^2 \sinh \alpha_i \left\{ 3 + \mu + \frac{2EI}{D} \beta_i \frac{1}{1-\mu} \coth \alpha_i + \frac{1-\mu}{2} (i\pi)(\tanh \alpha_i - \coth \alpha_i)\right\}$$

$$+ \sum C_n F_1 \left\{ 2(2-\mu) \frac{a}{n\pi} - \frac{2a}{n\pi} - \frac{2(1-\mu)}{K} \frac{n\pi}{a}\right\}$$

$$= \frac{4q}{\beta_i} \sin \alpha_i \left[\frac{EI}{2Da} - \frac{1}{4}\right] + \frac{2\mu}{1-\mu} \frac{q(-1)^{\frac{i-1}{2}}}{a\, \beta_i^2} \left[(i-\mu) \tanh \alpha_i + \frac{EI}{D} \beta_i\right] - \sum \left[\frac{F_1}{\cosh_n} (-1)^{\frac{n-1}{2}} \frac{2\mu q}{n^5} \frac{a^4}{\pi^5 D}\right] \qquad (4.12)$$

where $\alpha_i = \frac{i\pi}{2}$, $\beta_i = \frac{i\pi}{a}$

$$\alpha_n = \frac{n\pi}{2}, \quad \beta_n = \frac{n\pi}{a}$$

$$K = \alpha_n^2 + \beta_n^2$$

$$F_1 = -D \sin\alpha_n \, (\beta_n)^3 \, \frac{4\beta_i}{aK} \sin\alpha_i \cosh\alpha_n \qquad (4.13)$$

A computer program was written to solve Equation 4.12. C_1, C_3, C_5, C_7 obtained by this solution are substituted in Equation 4.11. Thus, all A_n and C_n values are known. The deflection function of Equation 4.2 is now completely defined. An expression for bending moment at the center of the slab is developed in Equation 4.19.

The accuracy of the theoretical and computer work completed upto this step was checked with the help of the formulas given by Timoshenko,[37] et.al. Excellent correlation was observed as shown in the computer print-out of Appendix C.

A study was conducted to understand the convergence characteristics of the A_n and C_n series and also their effects on deflections and bending moments. Both series were found to converge very fast. In some cases, the first term only gives deflection values correct to three decimal places. Nevertheless, the computer program is capable of generating the terms upto A_7 and C_7, the last one being very small (of the order of 10^{-14}).

4.3 Analysis of Doubly Symmetric Flat Plates and Slabs for all the Possible Edge Conditions

4.3.1 Assumed Solution

There are five possible edge conditions for the doubly symmetric case. (i) Free edges (ii) Elastically Supported Edges Without Torsion (iii) Elastically Supported Edges With Torsion (iv) Simply Supported Edges (v) Fixed Edges. The assumed solution for the deflection surface of the slab should be such that deflection at the edges must be zero in edge conditions (iv) and (v). However, it must be finite and non-zero for the first three cases. Also, the assumed deflection function should have derivatives which yield zero bending moments at the edges for conditions (i), (ii) and (iv) but finite non-zero values for (iii) and (v). A careful study of the deflection function of Equation 4.2 will show that it is capable of satisfying all these requirements, if proper boundary conditions are used. Thus, this function is assumed to be a possible solution of differential equation 4.1 . The corresponding boundary conditions are discussed in the next article.

4.3.2 Boundary Conditions

The boundary condition given by Equation 4.3 is not valid. The torsional moment in the edge beam can be a non-zero value given by $-c(\partial^2 w/\partial x\,\partial y)$ along $y = a/2$. The right-hand-screw rule is used for the sign convention. This torsional moment varies along the edge, since the slab, rigidly connected with the beam, transmits continuously distributed twisting moments to the beam. The magnitude of these applied moments per unit length is equal and opposite to the bending moments M_y in the slab. Hence, from a consideration of the torsional equilibrium on an element of the beam, the boundary condition can be expressed in the following analytical form:

$$D\left[\frac{\partial^2 w}{\partial y^2} + \nu \frac{\partial^2 w}{\partial x^2}\right]_{y=\frac{a}{2}} = - C \frac{\partial}{\partial x}\left[\frac{\partial^2 w}{\partial y \partial x}\right]_{y=\frac{a}{2}} \tag{4.14}$$

The boundary condition given by Equation 4.4 is valid for all five edge conditions. The differential equation of the deflection curve of the beam remains the same. A close study of the boundary conditions given by Equations 4.4 and 4.14 reveals that they can generate all the five edge conditions by using proper combinations of EI and C values. For example, in edge condition (i), free edges, EI = 0, C = 0; in edge condition (iv), simply supported edges, EI = ∞, C = 0, etc. Thus, the boundary conditions given by Equations 4.4 and 4.14 are the most general type and can be used for all the possible edge conditions of the doubly symmetric system.

4.3.3 Formation of the Simultaneous Summation Equations

The boundary condition given by Equation 4.14 can be rewritten as:

$$\left[\frac{\partial^2 w}{\partial y^2} + \nu \frac{\partial^2 w}{\partial x^2}\right]_{y=\frac{a}{2}} = - \frac{C}{D} \frac{\partial}{\partial x}\left[\frac{\partial^2 w}{\partial y \partial x}\right]_{y=\frac{a}{2}} \tag{4.15}$$

A summation equation based on this boundary condition can be evaluted by using the appropriate derivatives of the deflection function w. After a few steps of simplification, the right hand side of Equation 4.15 becomes:

$$-\frac{C}{D}\sum A_n\left[-\left(\frac{n\pi}{a}\right)^3\cosh\frac{n\pi x}{a}\ \sin\alpha_n-\left(\frac{n\pi}{a}\right)^3\sinh\alpha_n\cos\frac{n\pi x}{a}\right]$$
$$-\frac{C}{D}\sum C_n\left[-\left(\frac{n\pi}{a}\right)^2\cosh\frac{n\pi x}{a}\ \sin\alpha_n-\left(\frac{n\pi}{a}\right)^2\cosh\frac{n\pi x}{a}\sin\alpha_n\right.$$
$$-x\left(\frac{n\pi}{a}\right)^3\sinh\frac{n\pi x}{a}\ \sin\alpha_n-\left(\frac{n\pi}{a}\right)^2\sinh\alpha_n\cos\frac{n\pi x}{a}$$
$$\left.-\frac{a}{2}\left(\frac{n\pi}{a}\right)^3\cosh\alpha_n\cos\frac{n\pi x}{a}\right] \qquad (4.16)$$

Now, using procedures (a) to (d) given on page 62, after a few pages of simplification, the boundary condition given by Equation 4.14 yields the first summation equation. In the same way, the boundary condition given by Equation 4.4 will yield another eqution. These two uncoupled equations are as follows:

$$A_i\left\{\left(\frac{i\pi}{a}\right)^2(1-\mu)\cosh\alpha_i\right\}+C_i\left\{\frac{2i\pi}{a}\quad\cosh\alpha_i+\frac{a}{2}\sinh\alpha_i\,(1-\mu)\right\}$$
$$+(-1)^{\frac{i+1}{2}}\ \frac{2\mu q a^2}{\pi^3 i^3 D}$$
$$=A_i\frac{C}{D}\left(\frac{i\pi}{a}\right)^3\ \sinh\alpha_i+C_i\ \frac{C}{D}\left[\left(\frac{i\pi}{a}\right)^2\ \sinh\alpha_i+\frac{a}{2}\left(\frac{i\pi}{a}\right)^3\cosh\alpha_i\right]$$
$$+\sum_{n=1,3,5}\frac{C}{D}\left\{A_n\left(\frac{n\pi}{a}\right)^3\sin\alpha_n+C_n\,2\left(\frac{n\pi}{a}\right)^2\sin\alpha_n\right\}\left[\frac{C}{D}\ \frac{4i\pi}{a^2K}\ \sin\alpha_i\cosh\frac{n\pi}{2}\right]$$
$$+\sum_{n=1,3,5}C_n\frac{C}{D}\left(\frac{n\pi}{a}\right)^3\sin\alpha_n\left[\frac{2}{K}\ \frac{i\pi}{a}\ \sin\alpha_i\sinh\ \frac{n\pi}{2}\right.$$
$$\left.-\frac{8}{aK^2}\left(\frac{n\pi}{a}\right)\left(\frac{i\pi}{a}\right)\sin\alpha_i\cosh\frac{n\pi}{2}\right] \qquad (4.17)$$

This is the 'GRH1' equation of the computer program. The 'GRH2' equation based on Equation (4) is:

$$-D\left(\frac{i\pi}{a}\right)^3 \cosh\alpha_i \left\{(1-\mu)\ \text{Tanh}\,\alpha_i + \frac{EI}{D}\left(\frac{i\pi}{a}\right)\right\} A_i$$

$$+D\left(\frac{i\pi}{a}\right)^2 \sinh\alpha_i \left\{1+\mu - \frac{EI}{D}\ \frac{a}{2}\left(\frac{i\pi}{a}\right)^2 - \frac{i\pi}{2}\ (1-\mu)\coth\alpha_i\right\} C_i$$

$$+\sum_{n=1,3,5}\left\{(1-\mu)A_n + 2(1-\mu)\frac{a}{n\pi}C_n\right\}\left[-D\sin\alpha_n\left(\frac{n\pi}{a}\right)^3 \frac{4i\pi}{a^2K}\sin\alpha_i\cosh\frac{n\pi}{2}\right]$$

$$+\sum_{n=1,3,5} C_n F_1\left\{(1-\mu)\left[\frac{a}{2}\ \tanh\frac{n\pi}{2} - \frac{2}{K}\left(\frac{n\pi}{a}\right)\right]\right\}$$

$$= \frac{4qa}{i\pi}\sin\alpha_i\left[\frac{EI}{2Da} - \frac{1}{4}\right] \qquad (4.18)$$

4.3.4 Deflection Equation

The two uncoupled equations 4.17 and 4.18 are to be solved for A_n and C_n in an open form, each set yielding a finite number (say N) of simultaneous linear equations, each equation having all unknowns A_1 to A_N and C_1 to C_N. Thus, there will be 2N equations each having 2N unknowns to be evaluated. It may be noted here that it is not possible to eliminate any of the A_n or C_n summation constant from Equations 4.17 and 4.18 . This is because these constants appear both inside and outside of the summation terms as indicated by A_i and A_n and C_i and C_n. This is contrary to Equations 4.7 and 4.10 which can be coupled in Equation 4.12 . The value of N to be selected depends on the convergence of the A_n and C_n series and their effects on the deflection function w. It is observed that the function is not affected at all because of A_5 and C_5, both of them being of the order of 10^{-10}. The computer print-out given in Appendix C shows that even A_3 and C_3 are of very small magnitude (of the order of 10^{-6} and 10^{-7} respectively). Nevertheless, these values are generated in the computer making the deflection function w and its derivatives reliable enough for the further computations shown in the following sections.

4.3.5 Bending Moment at the Center of Slab

The analytical expression for bending moment at the center of the slab can be written as:

$$\left[M_x\right]_{0,0} = \left[M_y\right]_{0,0} = D\left[\frac{\partial^2 w}{\partial y^2} + \mu\frac{\partial^2 w}{\partial x^2}\right]_{0,0}$$

After taking the appropriate derivatives of w and substituting x=0, y=0, the expression becomes:

$$\left[M_x\right]_{0,0} = \left[M_y\right]_{0,0}$$

$$= -\frac{q}{16}a^2(1+\mu) + D(1+\mu)\sum_{n=1,3} C_n \frac{2n\pi}{a} \tag{4.19}$$

4.3.6 Torque Distribution Along Edge Beams

By using the boundary condition given by Equation 4.14, the required torque distribution may be written as:

$$-\left[M_x\right]_{x=\frac{a}{2}} = -D\left[\frac{\partial^2 w}{\partial x^2} + \mu\frac{\partial^2 w}{\partial y^2}\right]_{x=\frac{a}{2}} \tag{4.20}$$

$$\frac{\partial^2 w}{\partial x^2} + \mu \frac{\partial^2 w}{\partial y^2}$$

$$= \frac{q}{768D} (192x^2 - 48a^2)$$

$$+ \sum A_n \left[(\frac{n\pi}{a})^2 \cosh \frac{n\pi x}{a} \cos \frac{n\pi y}{a} - (\frac{n\pi}{a})^2 \cosh \frac{n\pi y}{a} \cos \frac{n\pi x}{a} \right]$$

$$+ \sum C_n \left\{ -y(\frac{n\pi}{a})^2 \sinh \frac{n\pi y}{a} \cos \frac{n\pi x}{a} \right.$$

$$\left. + \cos \frac{n\pi y}{a} \left[\frac{2n\pi}{a} \cosh \frac{n\pi x}{a} + x(\frac{n\pi}{a})^2 \sinh \frac{n\pi x}{a} \right] \right\}$$

$$+ \frac{\mu q}{768D} (192y^2 - 48a^2)$$

$$+ \mu \sum C_n \left\{ -x (\frac{n\pi}{a})^2 \sinh \frac{n\pi x}{a} \cos \frac{n\pi y}{a} \right.$$

$$\left. + \cos \frac{n\pi x}{a} \left[\frac{2n\pi}{a} \cosh \frac{n\pi y}{a} + y(\frac{n\pi}{a})^2 \sinh \frac{n\pi y}{a} \right] \right\}$$

$$+ \mu \sum A_n \left[- (\frac{n\pi}{a})^2 \cosh \frac{n\pi x}{a} \cos \frac{n\pi y}{a} + (\frac{n\pi}{a})^2 \cosh \frac{n\pi y}{a} \cos \frac{n\pi x}{a} \right]$$

Therefore the expression for the torque distribution becomes:

$$- \frac{\mu q}{768} (192y^2 - 48a^2) - D \sum C_n \frac{a}{2} (\frac{n\pi}{a})^2 \sinh \frac{n\pi}{2} \cos \frac{n\pi y}{a} (1 - \mu)$$

$$- D \sum A_n (\frac{n\pi}{a})^2 \cosh \frac{n\pi}{2} \cos \frac{n\pi y}{2} (1 - \mu) - D \sum C_n \cos \frac{n\pi y}{a} (\frac{2n\pi}{a} \cosh \frac{n\pi}{2})$$

Writing $\mu q(192y^2 - 48a^2)/(768D)$ in a Fourier series, the required expression for torque distribution along the edge beams will be:

$$- \frac{2\mu q a^2}{3D} \sum (-1)^{\frac{n+1}{2}} \frac{1}{n^3} \cos \frac{n\pi y}{a} - D \sum A_n (\frac{n\pi}{a})^2 \cosh \frac{n\pi}{2} \cos \frac{n\pi y}{2} (1 - \mu)$$

$$- D \sum C_n \cos \frac{n\pi y}{a} \left[\frac{a}{2} (\frac{n\pi}{a})^2 (1 - \mu) \sinh \frac{n\pi}{2} + \frac{2n}{a} \cosh \frac{n\pi}{2} \right]$$

This is an expression of torque (say lb-ft/ft) transmitted to the edge beam at any section y. If this expression is written as

$t = f(\cos \frac{n\pi y}{a})$, then the torque (say lb-ft) 'T' resisted by any section y is given by

$$T = \int_0^y t \, dy = \int_0^y f(\cos \frac{n\pi y}{a}) \, dy$$

4.3.7 Torsional Rotation of Edge Beams

The angle of rotation of any cross section of an edge beam can be written as $-(\partial w/\partial y)$. The right-hand-screw rule is used for the sign of the angle. By differentiating the deflection function of Equation 4.2 , the rotation is given by:

$$\begin{aligned} -\frac{\partial w}{\partial y} = & -\frac{q}{768D}\left[64y^3 - 48a^2 y\right] \\ & - \sum_{n\,odd} A_n \left[\frac{n\pi}{a} \sinh \frac{n\pi y}{a} \cos \frac{n\pi x}{a} - \frac{n\pi}{a} \cosh \frac{n\pi x}{a} \sin \frac{n\pi y}{a}\right] \\ & - \sum_{n\,odd} C_n \left[\sinh \frac{n\pi y}{a} \cos \frac{n\pi x}{a} + y \frac{n\pi}{a} \cosh \frac{n\pi y}{a} \cos \frac{n\pi x}{a} \right. \\ & \left. - x \sinh \frac{n\pi x}{a} \left(\frac{n\pi}{a}\right) \sin \frac{n\pi x}{a}\right] \end{aligned} \tag{4.21}$$

The expression for the torsional rotation of the beam central section becomes:

$$\begin{aligned} -\left[\frac{\partial w}{\partial y}\right]_{x=0,\, y=-\frac{a}{2}} = & \frac{qa^3}{48D} - \sum_{n\,odd} A_n \left[\frac{n\pi}{a} \sinh \frac{n\pi}{2} - \frac{n\pi}{a} \sin \frac{n\pi}{2}\right] \\ & - \sum_{n\,odd} C_n \left[\sinh \frac{n\pi}{2} + \frac{n\pi}{2} \cosh \frac{n\pi}{2}\right] \end{aligned} \tag{4.22}$$

4.3.8 Computer Program

A general computer program based on this theoretical work is written and incorporated in Appendix C. The program is capable of analyzing an almost unlimited number of different structures, each having an unlimited number of load stages, for all the five possible edge conditions, in one compilation only. The compilation time of the program is 3.92 seconds, while the execution time is 0.24 second per structure per load stage. The computer prints out slab central deflections, bending moments and all the necessary data to be used for evaluating any set of generalized forces and displacements involved in the system. For example, the summation constants A_n and C_n printed out by the computer are used to compute torsional rotations of the beam central section as shown in Appendix D. As discussed earlier, Equations 4.7 and 4.10 can be coupled in Equation 4.12 but Equations 4.17 and 4.18 must be solved in the uncoupled open form of 2N equations each having 2N unknowns. So, the uncoupling effect involved in this computer work is accounted for by using an uncoupling correction factor which is also printed out by the computer.

The elastic constants of the material, bending stiffness of the slab, bending and the torsional stiffness of the edge beams, load stage and the experimental value of deflection are the variables to be supplied to the computer. All these variables are in kip and foot units except the torsional stiffness and the experimental deflection value which are in kip and inch units. In place of the experimental value of deflection one may use the values obtained by formulas given in Reference (37) for the edge conditions (i), (iv) and (v). Any arbitrary deflection may be used in the absence of experimental and formula values so as to complete the execution of the program, otherwise, the computer will give an error message for missing data. Various uses of this computer program are illustrated while comparing theoretical and experimental results.

4.3.9 Accuracy of the Theoretical and Computer Work

Considering the complex nature of the calculation procedure and also of the subsequent computer programming, various checks and counter-checks were used at different stages of the work. Formulas of bending moments and deflections given in Reference (37) served this purpose very effectively. Also, the experimental values of deflections and torsional rotations were compared to the corresponding theoretical values as shown in the next chapter. The graph comparing the values of the slab central bending moments as obtained by the computer program and also by the formulas is given in Figure 4.2. In the computer print-out shown in Appendix C, analyses numbered 1 and 2 are for free edges (EI/aD = 0, TS = 0), those numbered 3 and 4 for elastic supports without torsion (EI/aD = 3.0 , TS = 0), those numbered 5 and 6 for simple supports (EI/aD = 99999---, TS = 0) and those numbered 7 and 8 for fixed edges (EI/aD = 99999---, TS = 99999---). Excellent correlation is

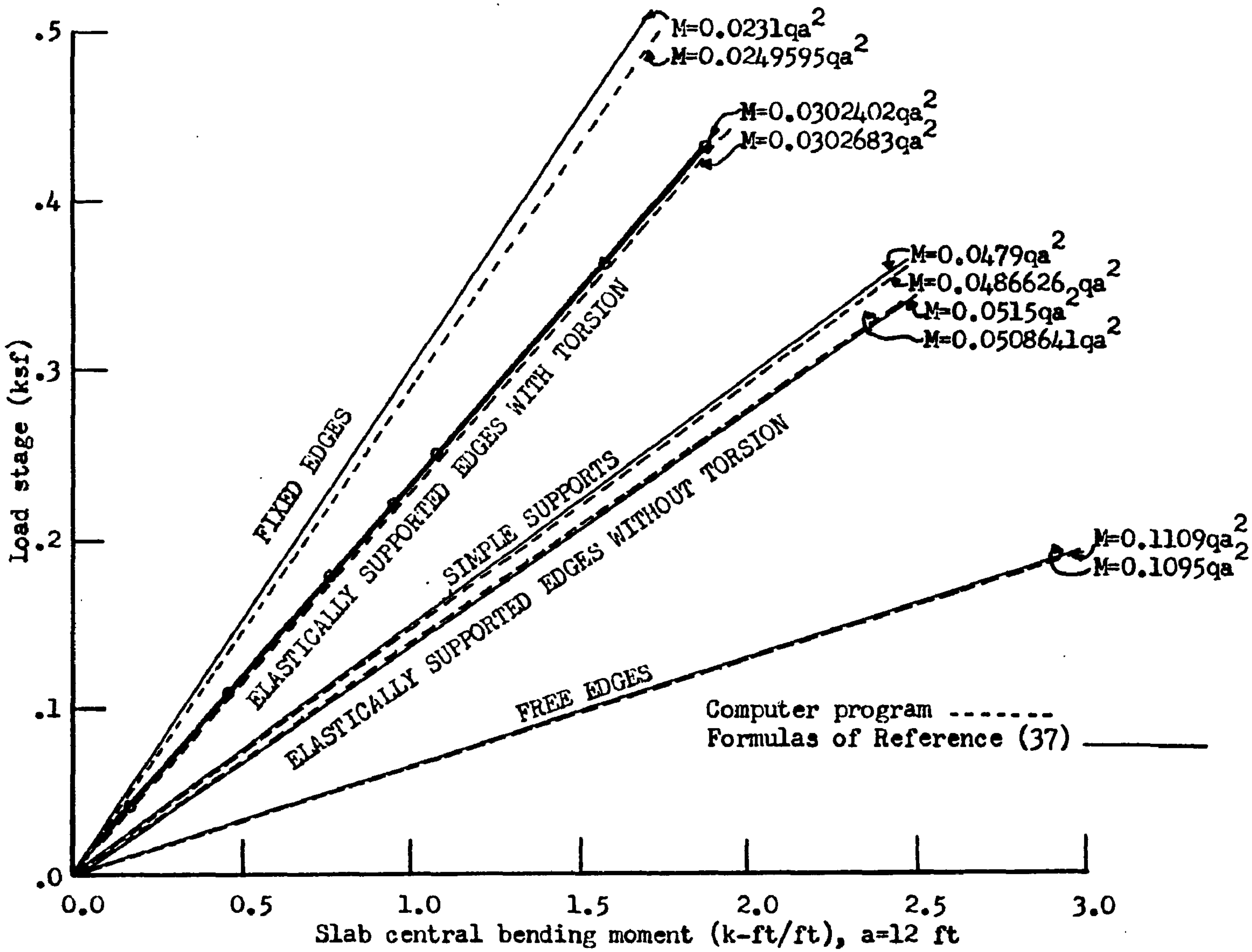

Figure 4.2 Comparison of the current computer program and the formulas of Reference (37)

observed between the values obtained by the computer program and the corresponding values given by the formulas from Timoshenko, et.al.[37] as shown in Appendix C. Some difficulty experience in the case of fixed edges because of the two infinite values involved and the slow convergence of the A_n and C_n series. Nevertheless, the particular integrals and complimentary functions obtained by the program check within 2 percent of the corresponding formula values, indicating the accuracy of the theoretical derivation even for the fixed edge condition.

The over-all algebraic check used for this theoretical work runs into several pages and need not be repeated here. The idea behind this check is to use c = 0 in Equations 4.17 and 4.18 then to couple them in one equation (by eliminating A_n) to see that the final coupled equation is the same as Equation 4.12 . Thus, after establishing the reliability of this theoretical and computer work, it was used to correlate the experimental data, as shown in the next chapter.

4.4 Cracking Loads for Doubly Symmetric Panels

4.4.1 Flexural Cracking of the Slab

The serviceability of a structure is of prime importance to the engineer and requirements such as deflection and crack control must be met regardless of whether the ultimate strength or the working stress design is employed. The flexural cracking load of the slab can be calculated with the help of 1971 ACI Code (9.5.2.2) and the computer program given in Appendix C. The required procedure is to calculate the cracking moment M_{cr} by $M_{cr} = z f_r$, then to run the computer program for different load intensities which can be done in one compilation only. The computer will print the load stages and the corresponding slab central bending moments and then select that load stage as a cracking load, at which the printed moment is the same as M_{cr}.

For example, consider a normal weight concrete structure similar to model specimen 1. Taking a unit strip at the center of the slab, the section modulus z per foot is $z = bh^2/6 = 12 \times 1^2/6 = 2 \text{ in}^3$ per ft of slab. $f_r = 7.5\sqrt{f'_c} = 7.5\sqrt{4242} = 488$ psi.

$$
\begin{aligned}
M_{cr} &= 488 \times 2 \text{ lb-in per ft} \\
&= 488 \times 2/12000 \text{ k-ft/ft} \\
&= 0.08133 \text{ k-ft/ft}
\end{aligned}
\tag{4.23}
$$

By the computer print-out of Analysis Numbers 54 and 55, the load at which this $M_{cr} = 0.08133$ k-ft/ft occurs is obtained by linear interpolation between the values of the two solutions;

For the Analysis Number 54: $M = 0.0800668$ k-ft/ft
$q = 0.290$ k/ft^2

For the Analysis Number 55: $M = 0.0924910$ k-ft/ft
$q = 0.335$ k/ft^2

By linear interpolation:

$$q_{cr} = 0.290 + (0.335 - 0.290)\ \frac{0.08133 - 0.0800668}{0.0924910 - 0.0800668}$$

$$= 0.29447 \quad k/ft^2$$

$$= 294.47 \text{ say } \underline{295} \quad lb/ft^2$$

Micro-concrete models tend to exhibit higher cracking strength [9]. The experimentally observed cracking load was approximately 330 lb/ft^2. This ten percent increase in the observed value may be attributed to several facts, e.g. (a) the formula for f_r is empirical, (b) the first crack was observed with the naked eye with the possibility of skipping the earlier and true load intensities and (c) the calculated cracking load is for the central section of the slab and it may take some extra load for the crack to propagate long enough so as to make itself visible. Nevertheless, this procedure for calculating flexural cracking load of the slab appears satisfactory for all practical purposes.

4.4.2 Formula for Flexural Cracking of Edge Beam

Torsional stiffness and EI/aD ratio are the two important factors governing the behavior of a doubly symmetric structure of slab terminating in edge beams. Magnitudes of these two factors may vary considerably and it is difficult to come up with a general formula for a flexural cracking load unless reasonably conservative values are assumed for shear forces, torques and bending moments. Using this approach it is possible to develop formulas for the flexural cracking load and the permissible load for the combined torsion and shear requirement of the edge beams. The following is the derivation for the flexural cracking load of the slab.

Total load 'W' on the slab = qa^2. Vertical reaction 'V_B' at each end of the beam = (w/8) + (R/2), where R is a reactive force per column which is $0.065qa^2$ or $qa^2/16$ for design purposes.

$$V_B = \frac{W}{8} + \frac{W}{32} = \frac{5W}{32} \tag{4.23.A}$$

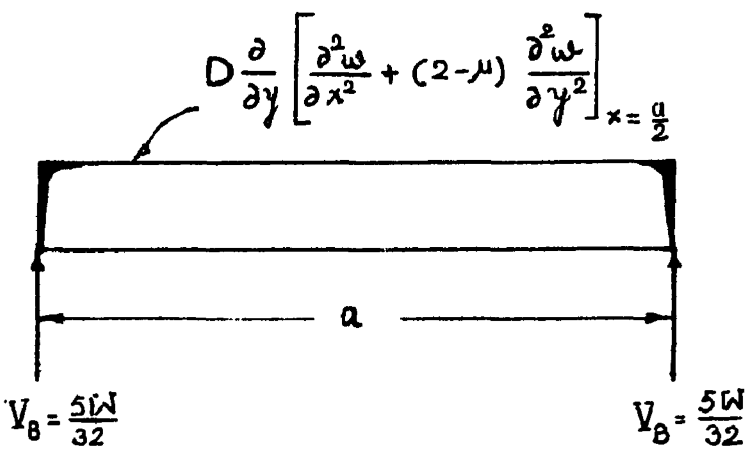

Figure 4.3 Vertical load transmitted to edge beam

As shown in Figure 4.3, the vertical shear transmitted to the edge beam by the slab is a curve consisting of the harmonic terms of the cosine series and can be approximated by a rectangle because of the large magnitude of a/h ratio. Therefore, the load intensity on the edge beam is $(\frac{5W}{32} \times \frac{2}{a}) = 5W/16a$ per unit length. (Wood [39] has recommended W/3a as the probable load intensity). Therefore the negative moment developed at the column faces

$$= \frac{5W}{16a} \frac{a^2}{12} = \frac{5Wa}{192} \qquad (4.23.B)$$

On the basis of the ACI Building Code the modulus of rupture 'f_r' of concrete = $7.5\sqrt{f'_c}$

$$\frac{5Wa}{192} = (7.5\sqrt{f'_c})(\frac{bd_o^2}{6})$$

Using $W = q_{cr}a^2$,

$$q_{cr} = \frac{7.5 \times 192}{5 \times 6} \frac{bd_o^2\sqrt{f'_c}}{a^3}$$

$$= \frac{48bd_o^2\sqrt{f'_c}}{a^3} \qquad (4.24)$$

4.4.3 Formula for Combined Shear and Torsion Edge Beam Requirements

The bending moment along the edge of the slab is transmitted to the beam as a distributed torque. This torque distribution consists of harmonic cosine terms (see the theoretical analysis), with a maximum value at the center, and zero at the columns. The maximum value is absolutely maximum at $0.0513qa^2$ when the slab edges are fixed ($TS = \infty$, $EI = \infty$). Therefore, the maximum torque at any section of the beam is always less than:

$$T = \int_o^{a/2} M_y dx = \int_o^{a/2} \sum_{m=1,3} (-1)^{\frac{m-1}{2}} E_m \cos \frac{m\pi x}{a} \; dx$$

$$= \sum_{m=1,3} (-1)^{\frac{m-1}{2}} \frac{Ema}{m\pi} \left[\sin \frac{m\pi}{2} \right]$$

$$= \frac{a}{\pi} \left[E_1 + \frac{E_3}{3} + \frac{E_5}{5} + \frac{E_7}{7} \right]$$

$$= \frac{4}{\pi^4} qa^3 \left[0.3722 - 0.0126 - 0.0036 - 0.0012 \right]$$

$$= 0.01456 \; qa^3 \tag{4.25}$$

Thus the maximum possible torque (occurring at the column faces) is $T = 0.01456 \; qa^3$. Considering a circular interaction between torsion and shear, their combined requirement may be expressed as:

$$\left(\frac{V_u}{V_c}\right)^2 + \left(\frac{V_{tu}}{V_{tc}}\right)^2 \leqslant 1 \tag{4.26}$$

where V_u = nominal total design shear stress

$$= \frac{V_u}{\varnothing bd} = \frac{5W}{32\phi bd} = \frac{5qa^2}{32\phi bd} \tag{4.27}$$

V_{tu} = nominal total design torsional stress

$= \dfrac{KT_u}{\varnothing \Sigma x^2 y}$ by ACI Code (1).

Taking K = 3 according to the ACI Code and using $T = 0.01456qa^3$,

$$v_{tu} = \frac{3 \times 0.01456qa^3}{\phi \Sigma x^2 y}$$

$$v_{tu} = \frac{0.04368qa^3}{\phi \Sigma x^2 y} \tag{4.28}$$

Substituting for v_u and v_{tu} in Equation 4.26 and after simplification, the expression for q becomes:

$$q \leqslant \frac{1}{a^2 \left[\left(\frac{5}{32\phi b d v_c}\right)^2 + \left(\frac{0.04368a}{\phi \Sigma x^2 y v_{tc}}\right)^2 \right]^{\frac{1}{2}}}$$

Using $x = b$, $b < d_o$,

$y = d_o$ the overall depth of beam,

$v_c \cong 2\sqrt{f'_c}$ as a conservative value

$v_{tc} = 6.25\sqrt{f'_c}$ for uniformly distributed torque along the beam length, in the limit q becomes:

$$q = \frac{1}{a^2 \left[\left(\frac{5}{32\phi b d 2\sqrt{f'_c}}\right)^2 + \left(\frac{0.04368a}{\phi b^2 d_o 6.25\sqrt{f'_c}}\right)^2 \right]^{\frac{1}{2}}}$$

replacing d by $0.85d_o$, the final expression for q can be written as:

$$q = \frac{100\ b^2 d_o}{a^2 \sqrt{84.48b^2 + 0.4884a^2}} \qquad (4.29)$$

When the total load intensity (including live and dead loads) on the slab is less than the above q value, combined torsion and shear requirement expressed in Inequality 4.26 will be satisfied.

4.4.4 Design Formulas for Edge Beam

Using the derived Equations 4.24 and 4.29 and required safety factors, general expressions for width and depth of the edge beams can be developed.

Let f_{sf} = Factor of safety against flexural cracking

f_{sts} = Factor of safety against the combined effect of the torsion and shear interaction.

By Equation 4.24 -

$$q = \frac{48bd_o^2}{f_{sf}a^3} \tag{4.30}$$

and by Equation 4.29 -

$$q = \frac{100\phi b^2 d_o \sqrt{f'_c}}{f_{sts}a^2 \sqrt{84.48b^2 + 0.4884a^2}} \tag{4.31}$$

Using $\phi = 0.85$, Equations 4.30 and 4.31 yield:

$$d_o = \frac{85abf_{sf}}{48f_{sts}\sqrt{84.48b^2 + 0.4884a^2}}$$

Substituting this value in Equation 4.30 the expression for b^3 can be written as

$$b^3 = C_2 + C_1 b^2 \tag{4.32}$$

$$\text{where } C_2 = \frac{qf_{sts}^2 a^3}{308.2f_{sf}\sqrt{f'_c}} \tag{4.33}$$

$$C_1 = \frac{aqf_{sts}^2}{1.782f_{sf}\sqrt{f'_c}} \tag{4.34}$$

The slab transmits the load to the edge beam through the clear span (a_c). Also, the design section is at the end of the clear span. Therefore, the use of clear span 'a_c' in place of 'a' is justified. In order to calculate the b and d_o parameters for the edge beams, the final procedure becomes:

(i) Calculate b by $b^3 = c_2 + c_1 b^2$

$$\text{where} \quad c_2 = \frac{q f_{sts}^2 a_c^3}{308.2 f_{sf} \sqrt{f_c'}} \tag{4.35}$$

$$c_1 = \frac{a_c q f_{sts}^2}{1.782 f_{sf} \sqrt{f_c'}} \tag{4.36}$$

As a first trial use $b = (C_2)^{\frac{1}{3}}$

(ii) Use the exact value of b (satisfying $b^3 = C_2 + C_1 b^2$), in the following equation and get d_o

$$d_o = \left[\frac{q f_{sf} a_c^3}{48 b \sqrt{f_c'}}\right]^{\frac{1}{2}} \tag{4.37}$$

Two examples will be solved to illustrate this procedure.

Example 1:

Data: $a_c = 240"$ $q = 1.55$ psi $f_c' = 3600$ psi

$f_{sf} = f_{sts} = 1$

Required: b and d_o

Solution:

By Equation (4.35) $C_2 = \dfrac{1.55(240)^3}{308.2 \times 60} = 1160$

By Equation (4.36) $C_1 = \dfrac{240 \times 1.55}{1.782 \times 60} = 3.48$

First trial: $b = (C_2)^{\frac{1}{3}} = 10.9$, try $b = 11.0$ in.

$b^2 = 121 \qquad b^3 = 1331$

R.H.S. of $(b^3 = C_2 + C_1 b^2)$ is $1160 + 3.48 \times 121 = 1581 > 1331$

Second trial: $b = 11.8$, $b^2 = 139.5$, $b^3 = 1648$

R.H.S. $= 1160 + 3.48 \times 139.5 = 1645 \approx 1648$ ok.

By Equation 4.37, $d_o = \left[\dfrac{1.55 \times 240^3}{48 \times 11.8 \times 60}\right]^{\frac{1}{2}} = 25.1$

Use edge beams 11.8 in. wide and 25.1 in. deep. Kemp and Wilhelm have used 12 x 24 inch edge beams for the same data [21]. If 11.8 is rounded to 12 for practical use, d_o will be slightly less than 25.1 by Equation 4.37 and may be taken as 24.

Example 2:

Data: Same as above except $f_{sf} = 1.1$, $f_{sts} = 0.9$

Required: b and d_o

Solution: By Equation 4.35, $C_2 = \dfrac{1.55 \times .81 \times 240^3}{308.2 \times 1.1 \times 60} = 852$

By Equation 4.36, $C_1 = \dfrac{240 \times 1.55 \times 0.81}{1.782 \times 1.1 \times 60} = 2.561$

First trial: $b = (C_2)^{\frac{1}{3}} = 9.48$, try $b = 10$ in., $b^2 = 100$, $b^3 = 1000$

R.H.S. of $(b^3 = C_2 + C_1 b^2)$ is $852 + 2.561 \times 100 = 1108.1 > 1000$

Second trial: $b = 10.47$, $b^2 = 109.5$, $b^3 = 1145$

R.H.S. $= 852 + 2.561 \times 109.5 = 1133 > 1145$

Third trial: $b = 10.41$, $b^2 = 108.5$, $b^3 = 1131$

$$\text{R.H.S.} = 852 + 2.561 \times 108.5 = 1130 \approx 1131 \quad \text{ok.}$$

$$\text{By Equation } 4.37\text{ , } d_o = \left[\frac{1.55 \times 1.1 \times 240^3}{48 \times 10.41 \times 60}\right]^{\frac{1}{2}} = 28.0$$

Use edge beams 10.41 in. wide and 28 in. deep. In the given data $f_{sts} < 1$ and $f_{sf} > 1$. This is a condition in which torsional hinges are formed but the beam is strong in flexure. Such a structure may be used by research workers studying torsional behavior of spandrel beams. For a wider range of loads in which torsional hinges are formed but the flexural cracking does not occur, one may use a higher value of f_{sf} but lower value of f_{sts}. For example, if $f_{sf} = 1.2$ and $f_{sts} = 0.8$ then the corresponding b and d_o values will be 9.15 in. and 31.2 in. respectively.

4.5 Yield Line Analysis

The failure mode of a system consisting of a rectangular slab terminating in edge beams can be explained by (1) Conventional Yield Line Theory in which failure is caused by the formation of positive and negative yield lines in the slab, (2) Modified Yield Line Theory given by Kemp and Wilhelm [21] in which failure occurs as a result of the formation of positive yield lines in the slab and torsional hinges in the edge beams, (3) combined mode of failure in which positive yield lines are formed in the slab, torsional hinges in only one pair of the two opposite edge beams and two negative yield lines along the edges parallel to the remaining pair of edge beams.

4.5.1 Conventional Yield Line Theory

Equilibrium equation based on this failure mode can be written as

$$m = \frac{q\alpha^2 L^2}{6\gamma_{34}^2}\left\{\sqrt{3 + \left(\frac{\alpha\gamma_{12}}{\gamma_{34}}\right)^2} + \frac{\alpha\gamma_{12}\sqrt{\mu}}{\gamma_{34}}\right\}^2 \tag{4.38}$$

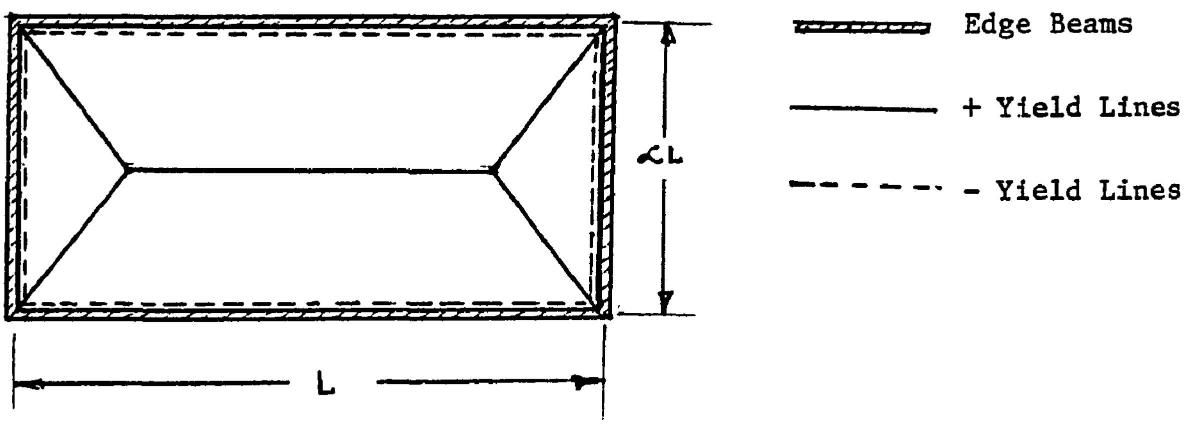

Figure 4.4 Conventional mode of failure

Derivation of Equation 4.38 is given in Reference (19).

4.5.2 Modified Yield Line Theory

Kemp and Wilhelm have given the details of this theory in Reference (21). According to their discussion, the total load carrying capacity of the beam-slab system results from the torque carrying capacity of the beams and the ultimate moment capacity of the isotropic slab along the path of positive yield lines. The equilibrium equation balancing actuating and resisting moments can be written for each edge separately, leading to a general expression for ultimate load based on this Modified Yield Line Theory.

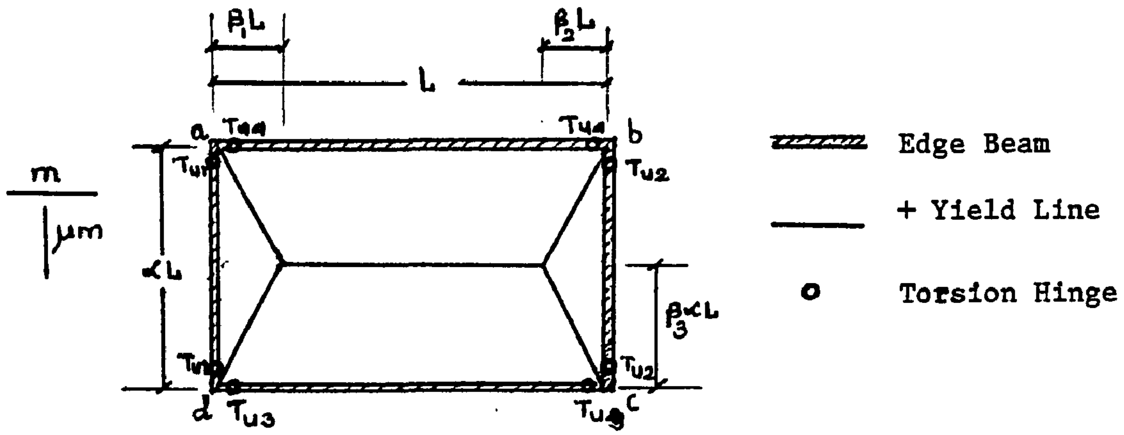

Figure 4.5 Failure mode based on Modified Yield Line Theory

Let the ultimate torque carrying capacities of the four beams be given by:

$T_{u1} = \mu m \alpha L j_1$ of beam ad

$T_{u2} = \mu m \alpha L j_2$ of beam bc

$T_{u3} = mLj_3$ of beam dc

$T_{u4} = mLj_4$ of beam ab $\quad$ (4.39)

Moment equilibrium equations for the edges are as follows:

Edge ad: $\mu m \alpha L(1 + 2j_1) = \frac{1}{6} q \alpha L \times \beta_1^2 L^2$

$$\mu m(1 + 2j_1) = \frac{1}{6} q \beta_1^2 L^2 \qquad (4.40)$$

Edge bc: $\mu m(1 + 2j_2) = \frac{1}{6} q \beta_2^2 L^2$ $\quad$ (4.41)

Edge dc: $mL(1 + 2j_3) = q\left[\frac{1}{2}\beta_3^2\alpha^2L^2(1 - \beta_1 - \beta_2) + \frac{1}{6}\beta_3^2\alpha^2L^2(\beta_1 + \beta_2)\right]$

$$\therefore m(1 + 2j_3) = \frac{1}{6}q\alpha^2\beta_3^2L^2\left[3 - 2(\beta_1 + \beta_2)\right] \tag{4.42}$$

Edge ab: $m(1 + 2j_4) = \frac{1}{6}q\alpha^2(1 - \beta_3)^2L^2\left[3 - 2(\beta_1 + \beta_2)\right]$ (4.43)

Eliminating unknown parameters $\beta_1, \beta_2, \beta_3, \beta_4$ and using

$$\lambda_{34} = \sqrt{1 + 2j_3} + \sqrt{1 + 2j_4} \tag{4.44}$$

$$\lambda_{12} = \sqrt{1 + 2j_1} + \sqrt{1 + 2j_2} \tag{4.45}$$

equation containing ultimate load can be simplified to

$$m = \frac{q\alpha^2L^2}{6\lambda_{34}^2}\left\{\sqrt{3 + \mu\left(\frac{\alpha\lambda_{12}}{\lambda_{34}}\right)^2} - \frac{\alpha\lambda_{12}\sqrt{\mu}}{34}\right\}^2 \tag{4.46}$$

For a square slab:

$$\alpha = 1,\ \mu = 1,\ T_{u1} = T_{u2} = T_{u3} = T_{u4} = T_u = mLj_3$$

$j_3 = T_u/(mL) = C$ a new constant.

$\lambda_{12} = \lambda_{34}$ by symmetry,

by Equation 4.46 , $m = \frac{qL^2}{6\lambda_{34}^2}\left\{\sqrt{3 + 1} - 1\right\}^2 = \frac{qL^2}{6\lambda_{34}^2}$

$$q = \frac{6m\lambda_{34}^2}{L^2} \tag{4.47}$$

$\lambda_{34} = 2\sqrt{1 + 2j_3}$ $\qquad$ $\lambda_{34}^2 = 4(1 + 2j_3)$

$= 4(1 + 2C)$

This value of λ_{34}^2 in Equation 4.7

$$q = \frac{24m(1 + 2C)}{L^2} \tag{4.48}$$

Equation 4.48 is the same as the one derived by Kemp and Wilhelm by using the Energy Approach and a particular design condition $T_u = T_c$.

4.5.3 Combined Mode of Failure

The slab-spandrel structure may fail according to the Conventional Yield Line Theory, the Modified Yield Line Theory or the combination of these modes depending on the magnitudes of the various design parameters. In the combined mode of failure any two opposite edges may fail because of the development of torsional hinges in the beams and the remaining two because of the negative yield lines in the slab. In general, any edge under consideration will fail because of the presence of torsional hinges and not because of the occurrence of negative yield lines, if

$$mi > \frac{2T_u}{L} \tag{4.49}$$

Writing $T_u = K\ T_c = K \frac{1}{3} (b^2 d_o)\ 5 \sqrt{f'_c}$, the condition for formation of torsional hinges becomes:

$$mi > \frac{10 b^2 d_o K \sqrt{f'_c}}{3L} \tag{4.50}$$

The appropriate value of K based on the designed reinforcement in the beam can be used in Inequality 4.50 . If any two opposite edges satisfy this inequality and the remaining two do not, a combined failure mode occurs; A general equation may be written as

$$m = \frac{q \alpha^2 L^2}{6 \epsilon_{34}^2} \left\{ \sqrt{3 + \left(\frac{\alpha \epsilon_{12}}{\epsilon_{34}}\right)^2} - \frac{\alpha \epsilon_{12} \sqrt{\mu}}{\epsilon_{34}} \right\}^2 \tag{4.51}$$

where
$$\left.\begin{aligned}\epsilon_{12} &= \nu_{12}\\ \epsilon_{34} &= \nu_{34}\end{aligned}\right\}\text{ if } mi < (10b^2 d_o K \sqrt{f'_c}\,/3L)$$

$$\left.\begin{aligned}\epsilon_{12} &= \lambda_{12}\\ \epsilon_{34} &= \lambda_{34}\end{aligned}\right\}\text{ if } mi \geqslant (10b^2 d_o K \sqrt{f'_c}\,/3L)$$

Example:

Data: Doubly symmetric slab of clear span 57 inches

$f'_c = 3900$ psi, $b = d_o = 3$ inches,

$mi = 334$ lb-in/in, $K = 1$

Required: Failure mode of the structure. solution:

$$(10b^2 d_o K \sqrt{f'_c}\,/3L) = 10 \times 9 \times 3 \times 1 \times \;\; 3900/(3 \times 57)$$
$$= 98.5 \text{ lb-in/in}$$
$$< 334 \text{ lb-in/in}$$

Inequality 4.50 is satisfied and the structure will fail according to the Modified Yield Line Theory. These data are for the "University of Illinois Slab" analyzed by Kemp and Wilhelm [20]. They also reached the same conclusion that the slab must have failed by a combination of positive yield lines in the slab and torsional hinges in the edge beams.

4.5.4 Analysis of Test Specimens

Yield Line patterns for the three micro-concrete models were observed and traced carefully during the testing process. Model specimen 1 was identical to prototype specimen 2 whose detailed analysis is given in Reference (33) and will not be repeated here. The model specimens 2 and 3 were found to fail by the combination of positive and negative yield lines in the slabs, as expected from the general condition $mi < (10b^2 d_o K \sqrt{f'_c}/3L)$. Therefore, Equation 4.38 will be used to analyze these specimens.

$\alpha = 0.5$ for specimen 2

$\alpha = 0.667$ for specimen 3

For both the specimens: $i_1 = i_2 = i_3 = i_4 = 1$

$\mu = 1$, $m = 146.5$ lb-in/in

$\gamma_{12} = \sqrt{1 + i_1} + \sqrt{1 + i_2} = 2.828$

$\gamma_{12} = \gamma_{34}$, $\gamma_{34}^2 = 8$

Substituting these values in Equation 4.38 and solving for q:

q = 12.850 psi = 1850 psf for specimen 2,

q = 8.749 psi = 1260 psf for specimen 3.

These calculated values are shown on the graphs of load stage vs. deformation (Figures 3.12 thru 3.16). The experimentally observed ultimate loads were 25 to 30 percent higher than the corresponding calculated values because of the presence of considerable extra membrane effect usually associated with such type of failure in which the beams do not yield [(19)].

5. COMPARISON OF THEORETICAL AND EXPERIMENTAL RESULTS

5.1 Introduction

A general elastic theory of doubly symmetric flat plates and slabs developed as a part of this research program is applied to the prototype [33] and the model slabs tested at West Virginia University. The study indicates that the theoretical analysis accurately predicts the elastic behavior of both the model and the prototype structures. By using dimensional analysis, appropriate multipliers are developed to convert the model variables of the homologous points to the corresponding prototype values. The latter quantities termed as the 'model prediction values' are compared to the prototype test results, thus establishing the reliability of the modeling technique. The comparison also serves to check fabrication accuracy and dependability of the instrumentation. The computer print-outs of the analysis of these various structures at all the load stages are given in Appendices C and D. The print-outs also help to compare the theoretical and experimental values at the particular integral and complimentary function levels of the deflection function of Equation 4.2 .

5.2 Dimensional Analysis

The dimensionless multipliers to predict the prototype variables corresponding to those of the model and vice versa are derived by using dimensional analysis. Equation 4.2 of the deflection function indicates that 'w' can be expressed dimensionally as:

$$[w] = \left[\frac{qa^4}{D}\right]$$

$$\frac{w_p}{w_m} = \left(\frac{qa^4}{D}\right)_p / \left(\frac{qa^4}{D}\right)_m$$

But $[D] = [Eh^3] = [Ea^3]$

$$\frac{w_p}{w_m} = \frac{q_p}{q_m}\ \frac{a_p}{a_m}\ \frac{E_m}{E_p} \tag{5.1}$$

The ratio of slope at any section in the prototype to the slope at the homologous section in the model is given by Equation 4.22 which shows:

$$[\theta] = \left[\frac{qa^3}{D}\right]$$

$$\frac{\theta_p}{\theta_m} = \left(\frac{qa^3}{D}\right)_p / \left(\frac{qa^3}{D}\right)_m$$

But $[D] = [Eh^3] = [Ea^3]$

$$\frac{\theta_p}{\theta_m} = \frac{q_p}{q_m} = \frac{E_m}{E_p} \tag{5.2}$$

Equation 4.19 is used to find the moment ratio of the prototype and the model at any homologous point. By that equation, moment per unit length can be dimensionally expressed as:

$$[M] = [qa^2]$$

$$\frac{M_p}{M_m} = \frac{(qa^2)_p}{(qa^2)_m}$$

$$= \frac{q_p}{q_m}\left(\frac{a_p}{a_m}\right)^2 \tag{5.3}$$

These equations completely check with those given by Elstner [12].

Equation 4.17 is used to obtain a dimensionless multiplier to convert the torsional stiffness of the edge beam of the model to the corresponding value of the prototype and vice versa. In order that Equation 4.17 is to be dimensionally correct, the following dimensional identity should be satisfied.

$$\left[\frac{\cancel{r}qa^2}{D}\right] = \left[C_i \frac{C}{Da^2}\right]$$

C_i is dimensionless as observed from the deflection function of Equation 4.2 .

$$[qa^2] = [c/a^2] \qquad \therefore \; [c] = [qa^4]$$

When $q_p = q_m$, $\frac{C_p}{C_m} = (\frac{a_p}{a_m})^4$ (5.4)

It may be noted that Equation 5.4A given by Chander, Kemp and Wilhelm [8] will lead to the same results when $(f_c)_p = (f_c)_m$, which is generally true in model testing.

Equations 5.1 , 5.2 and 5.3 will be used to compute the dimensionless multipliers for a scale ratio 1:4 and the load intensity q_p equals to the load intensity q_m. Thus, $\frac{a_p}{a_m} = 4.0$, $q_p = q_m$, $E_p = 3.68 \times 10^6$, $E_m = 2.60 \times 10^6$. Therefore by Equation 5.1

$$\frac{w_p}{w_m} = 4 \times \frac{2.6 \times 10^6}{3.68 \times 10^6} = 2.8260$$

In the same way, by Equation 5.2 :

$$\frac{\theta_p}{\theta_m} = \frac{2.60 \times 10^6}{3.68 \times 10^6} = 0.7065$$

In the same way, by Equation 5.3 :

$$\frac{M_p}{M_m} = 4^2 = 16$$

As a further check (in addition to the one of Reference (11)), to this dimensional analysis work, the model variables were obtained by using expressions of I, D, C, etc.

$$I = \frac{1}{12}bd^3, \; D = \frac{Eh^3}{12(1 - \nu^2)}$$

$$C = 9925b^3df_c'^{\,0.5}(1 - 0.7691\,\frac{b}{d} + 0.2030\,\frac{b^2}{d^2}) \qquad (5.4A)$$

These variables were employed in the computer program to calculate the slab central deflections and bending moments at different load intensities of Analysis Numbers[1] 43 thru 54. The deflections and bending moments printed out by the computer are summarized in Table 5.1, which verifies the constants 2.8260 and 16.0000 derived earlier. It may however be noted that in these computations Poisson's ratio for the prototype is 0.16 whereas for the model it is 0.17. This small difference has caused a slight deviation in the deflection and the moment ratios from 2.8260 and 16.0000 respectively, which may be observed from Table 5.1.

5.3 Slab Central Deflections

5.3.1 Theoretical, Prototype Specimen 2 and Model Prediction Values

The computer program based on the general elastic theory of flat plates and slabs is given in Appendix C. This program is used

1 These Analysis Numbers are corresponding to those printed out by the computer during the execution of the program of Appendix C.

Table 5.1 Summary of computer analysis of model specimen 1

Computer Analysis Number	Applied Load (k/ft^2)	Deflection w_m (in)	Moment M_m (k-ft/ft)
43	0.030	0.0052816	-0.0082828
44	0.050	0.0088026	-0.0138046
45	0.070	0.0123237	-0.0193264
46	0.090	0.0158447	-0.0248482
47	0.110	0.0193657	-0.0303699
48	0.130	0.0228872	-0.0358919
49	0.150	0.0264082	-0.0414137
50	0.170	0.0299292	-0.0469356
51	0.190	0.0334501	-0.0524572
52	0.210	0.0369712	-0.0579790
53	0.245	0.0431329	-0.0676422
54	0.290	0.0510558	-0.0800668

to analyze the prototype specimen 2. The Analysis Numbers 9 thru 34 of the computer print-out show all the important steps followed during the execution of each load intensity. The twenty-five stages for which the structure is analyzed are those observed in the prototype testing [33]. The graph of theoretical central deflection versus load intensity is a straight line (Figure 5.1) as expected from the elastic theory. In the same figure the graph of experimentally observed slab central deflection versus load stage is plotted to the same scale. The modulus of elasticity for concrete given by the 1971 ACI Code is used in the computer program. The model prediction values given in Table 3.6 are also plotted in Figure 5.1 which shows that the elastic theory, prototype testing and the model predictions give the same slab central deflections in the elastic limit.

5.2.2 Theoretical and Model Test Results

The data obtained by means of the dimensional analysis work and the direct formulas of the slab bending rigidity, the beam bending and torsional rigidity, etc. are supplied to the computer to analyze model specimen 1. These theoretical results are summarized in Table 5.2. Test results are also incorporated in the same table for direct comparison. The study shows a close agreement between the theoretical and the corresponding experimentally observed values in the elastic zone of model specimen 1. These experimentally observed values when multiplied by 2.826 can predict the prototype

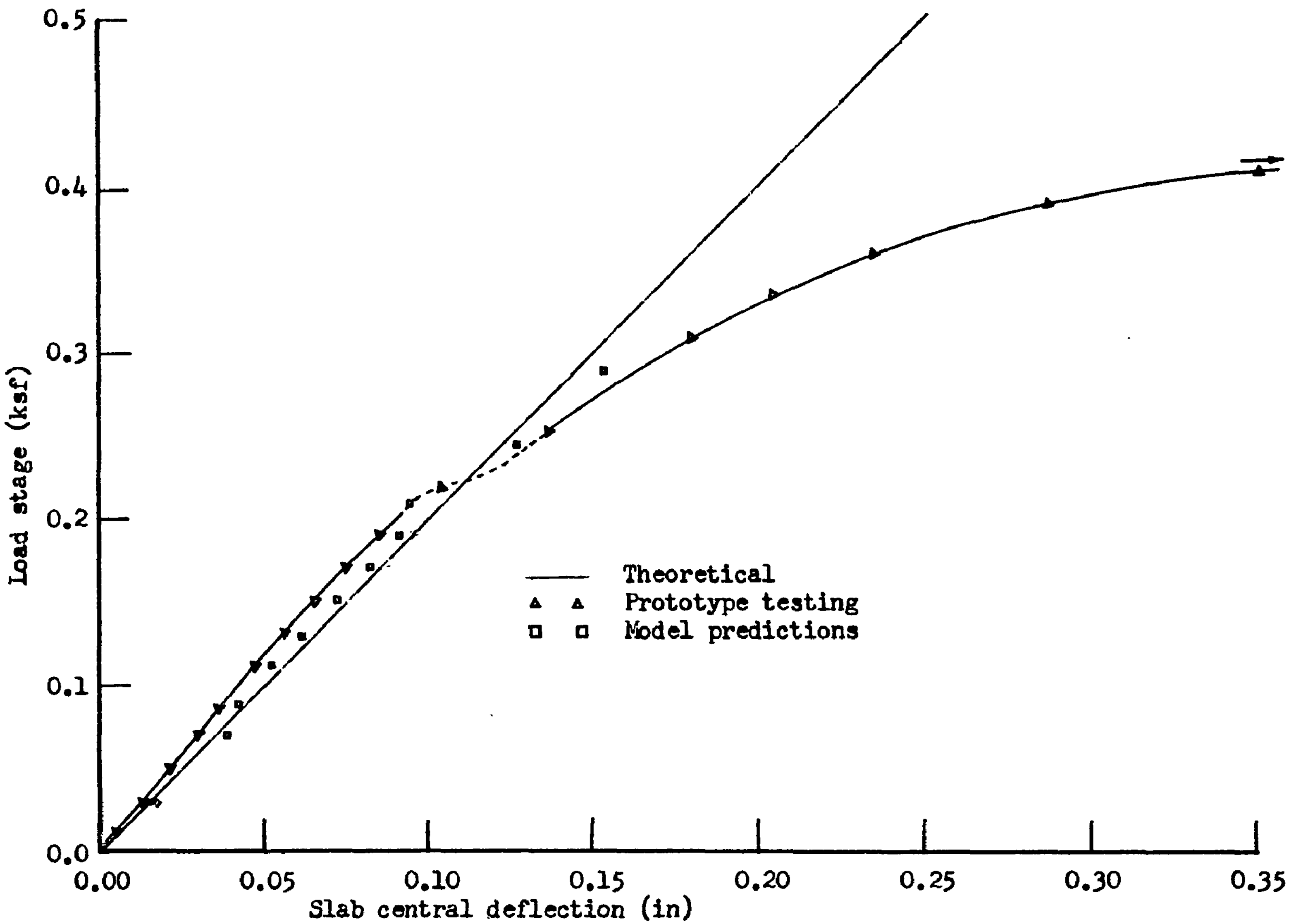

Figure 5.1 Comparison of slab central deflection values of prototype specimen 2

Table 5.2 Comparison of theoretical and observed results of model specimen 1

Computer Analysis No.	Applied Load (k/ft^2)	Theoretical Deflection (in)	Experimental Deflection (in)	$\frac{\text{Theo } \omega}{\text{Exp } \omega}$
43	0.030	0.0052816	0.0055	0.96
44	0.050	0.0088026	0.0090	0.98
45	0.070	0.0123237	0.0140	0.88
46	0.090	0.0158447	0.0155	1.02
47	0.110	0.0193567	0.0190	1.02
48	0.130	0.0228872	0.0220	1.04
49	0.150	0.0264082	0.0260	1.02
50	0.170	0.0299292	0.0290	1.03
51	0.190	0.0334501	0.0320	1.02
52	0.210	0.0369712	0.0335	1.10
53	0.245	0.0431329	0.0455	0.95
54	0.290	0.0510558	0.0540	0.95

deflections with reasonable accuracy as illustrated in Figure 5.1.

5.3.3 Theoretical and Prototype Specimen 3

The elastic and sectional constants of prototype specimen 3 are supplied to the computer. The results of the analysis as printed by the computer are given in Appendix C (Analysis Numbers 35 thru 42). The eight load stages for which the structure is analyzed are those observed in the laboratory test whose results are given in the print-out of Appendix C. These experimentally observed and theoretically calculated values of the slab central deflections are plotted in Figure 5.2. The small difference in the slopes of the elastic straight line portions may be attributed to the fact that the modulus of elasticity of concrete used in the theoretical analysis is derived from the empirical formula of the 1971 ACI Code. Nevertheless, the agreement between these theoretical and experimentally observed values are satisfactory for all practical purposes.

5.4 Beam Central Torsional Rotation

5.4.1 Theoretical, Semitheoretical[2], Prototype and Model Prediction Values

Equation 4.22 gives a general expression for the torsional rotation of the edge beam central section. The equation is employed

---

2 Significance of the term 'semitheoretical value' and the detail procedure to compute it, are given in the subsequent pages of this report.

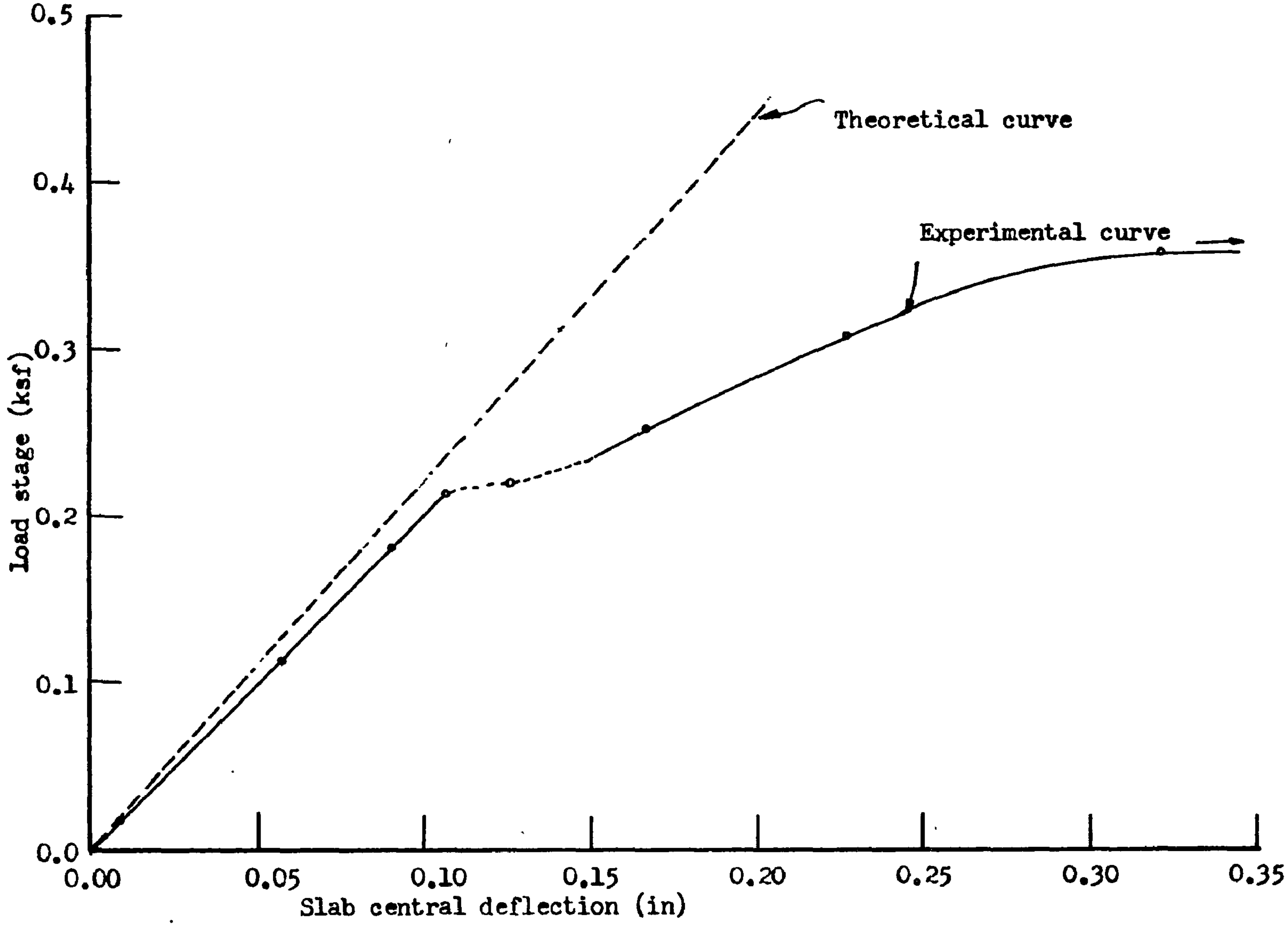

Figure 5.2 Comparison of slab central deflection values of prototype specimen 3

to compute both the theoretical and the semitheoretical values of the rotational angle. The summation constants A_n and C_n printed during the execution of the general computer program of Appendix C are used in Equation 4.22 to obtain the theoretical values. The graph between these values and their corresponding load stages is a straight line (Figure 5.3) as expected from the elastic theory. The print-outs of Appendix C clearly show the characteristic of rapid convergence of both A_n and C_n series. Therefore, the terms upto A_3 and C_3 only are used to calculate the theoretical rotations. These terms are approximately of the order of 10^{-7}. The higher order terms are smaller than 10^{-10} and are conveniently neglected.

As in the case of theoretical values, the semitheoretical ones also involve computerization of Equation 4.22 which is carried out in the subprogram of Appendix D. The summation constants A_n and C_n of Equation 4.22 are those corresponding to the experimentally observed slab central deflections. This technique of calculating the semitheoretical values of any generalized force and displacement may be summarized as follows:

(i) Compute the theoretical values of the constants A_1, A_3--------, C_1, C_3 ------------, etc. and find theoretical ΣA_n as

$$A_n = A_1 + A_3 + \text{-----------}, \text{ etc.}$$

(In the computer program this ΣA_n is denoted by 'TSUMAN', the abbreviation of 'Theoretical Sum of A_n').

(ii) Calculate experimental value of ΣA_n (denoted by 'ESUMAN') given by the equation:

$$w_{expt} = \frac{qa^4}{76.8D} + 2 \quad \sum A_n \tag{5.5}$$

where w_{expt} is the experimentally observed central deflection at the load stage q.

(iii) Calculate the factor 'FT' by:

$$FT = \text{Experimental} \quad \sum A_n/\text{Theoretical} \quad \sum A_n \tag{5.6}$$

(iv) Multiply A_1, A_3 -------- and C_1, C_3 ---------, etc. by 'FT' of step (iii) and get the new quantities called the 'semitheoretical summation constants', A_1', A_3' ---------- and C_1', C_3' ---------, etc.

(v) These semitheoretical constants A_1', A_3' --------- and C_1', C_3' -------, etc. of step (iv) are used in the expressions of any generalized forces and displacements to calculate their 'semitheoretical values'.

As illustrated in Figure 5.3 and also in the computer program of Appendix D, this technique of computing the semitheoretical values is found to be successful not only in the elastic zone but also in the inelastic portion of the load versus deformation curve. It may be noted here that the elastic and related constants (such as μ, E, D, etc.) and also the sectional constants (e.g. area, moment of inertia, section modulus, etc.) used in the expressions of generalized forces and displacements are the same for both the elastic and inelastic zones. Inspite of this apparent limitation the technique is capable of calculating the nonelastic values also because Equation 5.6 of factor 'FT' takes into account this change in the sectional and elastic properties by automatically adjusting the numerator

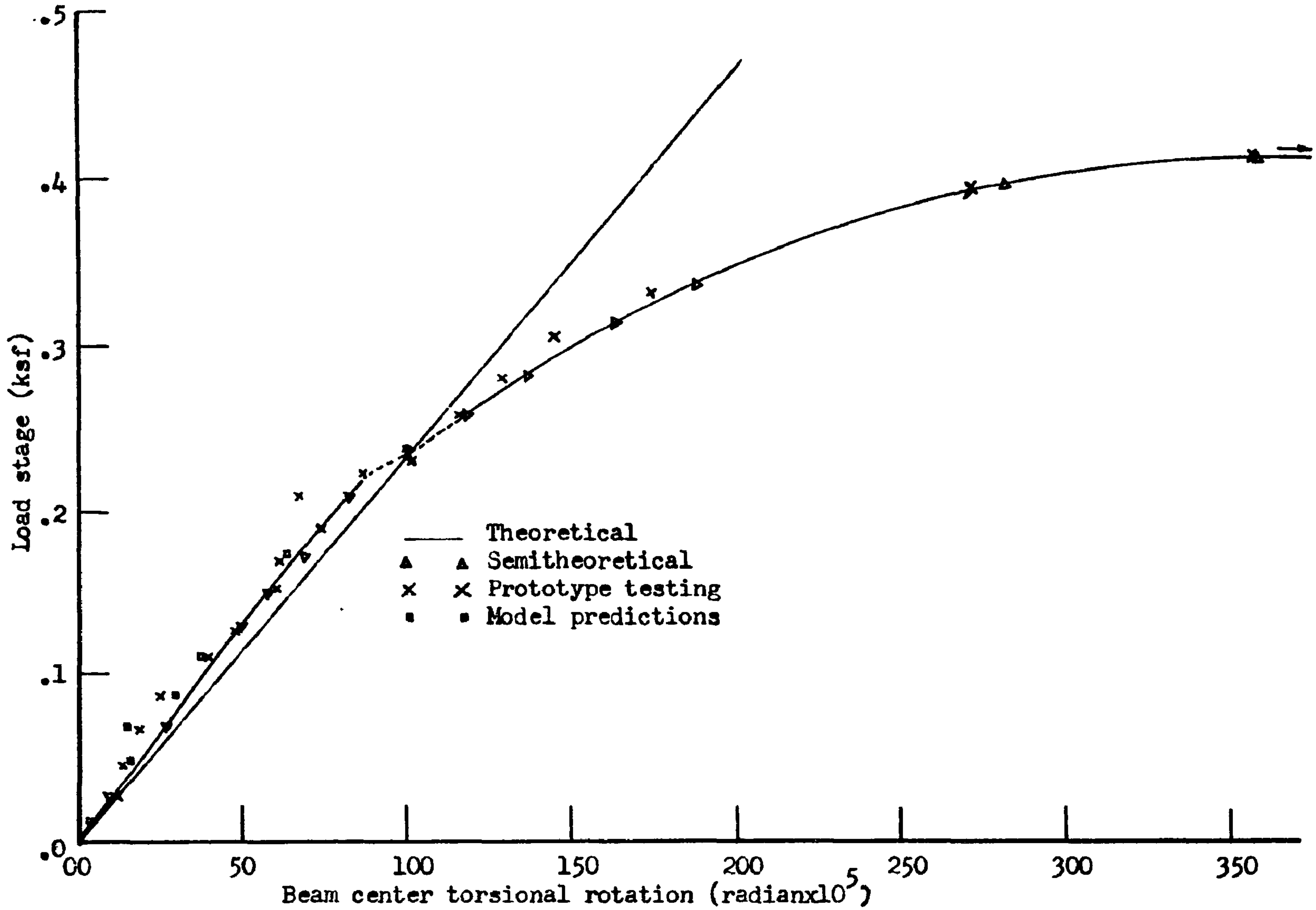

Figure 5.3 Comparison of beam center torsional rotations

(Experimental ΣA_n). This is an introductory work of the technique with one example of its success. Further research is clearly needed in this area.

The experimentally observed beam central torsional rotation in prototype specimen 2 of Appendix D and the model prediction values of Table 3.6 are also plotted in Figure 5.3. The study indicates a reasonable correlation between the theoretical, semitheoretical, prototype observed and the model prediction values of the torsional rotation of the spandrel beam.

6. DESIGN PROCEDURE BASED ON THE EXACT ELASTIC SOLUTION AND THE MODIFIED YIELD LINE THEORY

6.1 Design Procedure

This investigation leads to a new procedure for designing slab-spandrel floor systems. Accordingly, the serviceability requirements of the structure are satisfied by using the "exact" elastic solution developed in Chapter 4, which enables the designer to calculate immediate elastic deflections and also to proportion the slab and the spandrel beams so as to obtain the desired factor of safety against flexural cracking of the slab and also against the flexural, torsion and shear cracking of the edge member. Reinforcement in the structure can be very conveniently and economically designed by using the Ultimate Strength Design given by the Modified Yield Line Theory for which the required formulas are derived in Chapter 4. The Ultimate Design Load for the slab may be obtained by using the load factors given in the ACI Building Code or any other suitable code. To start with, any rectangular area can be converted to a suitable number of square panels. Further design procedure is summarized in the following steps.

1. Problem Statement: To design a single square panel supported by spandrel beams and corner columns.

   Given: Dimensions of the columns, center distance (a or L) between the columns, compressive strength of the concrete (f'_c), factor of safety against flexural cracking (f_{sf}), factor of safety against the combined torsion and shear interaction effect (f_{sts}), service live load intensity on the slab (q_L), load factors for dead and live loads.

2. <u>Proportioning the Slab</u>: Assume a slab thickness (h) which will be checked after proportioning the spandrel beams. Deflection control requirements of the ACI Building Code or any other suitable code can give the first trial thickness of the slab. Calculate clear span a_c = a - column width, calculate dead load q_D and the total service load $q = q_L + q_D$.

3. <u>Proportioning the Spandrel Beam</u>: Obtain width (b) of the beam by Equation 4.32 , and the overall depth (d_o) of the beam by Equation 4.37 .

4. <u>To Check for the Permissible Deflection (w_{code}) and Cracking Strength (M_{code})</u>: Calculate w_{code} = a/360 in, $M_{code} = f_r z$ where 'f_r' is the rupture modulus of concrete and 'z' is the section modulus of the slab central section. Find w_{actual} and M_{actual} by the computer program of Appendix C. If the program is not available use:

$w_{actual} = 0.0034qa^4/D$, $M_{actual} = 0.032qa^2$

(These are the approximate values of deflection and bending moment based on the elastic theory).

See that: $w_{actual} < w_{code}$

$$M_{actual} < (M_{code}/f_{sf}),$$

if not, use a higher value of slab thickness and repeat steps 1 thru 4.

5. <u>To Design the Reinforcement</u>:

(i) Positive reinforcement in the slab is designed for the moment m, given by the Modified Yield Line formula of Equation 48 ,

$$q_u = \frac{24m(1 + 2c)}{L^2}$$

where q_u is obtained by using suitable load factors given in the ACI Building Code or any other code.

(ii) Negative reinforcement in the slab is designed for the moment 'mi', which will give simultaneous formation of torsional hinges in the beam and negative yield lines around the periphery for the maximum utilization of the reinforcement,

$$mi = \frac{10b^2 d_o K \sqrt{f'_c}}{3L} \quad \text{from Equation 4.50}$$

(iii) The torsional steel in the edge beam is designed for

$$T_u = KT_c = K\,\frac{1}{3}(b^2 d_o)5\sqrt{f'_c}$$

It should be noted that this equation is based upon the ACI Building Code (ACI 318-71) and Commentary [1,2]. Here, T_c represents the cracking torque and not the vertical axis intercept on the torque-reinforcement factor curve [21].

(iv) The flexural steel in the beam is designed for $M_u = \frac{5q_u a^3}{192}$ (Equation 4.23.B.). Suitable load factors can be used in computing the value of q_u.

(v) The shear reinforcement in the beam is designed for the shear force (V_B) given by Equation 4.23.A, $V_B = 5q_u a^2/32$. If the spandrel beam is supporting the load of the on-coming wall, proper provision should be made in calculating q_u of Equations 4.23.A and 4.23.B.

Thus, the magnitudes of torque and flexural shear of the spandrel beam are known, from which shear and torsional stresses can be computed. Then, the torsion and flexural shear steel can be proportioned accordingly by using the ACI Code [1], as shown in the following design example.

6.2 Design Example

1. Problem Statement: Design a single square panel supported by spandrel beams and corner columns 12 in. square and 12 ft. on centers.

Given: f'_c = 4151 psi, factor of safety against flexural cracking (f_{sf}) = factor of safety against the combined torsion and shear interaction effect (f_{sts}) = 1.1 an arbitrary value

Live load intensity on the slab, q_L = 150 psf.

Load factors 1.4 and 1.7 for the dead and live loads respectively.

2. Proportioning the Slab: Assume slab thickness $h = 4''$. The minimum permissible thickness by the ACI Building Code [1] (Section 9.5.3.1) is 3-1/2 in.

Clear span $a_c = 12 - 1 = 11$ ft. $= 132$ in.

Dead load of the slab $q_D = 144 \times 4/12 \approx 50$ psf

Total service load $q = q_L + q_D = 150 + 50 = 200$ psf $= 1.39$ psi

3. Proportioning the Spandrel Beam: Width of the beam is given by Equation (4.32) $b^3 = c_2 + c_1 b^2$

$$c_2 = \frac{q f_{sts}^2 a_c^3}{308.2 f_{sf} \sqrt{f_c'}} = \frac{1.39 \times 1.1^2 \times 132^3}{1.782 \times 1.1 \times \sqrt{4151}} = 177.101$$

$$c_1 = \frac{a_c q f_{sts}^2}{1.782 f_{sf} \sqrt{f_c'}} = \frac{132 \times 1.39 \times 1.1^2}{1.782 \times 1.1 \times \sqrt{4151}} = 1.758$$

First trial: $b = (c_2)^{\frac{1}{3}} = (177.101)^{\frac{1}{3}} = 5.6147$ in.

try $b = 5.8''$, $b^2 = 33.64$, $b^3 = 195.11$

R.H.S. of ($b^3 = c_2 + c_1 b^2$) is $177.101 + 1.758 \times 33.64 = 236.2 > 195.11$

Second trial: $b = 6.25''$, $b^2 = 39.06$, $b^3 = 244.14$

R.H.S. $= 177.101 + 1.758 \times 39.06 = 245.5 \approx 244.14$

$b = 6.25$ in.

By Equation 4.37 $$d_o = \left[\frac{q \times f_{st} \times a_c^3}{48 \times b \times \sqrt{f_c'}}\right]^{\frac{1}{2}} = \left[\frac{1.29 \times 1.1 \times 132^3}{48 \times 6.25 \times \sqrt{4151}}\right]^{\frac{1}{2}}$$

$= 13.5$ in.

4. <u>To Check for the Permissible Deflection (w_{code}) and Cracking Strength</u> (M_{code}): $w_{code} = a/360 = 144/360$

$\therefore w_{code} = 0.4$ in.

$M_{code} = f_r \times z = (7.5\sqrt{4151})(12 \times 4^2/6)$ lb-in/ft of slab

$= 1.290$ k-ft/ft

$M_{code}/f_{sf} = 1.290/1.1 = 1.172$ k-ft/ft

By the computer program of Appendix C, for $q = 0.2$ k/ft^2,

$w_{actual} = 0.1001$ in.

$M_{actual} = 0.921$ k-ft/ft

If the computer program is not available, using approximate elastic constants:

$w_{actual} = 0.0034\ qa^4/D$, $M_{actual} = 0.032qa^2$, as explained earlier.

In this example, $q = 0.2$, $a = 12.0$, $D = 1675$ (all in kip and ft units).

$w_{actual} = (0.0034 \times 0.2 \times 12^4/1675) \times 12 = 0.101$ in.

$M_{actual} = (0.0032 \times 0.2 \times 144) = 0.0922$ k-ft/ft

$w_{actual} < w_{code}$ and $M_{actual} < (M_{code}/f_{sf})$

Slab thickness 4" is OK. Use spandrel beams of depth 13.5" and width 6.25".

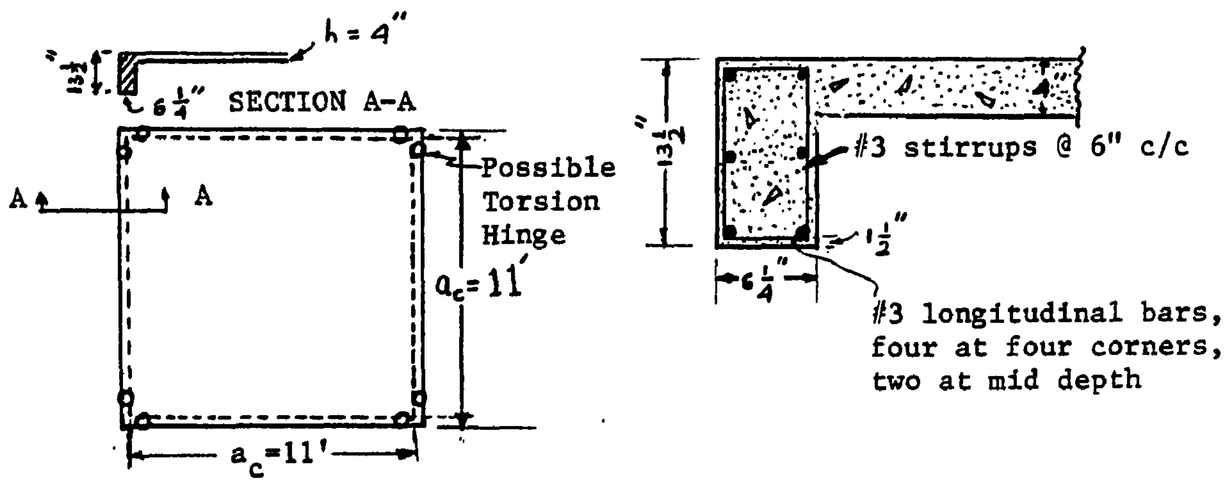

Figure 6.1 Designed sections of the square panel.

5. <u>To Design the Reinforcement:</u>

(i) Positive reinforcement in the slab is designed for the moment 'm', given by the Modified Yield Line formula

$$q_u = \frac{24m(1 + 2c)}{L^2} \quad , \quad c = T_u/mL$$

$$m = \frac{q_u L^2}{24} - \frac{2T_u}{L}$$

$$q_u = 1.4\ q_D + 1.7 q_L = 1.4 \times 50 + 1.7 \times 150 = 330 \text{ psf}$$

$$T_u = KT_c = K\ \frac{1}{3}\ (b^2 d_o)\ 5\sqrt{f_c'}$$

$$= 1 \times \frac{1}{3}\ (6.25 \times 13.5)\ 5\ \sqrt{4151}$$

$$= 56{,}600 \text{ lb-in} = 4717 \text{ lb-ft}$$

$$m = \frac{345 \times 12^2}{24} - \frac{2 \times 4717}{12} = 1284 \text{ lb-ft/ft}$$

$$= 1.284 \text{ k-ft/ft}$$

(ii) Negative reinforcement in the slab is designed for the moment 'mi', which will give simultaneous formation of torsional hinges and the negative yield lines in the beams and the slab respectively.

$$mi = \frac{10 b^2 d_o K \sqrt{f_c'}}{3L}$$

$$= \frac{10 \times 6.25^2 \times 13.5 \times 1 \times \sqrt{4151}}{3 \times 144}$$

$$= 785 \text{ lb-in/in} = 0.785 \text{ k-ft/ft}$$

(iii) Torsional steel in the beam is designed for $T_u = KT_c =$ 56,600 lb-in = 4717 lb-ft, as calculated earlier. Details of longitudinal torsional steel and the web reinforcement for both torsion and shear are given in step (v) ahead.

(iv) Flexural steel in the beam is designed for

$M_u = 5q_u a^3/192 = 5 \times 330 \times (12)^3/192$ lb-ft

$= 14,820$ lb-ft

A standard procedure [20] utilizing $M_u = bd^2 f'_c q(1 - 0.59q)$ etc. is used to calculate area of flexural steel.

(v) Shear reinforcement in the beam is designed for the shear given by Equation 4.23.A.

$V_B = 5q_u a^2/32 = 5 \times 330 \times (12)^2/32$ lb

$= 7500$ lb.

The minimum torsional reinforcement required can be determined from the ACI Tentative Recommendations [20].

$$A_t = \text{web reinforcement} = \frac{125\ xys}{f_y(x_1 + y_1)} \quad \frac{z_u}{V_u + z_u}$$

Let $x_1 = 4.75$ in, $y_1 = 10.5$ in. Calculate the nominal torsional and flexural shear magnitudes of steps (iii) and (v).

$$V_u = \frac{Vu}{bd} = \frac{7500}{6.25 \times 12} \qquad \text{using } d = 13.5 - 1.5 = 12 \text{ in.}$$

$$= 100 \text{ psi} < 2\phi\sqrt{f'_c} = 2 \times 0.85 \times \sqrt{4151} = 109.5 \text{ psi}$$

hence no stirrups are required for flexural shear.

$$z_u = \frac{3T_u}{x^2 y} = 3 \times \frac{56,600}{6.25^2 \times 13.5} = \frac{169800}{39.06 \times 13.5} = 322 \text{ psi}$$

$$\therefore \frac{A_t}{s} = \frac{125 \times 6.25 \times 13.5}{36,000(4.75 + 10.5)} \quad \frac{322}{422} = 0.01465$$

$\therefore A_t = 0.01465 \times 6 = 0.0879$ @ 6 in c/c, use #3 bar closed stirrups.

An equal amount of longitudinal steel must be provided. Again using the Tentative Recommendations:

$$A_L = 2 \times A_t \frac{x_1 + y_1}{s} = 2 \times 0.11(\frac{15.25}{6}) = 0.560 \text{ in}^2$$

use six #3 longitudinal bars, four in the corners and two at mid depth to satisfy both minimum ACI torsional strength requirements and acceptable detailing requirements.

In a similar manner the reinforcement can be designed for the rest of the spandrel beam. The cross section of the spandrel at the column face showing the reinforcement is illustrated in Figure 6.1.

7. TENTATIVE RECOMMENDATIONS FOR THE RECTANGULAR PANELS

7.1 Introduction

The experimental investigation and the theoretical analysis carried out for this research are used for recommending a tentative design procedure for the rectangular panels of the slabs terminating in edge beams. Modified Yield Line Theory can be conveniently used in predicting failure loads and also for the provision of the economic reinforcement in the slab and the edge beams. Difficulty is experienced in proportioning the slab and spandrels for the service load conditions, in the absence of 'exact' elastic solutions of the rectangular panels. This difficulty is overcome by using the procedure of Section 4.4.2 with appropriate modifications. For example, in the absence of the elastic solution, instead of integrating along the cosine curve (Figure 7.1), integration is carried out along a straight line, thereby neglecting the shaded area, during the calculation of maximum torque carried by the spandrel beam.

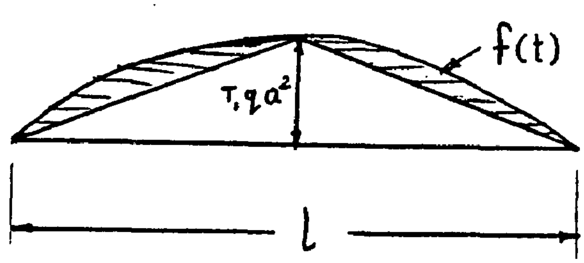

Figure 7.1 Torque distribution on the edge beam

Reduction in the torque value is justified because of the conservative values of T_1 used for $TS = \infty$, $EI = \infty$ (i.e. fixed edge) condition. The torque obtained by the exact integration of the cosine curve (of a square panel) will be checked with the value calculated by integrating along the straight line, thereby establishing the reasonableness of the later procedure.

Wood's recommendations [39] are used for the design load conditions of the edge beams. Formulas for the cracking loads for the edge beams and also for their design widths and depths are derived. Their reasonableness is checked with the width and depth obtained by the more exact formulas of Section 4.4.4.

Based on this theoretical and experimental work, a procedure is originated for the design of the rectangular panels. An illustrative design example is given in Section 7.7.

7.2 Flexural Cracking Loads of the Edge Beams

As explained in Section 7.1, using Wood's recommendation [39]:

$$q_{Beam} = \frac{qa}{2} \quad 1 - \frac{1}{1 + \frac{B}{a} + \frac{B^2}{a^2}}$$

$$\text{using } K_1 = 1 - \frac{1}{1 + \frac{B}{a} + \frac{B^2}{a^2}}$$

$$q_{Beam} = \frac{qaK_1}{2} \tag{7.1}$$

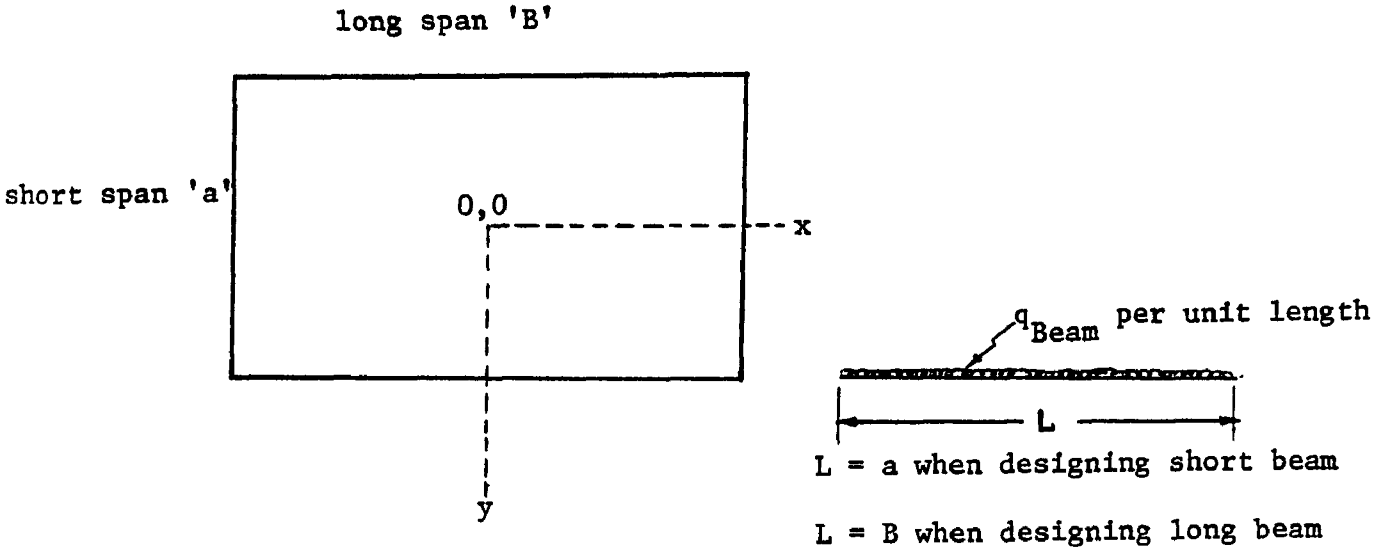

Figure 7.2 Rectangular panel

Negative moment developed at column faces = $q_{Beam}L^2/12$. In a limit of service load stage, this moment is equal to the flexural cracking moment of the edge beam.

$$q_{Beam}L^2/12 = (7.5\sqrt{f'_c})\left(\frac{bd_o^2}{6}\right)$$

$$q_{beam} = 15\sqrt{f'_c}\,\frac{bd_o^2}{L^2} \tag{7.2}$$

From the Equations 7.1 and 7.2 and using q on the slab as q_{cr}, the load intensity on the slab which causes flexural cracking in the edge beam, is given by:

$$q_{cr} = \frac{30bd_o^2\sqrt{f'_c}}{al^2K_1} \tag{7.3}$$

7.3 Formula for Combined Torsion and Shear Edge Beam Requirements

As explained in Section 7.1, the maximum torque to which an edge beam section is subjected, is given by:

$$T = \int_0^{L/2} f(t)'dl'$$

Integrating along the straight line (Figure 7.1)

$$T = T_1 qa^2 L/4 \tag{7.4}$$

This integration along a straight line instead of the cosine curve will give the torque value for the square panel as:

$$T = 0.0513qa^2(a)/4 = 0.0128qa^3$$

The exact calculations (by integrating along the cosine curve) of Section 4.4.3 have shown that:

$$T = 0.01456qa^3$$

This small reduction in T is justified because, the later value ($T = 0.01456qa^3$) is already conservative based on $TS = \infty$, $EI = \infty$.

Using a circular interaction curve, the necessary condition to be satisfied for the combined torsion and shear requirement, is given by:

$$\left(\frac{V_u}{V_c}\right)^2 + \left(\frac{V_{tu}}{V_{tc}}\right)^2 \leq 1 \tag{7.5}$$

$$\text{where } V_u = \frac{Vu}{\phi\, bd} = \frac{q_{Beam}L}{2\phi bd} \tag{7.6}$$

$$V_{tu} = \frac{KT_u}{\phi \Sigma x^2 y}$$

$$= 3 \frac{T_1 qa^2 L}{4} \frac{1}{\phi \Sigma x^2 y}$$

$$= \frac{3T_1 qa^2 L}{4\phi \Sigma x^2 y} \tag{7.7}$$

Substituting $q_{Beam} = \frac{qak_1}{2}$, Equation 7.6 becomes:

$$V_u = \frac{qak_1}{2} \frac{L}{2\phi bd} = \frac{qak_1 L}{4\phi bd}$$

Substituting for V_u and V_{tu} in Equation 7.5 and after simplification, the expression for q becomes:

$$q \leqslant \frac{1}{\left[\left(\frac{aK_1 L}{4\phi bdV_c}\right)^2 + \left(\frac{3T_1 a^2 L}{4\phi \Sigma x^2 y} \frac{1}{V_{tc}}\right)^2 \right]^{\frac{1}{2}}}$$

using $x = b$ $b \leqslant d_o$

$y = d_o$ the overall depth

$V_c = 2\sqrt{f_c'}$ as a conservative value

$V_{tc} = 6.25\sqrt{f_c'}$ for a reason explained in Section 4.4.3

in a limit q is given by:

$$q = \frac{1}{\left[\left(\frac{aK_1 L}{4\phi bd2\sqrt{f_c'}}\right)^2 + \left(\frac{3T_1 a^2 L}{25\ b^2 d_o \sqrt{f_c'}}\right)^2 \right]^{\frac{1}{2}}}$$

replacing d by $0.85d_o$ and after simplification

$$q = \frac{170\ b^2 d_o \phi \sqrt{f_c'}}{aL\sqrt{625K_1^2 b^2 + 416.2T_1^2 a^2}} \tag{7.8}$$

When the total load intensity (including live and dead loads) on the slab is less than the above q value, combined torsion and shear requirement expressed in Inequality 7.5 will be satisfied.
Note that T_1 and L also b and d_o are different for the short and long beams.

7.4 Design Formulas for Serviceability of the Edge Beams

Equations 7.3 and 7.8 will be used to derive the expressions for the widths and depths of both the short and long beams of a rectangular panel. Special consideration is to be given for the desired factor of safety against the flexural cracking and the combined torsion and shear requirement of the edge beams.

let f_{sf} = factor of safety against flexural cracking

f_{sts} = factor of safety against the combined effect of the torsion and shear interaction.

By Equation 7.3

$$q = \frac{30bd_o^2 \sqrt{f_c'}}{f_{sf}aL^2K_1} \tag{7.9}$$

By Equation 7.8

$$q = \frac{170\ b^2 d_o \phi \sqrt{f_c'}}{f_{sts}aL\left[625K_1^2b^2 + 416.2T_1^2a^2\right]^{\frac{1}{2}}} \tag{7.10}$$

Using $\phi = 0.85$, Equations 7.9 and 7.10 yield:

$$d_o = \frac{(170 \times 0.85) b f_{sf} L K_1}{30 f_{sf} \sqrt{625 K_1^2 b^2 + 416.2 T_1^2 a^2}}$$

substituting this value in Equation 7.9 and after simplification,

$$q = \frac{b^3 \sqrt{f_c'}\ f_{sf} K_1 (170 \times 0.85)^2}{30 a f_{sts}^2 (625 K_1^2 b^2 + 416.2 T_1^2 a^2)}$$

$$b^3 = c_2 + c_1 b^2 \tag{7.11}$$

where

$$c_2 = \frac{q f_{sts}^2 a^3 T_1^2}{1.672 K_1 f_{sf} \sqrt{f_c'}}$$

$$c_1 = \frac{a q f_{sts}^2 K_1}{1.114 f_{sf} \sqrt{f_c'}}$$

As explained in Section 4.4.4, use of clear span is justified in calculating b and d_o values. The final procedure becomes:

(i) Calculate b by $b^3 = c_2 + c_1 b^2$

$$\text{where } c_2 = \frac{q f_{sts}^2 a_c^3 T_1^2}{1.672 K_1 f_{sf} \sqrt{f_c'}} \tag{7.12}$$

$$c_1 = \frac{a_c q f_{sts}^2 K_1}{1.114 f_{sf} \sqrt{f_c'}} \tag{7.13}$$

As a first trial, use $b = (c_2)^{\frac{1}{3}}$

(ii) Use the exact value of b (satisfying $b^3 = c_2 + c_1 b^2$), in the following equation and get d_o

$$d_o = \left[\frac{q a_c L_c^2 K_1 f_{sf}}{30b\sqrt{f_c'}}\right]^{\frac{1}{2}} \qquad d_o \geqslant b \tag{7.14}$$

The procedure can be used for any aspect ratio of a rectangular panel. Different values of K_1, T_1 for short beam, T_1 for long beam, etc. corresponding to different aspect ratios, are given in Table 7.1.

To check the reasonableness of this procedure, the example of Section 4.4.4 will be solved by Equations 7.12 thru 7.14 and the b and d_o values thus obtained will be compared to those calculated by the more exact procedure of Section 4.4.4 of square panels.

Example 1:

Data: $a_c = B_c = 240''$ $\quad q = 1.55$ psi

$f_c = 3600$ psi, $\quad f_{sf} = f_{sts} = 1$

Required: b and d_o

Solution:

From Table 7.1, $T_1 = 0.0513$, $K_1 = 0.667$

By Equation 7.12, $c_2 = \dfrac{1.55 \times (240)^3 (0.0513)^2}{1.672 \times 0.667 \times 60} = 841$

By Equation 7.13, $c_1 = \dfrac{240 \times 1.55 \times 0.667}{1.114 \times 60} = 3.71$

First trial: $b = (c_2)^{\frac{1}{3}} = 9.4$,

try $b = 10''$ $\quad b^2 = 100 \quad b^3 = 1000$

R.H.S. of ($b^3 = c_2 + c_1 b^2$) becomes

R.H.S. $= 841 + 3.71 \times 100 = 1212 > 1000$

Table 7.1 Design table for the rectangular panels

B/a	w_{table} = Deflection at the slab center	T_1 for the short beam	T_1 for the long beam	M_{table} = B.M. at the slab center	K_1
1.0	0.00378 qa^4/D	0.0513	0.0513	0.0323 qa^2	0.6667
1.1	0.00450 qa^4/D	0.0581	0.0538	0.0370 qa^2	0.6979
1.2	0.00516 qa^4/D	0.0639	0.0554	0.0419 qa^2	0.7253
1.3	0.00573 qa^4/D	0.0687	0.0563	0.0458 qa^2	0.7494
1.4	0.00621 qa^4/D	0.0726	0.0568	0.0489 qa^2	0.7706
1.5	0.00660 qa^4/D	0.0757	0.0570	0.0515 qa^2	0.7895
1.6	0.00690 qa^4/D	0.0780	0.0571	0.0533 qa^2	0.8062
1.7	0.00714 qa^4/D	0.0799	0.0571	0.0549 qa^2	0.8211
1.8	0.00735 qa^4/D	0.0812	0.0571	0.0561 qa^2	0.8344
1.9	0.00747 qa^4/D	0.0822	0.0571	0.0569 qa^2	0.8464
2.0	0.00762 qa^4/D	0.0829	0.0571	0.0577 qa^2	0.8571
∞	0.0833 qa^4/D	0.0833	0.0571	0.0584 qa^2	1.0000

Second trial: $b = 10.9$, $b^2 = 118.81$, $b^3 = 1295.03$

R.H.S. $= 841 + 3.71 \times 118.81 = 1281 < 1295.03$

By third trial $b = 10.95$ is OK. Using $b = 11''$, d_o by Equation (7.14) is calculated as:

$$d_o = \left[\frac{1.55 \times 240 \times 240^3 \times 0.667}{30 \times 11 \times 60}\right]^{1/2} = (720)^{1/2} = 26.8$$

By Equations 7.12, 7.13, 7.14 $b = 11''$, $d_o = 26.8''$, whereas by the more exact procedure of Section 4.4.4, $b = 11.8''$ $d_o = 25.1''$. Thus, for the design purpose, this procedure of Section 7.4 may be found sufficiently accurate to proportion the spandrel beams of rectangular panels.

7.5 Bending Moment and Deflection Values for Serviceability of the Slab

The detail analytical and experimental work on the square panels (of Chapters 3,4,5 and 6) has shown that for a square panel $(0.032/0.0231) \approx 1.4$ is a suitable factor to obtain a moment at the center of a slab terminating in edge beams. In the same way, the deflection factor is given by $(0.0034/0.00126) \approx 3.0$. Applicability of these factors to the rectangular panels will be checked by the experimental work carried out in this investigation.

Consider model specimen 3, $B = 36$ in, $a = 24$ in, aspect ratio 1:1.5.

Maximum B.M. at the center of the slab

$= (0.0368 \times 1.4)q(24)^2 = 29.7q$ lb-in/in

$= 336.4q$ lb-in/ft.

Cracking moment of the slab of this model specimen

$M_{cr} = (7.5\sqrt{f'_c})(\frac{bd^2}{6}) = 488 \times 2 = 976$ lb-in/ft by Section 4.4.1.

$q = 976/336.4 = 2.91$ lb/in^2

$= 418$ lb/ft$^2 \leq 540$ lb/ft^2 the observed cracking load of the specimen. Therefore the moment constant 1.4 can be safely used.

Consider model specimen 2, B = 36 in, a = 18 in, aspect ratio 2.

Maximum B.M. at the center of the slab

$= (0.0571 \times 1.4)q(18)^2 = 25.92q$ lb-in/in

$= 311.04q$ lb-in/ft

M_{cr} for this specimen is also 976 lb-in/ft

$q = 976/311.04 = 3.122$ lb/in^2

$= 450$ lb/ft$^2 < 1050$ lb/ft^2 the observed cracking load of this model specimen 2.

In the same way the deflection factor '3' is also found very safe, once the cracking loads are in the permissible limit. The experimentally observed slab central deflections (0.018 in for specimen 2 and 0.035 in for specimen 3) corresponding to their designed cracking loads are very much safe as per the ACI Building Code [1] (which states that for the serviceability, deflection $w_{code} \leq a/360$).

Table 7.1 is thus completed by using these deflection and bending moment factors of 3 and 1.4 respectively. T_1 values for the long and short beams, given in the table are the conservative ones based on TS = ∞ , EI = ∞ as explained in Section 7.1 and 7.3. The load factor K_1 is also calculated and incorporated in the same table, for all the aspect ratios.

7.6 Design Procedure for Rectangular Panels

This experimental and theoretical work leads to a new procedure for designing slab-spandrel floor systems. Accordingly, the serviceability requirements of the rectangular panel are satisfied by using the work of Sections 7.1 thru 7.5, which enables the designer to calculate immediate deflections and also to proportion the slab and the edge beams so as to obtain the desired factor of safety against flexural cracking of the slab and also against the flexural, torsion and shear cracking of the edge member. The Ultimate Strength Design given by the Modified Yield Line Theory (for which required formulas are derived in Chapter 4) can be very conveniently and economically used to design the reinforcement. The ultimate load for the slab may be obtained by using the load factors given in the ACI Building Code or any other suitable code. The following steps explain this design procedure.

1. Problem Statement: To design a rectangular panel supported by spandrel beams and corner columns.

   Given: Dimensions of the columns, center to center distances (a and B) between the columns, compressive strength of the concrete (f_c'), factor of safety against flexural cracking (f_{sf}), factor of safety against the combined torsion and shear interaction effect (f_{sts}), Live load intensity on the slab (q_L), Load factors for dead and live loads.

2. Proportioning the Slab: Assume a slab thickness (h) which will be checked after proportioning the spandrel beams. Deflection

control requirements of the ACI Building Code or any other suitable code can give the first trial thickness of the slab. Calculate the clear spans B_c = B - column width, a_c = a - column width and aspect ratio B/a. Calculate dead load q_D and the total service load $q = q_L + q_D$.

3. Proportioning the Spandrel Beams: Obtain width (b) of the beams by Equation 7.11 . Use the appropriate values of T_1 (Table 7.1) and L_c for the short beam and the long beam. They will have different widths. In the same way calculate the depths of the short and long beams by using Equation 7.14 . Use the appropriate K_1 value (from Table 7.1) for the aspect ratio of the slab.

4. To Check for the Permissible Deflection (w_{code}) and Cracking Strength (M_{code}): Calculate w_{code} = a/360 in $M_{code} = f_r z$ where 'f_r' is the rupture modulus of concrete and 'z' is the section modulus of the slab central section. Find w_{table} and M_{table} by using Table 7.1.

   See that: $w_{table} < w_{code}$

   $M_{table} < (M_{code}/f_{sf})$,

   if not, use a higher value of slab thickness and repeat steps 1 thru 4.

5. To Design the Reinforcement:

   (i) Positive reinforcement in the slab is designed for the moment m, given by the Modified Yield Line formula of Equation 4.46

$$m = \frac{q\,{}^2L^2}{6\lambda_{34}^2}\left\{\sqrt{3+\mu\left(\frac{\alpha\lambda_{12}}{\lambda_{34}}\right)^2} - \frac{\alpha\lambda_{12}\sqrt{\mu}}{\lambda_{34}}\right\}^2$$

Appropriate values of ultimate torques of the edge beams should be used in this formula based on the Modified Yield Line Theory.

(ii) Negative reinforcement in the slab is designed for the moment 'mi', which will give simultaneous formation of torsional hinges in the beam and negative yield lines around the periphery for the maximum utilization of the reinforcement,

$$mi = \frac{10b^2 d_o K \sqrt{f'_c}}{3L} \quad \text{from Equation 4.50 .}$$

Calculate 'mi' parallel to the long and also the short beam edges. Use higher value of the two.

(iii) The torsional steel in the edge beam is designed for $T_u = KT_c = K \frac{1}{3} (b^2 d_o) 5\sqrt{f'_c}$. Explanation of this formula is given in Section 6.1.

(iv) The flexural steel in the beam is designed for $M_u = \frac{q_u a K_1 L^2}{24}$ obtained from Section 7.2.

(v) The shear reinforcement in the beam is designed for the shear $V_u = \frac{q_u a K_1 L}{4}$. Obtain 'q_u' of the slab, in above M_u and V_u formulas by using load factors from the ACI or any other suitable code

From these torques, bending moments and shear force values appropriate reinforcement in the beams can be designed, as shown in Section 6.2.

7.7 Design Example

1. Problem Statement: Same as Section 6.2 except that the panel is now rectangular 10 x 13 ft and f'_c = 3600 psi.

2. Proportioning the Slab: Assume slab thickness h = 4".

   Clear spans are a_c = 10 - 1 = 9 ft = 108 in.

   B_c = 13 - 1 = 12 ft = 144 in.

   aspect ratio = 13/10 = 1.3

   Total service load q = 200 psf = 1.39 psi as in Section 6.2.

3. Proportioning the Spandrel Beams: From Table 7.1, for the aspect ratio 1.3, K_1 = 0.749, T_1 = 0.0687 for short beam, T_1 = 0.0563 for long beam

   (i) Width and depth of long beam: L_c = 144 in. Width of the beam is given by Equation (7.11). $b^3 = c_2 + c_1 b^2$

$$c_2 = \frac{q f_{sts}^2 a_c^3 T_1^2}{1.672 K_1 f_{sf} \sqrt{f'_c}} = \frac{1.39 \times 1.1^2 \times (108)^3 \times 0.0563^2}{1.672 \times 0.749 \times 1.1 \times 60} = 811$$

$$c_1 = \frac{a_c q f_{sts}^2 K_1}{1.114 f_{sf} \sqrt{f'_c}} = \frac{108 \times 1.39 \times 1.1^2 \times 0.749}{1.14 \times 1.1 \times 60} = 1.869$$

First trial: $b = (c_2)^{\frac{1}{3}} = (811)^{\frac{1}{3}} = 9.31$ in.

try b = 10" $b^2 = 100$ $b^3 = 1000$

R.H.S. of $(b^3 = c_2 + c_1 b^2)$ is

R.H.S. = 811 + 1.869 x 100 = 998 $\approx$ 1000

$\therefore$ b = 10 in.

By Equation 7.14 , $d_o = \sqrt{\dfrac{qa_c l_c^2 K_1 f_{sf}}{30b\sqrt{f'_c}}}$ $\qquad d_o \geqslant b$

$$= \left[\frac{1.39 \times 108 \times (144)^2 \times 0.749 \times 1.1}{30 \times 10 \times 60}\right]^{\frac{1}{2}}$$

$= 11.92$ in. say 12 in.

Provide long beam 10" wide 12" deep. These dimensions may be revised after step 4.

(ii) Width and depth of short beam: $l_c = 108$ in.

Width of the beam is given by $b^3 = c_2 + c_1 b^2$

$$c_2 = \frac{qf_{sts}^2 \; a_c^3 T_1}{1.672 K_1 f_{sf}\sqrt{f'_c}} = \frac{1.39 \times 1.1^2 \times 108^3 \times (0.0687)^2}{1.672 \times 0.749 \times 1.1 \times 60}$$

$= 1210$

$$c_1 = \frac{a_c q f_{sts}^2 K_1}{1.114 f_{sf}\sqrt{f'_c}} = \frac{108 \times 1.39 \times 1.1^2 \times 0.749}{1.114 \times 1.1 \times 60} = 1.869$$

First trial: $b = (c_2)^{\frac{1}{3}} = (1210)^{\frac{1}{3}} = 10.6$

try $b = 11"$ $\quad b^2 = 121 \quad b^3 = 1331$

R.H.S. of $(b^3 = c_2 + c_1 b^2)$ is

R.H.S. $= 1210 + 1.869 \times 121 = 1436 > 1331$

Second trial: $b = 11.2 \quad b^2 = 125.4 \quad b^3 = 1404.9$

R.H.S. $= 1210 + 1.869 \times 125.4 = 1444 > 1404.9$

By third trial $b = 11.25$ in. is OK.

$$d_o = \left[\frac{q a_c l_c^2 K_1 f_{sf}}{30b\sqrt{f'_c}}\right]^2 , \; d_o \geqslant b$$

$$= \left[\frac{1.39 \times 108 \times 108^2 \times 0.749 \times 1.1}{30 \times 11.25 \times 60}\right]^{\frac{1}{2}}$$

$= 8.44 < 11.25$ Provide $d_o = 11.25$ in.

Provide short beam 11.25 x 11.25 inches. These dimensions may be revised after Step 4.

4. To Check for the Permissible Deflection (w_{code}) and Cracking Strength (M_{code}): $w_{code} = a/360 = \frac{120}{360}$

$\therefore w_{code} = 0.333$ in.

$M_{code} = f_r z = (7.5 \times \sqrt{3600})(12 \times 4^2/6)$ lb-in/ft of slab

$= 1.2$ k-ft/ft of slab

$M_{code}/f_{sf} = 1.2/1.1 = 1.09$ k-ft/ft

$M_{table} = (0.04578) \times 0.2 \times (10)^2$ k-ft/ft

$= 0.915 < 1.09$ OK.

$w_{table} = (0.00573) qa^4/D$

$= (0.00573 \times 0.2 \times (10)^4/1631) \times 12$ in

$= 0.084 < 0.333$ OK.

$M_{table} < (M_{code}/f_{sf})$

$w_{table} < w_{code}$

Slab thickness 4 in. is alright and provide the edge beams of the dimensions calculated above.

The remaining design procedure is similar to the one of Section 6.2 except that, one has to use the formulas for rectangular panels given in Section 7.6.

8. CONCLUSIONS AND RECOMMENDATIONS

8.1 Conclusions

This study of rectangular and square reinforced concrete floor slabs which terminate at edge beams leads to the following conclusions.

1. The span and depth of the short beam, the two fundamental variables in the experimental investigation, greatly influenced the deformation magnitudes (Sections 3.7 and 3.9), cracking loads (Sections 4.4 and 7.5), ultimate loads (Section 4.5.4) and the behavior in general (Section 3.8) of the slab-spandrel structural system. This influence is manifested by means of:

   (a) bending and torsional stiffnesses which govern the deformation magnitudes and cracking loads, (statistical methods can be used to separate the torsional stiffness effects from those of the bending rigidity, as shown in Appendix A);

   (b) ultimate torque which governs the type of failure modes (Sections 4.5.3 and 4.5.4) and the magnitude of ultimate load of the Modified Yield Line Theory (Sections 4.5.2 and 4.5.4).

   The conclusions based on the experimental work are derived from micro-concrete models which simulate the prototype behavior as shown by (i) the statistical analysis (Appendix A) of the experimental data (ii) the graphs of Figures 5.1 and 5.3 comparing experimentally observed and theoretically calculated elastic deformations and (iii) experimental works of many other investigators.

2. The Modified Yield Line Theory of Kemp and Wilhelm [21] is a valuable contribution to the field of concrete technology. The theory explains the failure mode of any geometric shaped (rectangular, square, circular, hexagonal, etc.) slab which terminates in edge beams. This failure mode is a combination of the positive yield lines in the slab and torsional hinges in the edge beams. The present investigation verifies the theory for rectangular slabs. Though the theory is equally applicable for a wide range of non-rectangular slabs, experimental data are lacking to verify it for these cases. Nevertheless, the theory can avoid the pitfall of a false sense of security in the design of reinforced concrete slabs terminating in edge beams. For example, the conventional yield line calculations will end up in a much larger magnitude of ultimate load than the one slab can actually sustain, when a large amount of negative steel is provided in the slab edges but the beams are not string enough against torsion. Also, the design becomes uneconomical because of the excessive amount of steel which does not play any appreciable role once the torsional hinges are formed in the edge beams.

The two inequalities based on Equations 4.50 and 4.31 (or 7.10) indicate when the structure will fail by the formation of torsional hinges in the edge beams (Modified Yield Line Theory) and not by the negative yield lines in the slab (Conventional Yield Line

Theory). This failure mode will occur when:

(i) $mi > 10b^2 d_o K\sqrt{f'_c}\,/(3L)$ of Equation (4.50)

where mi is ultimate yield moment of the slab per unit length parallel to the edge beam, K is the ratio of ultimate to cracking torque (T_u/T_c) for the edge beam and b, d_o and L are width, overall depth and length of the edge beam. This condition ensures the formation of torsional hinges in edge beams prior to the yielding of negative steel in the slab edges.

(ii) The safety factor f_{sts} against the combined effect of torsion and shear interaction is less than 1, i.e.

$$\frac{100\phi b^2 d_o\sqrt{f'_c}}{q a_c^2\sqrt{84.48b^2 + 0.4884a_c^2}} < 1.0 \text{ for square panel, (Equation 4.31)}$$

$$\frac{170\phi b^2 d_o\sqrt{f'_c}}{q a_c l_c\sqrt{625K_1^2 b^2 + 416.2T_1^2 a^2}} < 1.0 \text{ for rectangular panel,}$$

(Equation 7.10)

The slab test at the University of Illinois [21] (for which $mi > 10b^2 d_o K\sqrt{f'_c}\,/(3L)$ as shown in Section 4.5.3 and

$$f_{sts} = \frac{100 \times .85 \times 3^2 \times 3 \times \sqrt{3900} \times 144}{466 \times 56^2\sqrt{84.48 \times 3^2 + 0.4884 \times 56^2}} < 1.0)$$

and also of the present investigation (in which $mi < 10b^2 d_o K\sqrt{f'_c}\,/(3L)$ as stated in Section 4.5.3) provide experimental proof for these inequalities which are based on the concepts of Modified Yield Line Theory of Kemp and Wilhelm [21]. These test results verify that when torsional hinges are formed in the edge beam along with the positive yield lines in the slab, the Modified Yield Line Theory correctly predicts the ultimate loads.

However, when the beams do not yield, large membrane forces are developed resulting in ultimate loads which are much larger than those predicted by the yield line method which is based on a bending mechanism. This is in accordance with Wood's observations [39].

3. For the first time, an elastic theory is developed (Sections 4.3.1 through 4.3.9), which can account for the special boundary conditions imposed by slab edges being monolithic with the spandrel beams of the square panels. These special boundary conditions may be any combination of torsional and bending edge beam stiffnesses, both ranging between zero and infinity including the extremities. Comparison with existing formulas (of simply supported, free, fixed and elastically supported edges) indicate the reasonableness of the theory as shown in the computer print-out of Appendix C and the comparison graphs of Figure 4.2. Also, the theoretical results correlate well with those of the prototype and model tests in the elastic region before cracking occurs. (See Table 5.2, computer print-out of Appendix C and graphs of Figures 5.1, 5.2 and 5.3). Thus, the theory can be reliably used

to calculate elastic deformations and a set of generalized forces of a square panel loaded with uniform density.

4. A detailed study of the existing design methods of slabs which terminate at edge beams has shown that these methods fail to account for the influence of torsional stiffness of edge beams on load carrying capacity of the slab. Also, the important parameters such as elastic deformations of the slab, its flexural cracking load, proportions for the spandrels (to provide an adequate and economical factor of safety against failure caused by flexure and combined torsion and shear interaction), and an - economical and reasonable amount of slab reinforcement are not adequately accounted for in these existing design methods. This state of affairs may result in an unsafe or uneconomical structural design. The theoretical and experimental work of the current investigation helps to overcome these difficulties and leads to a new design procedure. Accordingly, the serviceability requirement of the structure is satisfied by an elastic solution and the formulas based on the theoretical and experimental work of this investigation. The Modified Yield Line Theory of Kemp and Wilhelm [21] is used to calculate ultimate load and to design economic reinforcement of the structural system. This new procedure, to design reinforced concrete floor slabs which terminate in edge beams, is summarized in the following steps, with appropriate references to the equation numbers, tables and sections of this report.

(i) Assume a slab thickness (h) of the square or rectangular panel.

(ii) Calculate the width of the spandrel beam by

$b^3 = C_2 + C_1 b^2$ Equation 4.32 or 7.11

where $C_2 = \dfrac{q f_{sts}^2 a_c^3}{308.2 f_{sf} \sqrt{f'_c}}$ for square panel (Equ. 4.35)

$C_1 = \dfrac{a_c q f_{sts}^2}{1.782 f_{sf} \sqrt{f'_c}}$ for square panel (Equ. 4.36)

$C_2 = \dfrac{q f_{sts}^2 a_c^3 T_1^2}{1.672 K_1 f_{sf} \sqrt{f'_c}}$ for rectangular panel (Equ. 7.12)

$C_1 = \dfrac{a_c q f_{sts}^2 K_1}{1.114 f_{sf} \sqrt{f'_c}}$ for rectangular panel (Equ. 7.13)

where: b = width of the edge beam (in)

a_c = clear span of short edge beam (in)

q = load intensity on the slab (psi)

K_1 = load factor for edge beam (Table 7.1)

T_1 = torque constant i.e. (torque per unit length divided by qa^2), defined in Figure 7.1

f_{sf} and f_{sts} = safety factors as defined earlier

f'_c = specified compressive strength of concrete (psi)

To solve this cubic equation use $b = (C_2)^{\frac{1}{3}}$ as a first trial. Values of K_1, T_1 for the short beam, and T_1 for long beam at different aspect ratios of slab are given in Table 7.1.

(iii) Calculate the depth of the edge beam by:

$$d_o = \left[\frac{q f_{sf} a_c^3}{48b\sqrt{f'_c}}\right]^{\frac{1}{2}} \quad \text{for square panel (Equ. 4.37)}$$

$$d_o = \left[\frac{q a_c l_c^2 K_1 f_{sf}}{30b\sqrt{f'_c}}\right]^{\frac{1}{2}} \quad d_o \geq b \quad \text{for rectangular panel}$$

(Equ. 7.14)

where: d_o = overall depth of edge beam (in)

l_c = clear span of edge beam to be designed (in)

Other notations are defined earlier.

Note that in a rectangular panel b and d_o for the short beam will be different than those of the long beam.

(iv) Check that

$w_{actual} < w_{code}$

$M_{actual} < (M_{code}/f_{sf})$

where $w_{code} = a/360$, $M_{code} = f_r z$.

w_{actual} and M_{actual} are obtained by the computer program (or by $w_{actual} = 0.0034qa^4/D$ and $M_{actual} = 0.032qa^2$ in absense of the computer program) for the square panel, and $w_{actual} = w_{table}$ of Table 7.1. $M_{actual} = M_{table}$ of Table 7.1

for rectangular panel. If $w_{code} < w_{actual}$ and $(M_{code}/f_{sf}) < M_{actual}$ use higher value of 'h' and repeat the steps i through iv.

(v) The positive reinforcement in the slab is designed for moment 'm' given by the Modified Yield Line Theory:

$$m = \frac{q_u l^2}{24} - \frac{2T_u}{L} \quad \text{for square panel (Equ. 4.48)}$$

$$m = \frac{q\alpha^2 l^2}{6\lambda_{34}^2}\left[\sqrt{3 + \mu\left(\frac{\alpha\lambda_{12}}{\lambda_{34}}\right)^2} - \frac{\alpha\lambda_{12}\sqrt{\mu}}{\lambda_{34}}\right]^2 \quad \text{for rectangular panel (Equ. 4.51)}$$

(vi) Negative reinforcement in the slab is designed for the condition of the simultaneous formation of the torsional hinges in edge beams and negative yield lines in the slab edges, given by:

$$mi = 10b^2 d_o K \sqrt{f'_c}\,/(3L) \qquad \text{(Equation 4.50)}$$

where: mi = ultimate moment of slab per unit length parallel to edge beam (lb-in/in)

K = ratio of ultimate to cracking torque of edge beam (T_u/T_c)

b = width of edge beam (in)

d_o = overall depth of edge beam (in)

L = length of edge beam (in)

(vii) Calculate the amount of flexural, torsional and shear steel in edge beams by using the formulas:

$$\left.\begin{aligned} M_u &= 5q_u a^3/192 \\ T_u &= 5Kb^2 d_o \sqrt{f'_c}\,/3 \\ V_u &= 5q_u a^2/32 \end{aligned}\right] \text{—— for square panel, given in Section 6.1.}$$

$$\left.\begin{aligned} M_u &= q_u a K_1 l^2/24 \\ T_u &= 5Kb^2 d_o \sqrt{f'_c}\,/3 \\ V_u &= q_u a K_1 l/4 \end{aligned}\right] \text{—— for rectangular panel, given in Section 7.6.}$$

8.2 Recommendations

The following areas in the field of reinforced concrete floor slabs which terminate at edge beams and its allied topics are recommended for further investigation.

1. Extent the present investigation of square slabs to include the solution of rectangular slabs which terminate in edge beams.
2. Test additional slabs to investigate collapse because of the formation of torsional hinges in a pair of two opposite edge beams and the negative yield lines in the slab at its junction with the remaining pair.

LIST OF REFERENCES

1. ACI Committee 318, "Building Code Requirements for Reinforced Concrete (ACI 318-71)", American Concrete Institute, Detroit, Michigan, February, 1971.

2. ACI Committee 318, "Commentary on Building Code Requirements for Reinforced Concrete (ACI 318-71)", American Concrete Institute, Detroit, Michigan, February, 1971.

3. Aldridge, W. W., and Breen, J. E. , "Useful Techniques in Direct Modeling of Reinforced Concrete Structures", Symposium on Models for Concrete Structures, ACI SP-26, Detroit, 1970, pp. 125-140.

4. Aldridge, W. W., Gamble, W. L., and Subnis, G. M., "Structural Models: Fabrication, Instrumentation and Test Techniques", Preprints, Symposium on Models of Concrete Structures, ACI Committee 444, Dallas, Texas, March 9, 1972.

5. ASTM Standards, "Concrete and Mineral Aggregates; Manual of Concrete Testing", American Society for Testing and Materials, Philadelphia, 1971, pp. 277-281.

6. Borges, F. J., and Pereira, J., "Dynamic Model Studies for Designing Concrete Structures", Symposium on Models for Concrete Structures, ACI SP-24, Detroit, 1970.

7. Carpenter, J. E., Roll, F., and Zelman, M. I., "Techniques and Materials for Structural Models", Symposium on Models for Concrete Structures, ACI SP-24, Detroit, 1970, pp. 41-63.

8. Chander, H., Kemp, E. L., Wilhelm, W. J., "Behavior of Prestressed Concrete Rectangular Members Subjected to Pure Torsion", Civil Engineering Studies Report No. 2007, West Virginia University,

9. Clark, L. A., "Crack Similtude in 1:3.7 Scale Models of Slabs Spanning One Way", Cement and Concrete Association (London), Technical Report, March, 1971.

10. Corley, W. G., and Jirsa, J. O., "Equivalent Frame Analysis for Slab Design", ACI Journal Proceedings V. 67, No. 11, Nov., 1970.

11. Dobbs, N., and Cohen, E., "Model Techniques and Response Tests of Reinforced Concrete Structures Subjected to Blast Loads", Symposium on Models for Concrete Structures, ACI SP-24, Detroit, 1970.

12. Elstner, R. C., "Tests of Elastic Models of Flat Plate and Flat Slab Floor System", Symposium on Models for Concrete Structures, ACI SP-24, Detroit, 1970, pp. 294.

13. Ersoy, U., and Ferguson, P. M., "Behavior and Strength of Concrete L-Beams Under Combined Torsion and Shear", ACI Journal, Vol. 64, No. 12, Dec., 1967, pp. 793-801.

14. Evans, P. R., Kemp, E. L., and Wilhelm, W. J., "The Behavior of T- and L-Shaped Plain and Reinforced Concrete Beams Loaded in Torsion", Civil Engineering Studies Report No. 2006, West Virginia University, 1970, Fed. Clearing House No. PB 194988.

15. Ferguson, Phil, M., Reinforced Concrete Fundamentals, John Wiley and Sons, Inc., New York, 1973.

16. Harris, H. G., Subnis, G. M., and White, R. N., "Reinforcement for Small Scale Models of Concrete Structures", Symposium on Models for Concrete Structures, ACI SP-24, Detroit, 1970, pp. 141-158.

17. Hsu, T. T. C., and Kemp, E. L., "Background and Practical Application of Tentative Design Criteria for Torsion", ACI Journal, Vol. 66, No. 1, January, 1969, pp. 12-23.

18. Jones, L. L., Altimate Load Analysis of Reinforced and Prestressed Concrete Structures, Frederick Ungan Publishing Co., New York, 1966.

19. Jones, L. L., Wood, R. H., Yield-Line Analysis of Slabs, American Elsevier Publishing Co., Inc., New York, 1967.

20. Kemp, E. L., "Behavior of Concrete Members Subject to Torsion Combined Torsion Bending and Shear", Torsion of Structural Concrete, ACI SP-18, 1968, pp. 179-202.

21. Kemp, E. L., and Wilhelm, W. J., "The Influence of Spandrel Beam Torsion on Slab Capacity Based on Yield Line Criteria", Presented at the 1971 Annual Convention, ACI, Denver, March 6-12, 1971.

22. Kemp, E. L., Brezny, F. S., and Unterspan, J. A., "Effect of Rust and Scale on the Bond Characteristics of Deformed Reinforcing Bars", ACI Journal, Vol. 65, No. 9, September 1968, pp. 743-756.

23. Kirk, Roger E., Experimental Design: Procedures for the Behavioral Sciences, Brooks/Cole Publishing Company, Belmount, California, 1968.

24. Klus, J. P., "Ultimate Strength of Reinforced Concrete Beams in Combined Torsion and Shear", ACI Journal, Vol. 65, No. 3, March, 1968, pp. 201-216.

25. Litle, W. A., Cohen, E., and Somerville, G., "Accuracy of Structural Models", Symposium on Models for Concrete Structures, ACI SP-24, Detroit, 1970.

26. Litle, W. A., Paparoni, M., "Size Effect in Small-Scale Models of Reinforced Concrete Beams", ACI Journal, Vol. 63, No. 11, Nov., 1966, pp. 1194-1204.

27. Metz, Gene, Alan, "Flexural Failure Tests of Reinforced Concrete Slabs", ACI Journal, Vol. 62, No. 1, January, 1965, pp. 105-115.

28. Mirza, S. M., White, R. N., and Roll, F., "Materials for Structural Models", Preprints, Symposium on Models of Concrete Structures, ACI Committee 444, Dallas, Texas, March 9, 1972.

29. Prager, W., Sectional Address, Eighth International Congress on Theoretical and Applied Mechanics, Istanbul, 1952.

30. Rocha, M., and Silveira, A. F., "Determination of Thermal Stresses in Concrete Dams by Means of Model Tests", Symposium on Models for Concrete Structures, ACI SP-26, Detroit, 1970.

31. Roll, F., "Materials for Structural Models", Proceedings ASCE, Vol. 94, ST6, June, 1968, pp. 1353-1382.

32. Salvadori, M. G., "Spandrel-Slab Interaction", Journal of the Structural Division, ASCE, Vol. 96, No. ST I, January, 1970, pp. 89-106.

33. Saunders, J. W., Jr., Wilhelm, W. J., Kemp, E. L., "The Design of Reinforced Concrete Floor Slabs Which Terminate at Edge Beams", Civil Engineering Studies Report No. 2017, West Virginia University, 1972.

34. Seather, K., Prachand, N. M., "Torsion in Spandrel Beams", ACI Journal, Vol. 66, No. 1, January, 1969, pp. 24-30.

35. Shoolbred, R. A., and Holland, E. P., "Investigation of Slab Restraint on Torsion Moments in Fixed-End Spandrel Girders", Torsion of Structural Concrete, ACI SP-18, 1968, pp. 999-1027.

36. Snedecor, George W., and Cochran, W. C., Statistical Methods, Iowa State University Press, Ames, Iowa, 1972.

37. Timoshenko, S. P., and Woinowsky-Krieger, S., Theory of Plates and Shells, McGraw-Hill Book Company, New York, 1959.

38. Wilhelm, W. J., and Kemp, E. L., "International Torsion Testing Facilities", Engineering Experiment Station Report No. 19, West Virginia University, March, 1972, Federal Clearing House.

39. Wood, R. H., Plastic and Elastic Design of Slabs and Plates, Thames and Hudson Limited, London, 1961.

A P P E N D I C E S

APPENDIX A

Computer Aided Statistical Analysis of the Experimental Data

A.1 Introduction

Model specimen 1 of the current investigation and the two prototype structures referred to as prototype specimen 2 and prototype specimen 3, tested at West Virginia University [33], constitute a source of the experimental data. The observed slab central deflections of the prototype structures and the model prediction values at the homologous point are given in one data matrix of Table A.1. The beam central torsional rotations of prototype specimen 2, the semitheoretical values corresponding to the slab central deflection of prototype specimen 2 and the model prediction values of the rotation for the same prototype structure are given in the rotational matrix of Table A.2.

The two prototype structures are of different concrete mixes. Therefore, in the deflection analysis, in addition to the column effect of load stages, the row effect of different mixes and test procedures is also studied. Thus, the deflection dependent variable is subjected to the different column treatment levels and also the row-blocking effect simultaneously, making a modified RB-k design appropriate for this deflection analysis. In this experiment, each block is composed of one specimen subjected to all treatment levels. So, it is unlikely that all the covariances will be equal [23]. In this situation, using an exact multivariate approach, Box [23] found that the true distribution of the univariate F statistic can be replaced by a conservative F-test. Therefore, this modified procedure along with the follow-up T^2 test, if found necessary, will be used.

The torsional rotation data is related to only one concrete mix, that of prototype specimen 2. The three different methods to obtain the rotational values are theoretically same through structural engineering concepts. Whatever may be the differences between the rotational values, at the same load stage, should be attributed to the nuisance variables (e.g. shape and size effects of the aggregates, unit weight effect, difference in instrumentation, etc.) and the row treatment effect induced in the analysis because of the source-wise variation in the data. The source of the data changes from row to row, e.g. quantities in the first row (Table A.2) are derived from the experimentally observed torsional rotations of model specimen 2, whereas in row 2, the readings are of prototype specimen 2. This results in the source-wise variation of the data. The design should give the level of significance of the row effect on the dependent variable under study (i.e. torsional rotation of the beam central section). Statistically speaking, the dependent variable (rotation) is subjected to the column treatment (load stage) and the row effect (induced because of the source-wise variation). The RB-k design can separate the two treatment effects. Therefore, the rotation data is also analyzed by the modified RB-k design.

A general computer program is written which is useful for RB-k design. The computer prints the following results.

(i) Preliminary quantities such as row means, column means, column variances, row variances, etc.,

(ii) Cochran's 'C' for homogeneity of column variances,

(iii) Cochran's 'C' for homogeneity of row variances,

(iv) ANOVA results of RB-k design,

(v) row and column variances for comparison,

(vi) d(i, j) matrix, F_{nonadd} etc. for nonadditivity test,

(vii) 'F' for linearity trend by orthogonal polynomial coefficients.

The structural significance of this statistical analysis is also discussed in details. Considering the wide applicability of this computer program; logic diagram and suitable hints are given for the prospective program users. Further analysis of the deflection data has shown that the univariate F statistic is to be replaced by the conservative F-test which is to be followed by 'A Posteriori' T^2 test. Therefore, another computer program is written and successfully used for the data analysis. The computer prints all the important matrices (including the variance-covariance matrix) and the final T^2 value for the data. Accuracy of these programs is tested with the help of a solved example of Reference (23). Both give the same results as shown in the computer print-outs of Appendix E.

A.2 Data Matrices

The data matrices of the slab central deflections and the beam central torsional rotations are given in Table A.1 and Table A.2 respectively. The data cards to be supplied to the computer are also given for each analysis.

Table A.1. Data Matrix

Slab Central Deflection (10^{-2}in), RB-10 Design

b - Treatment Levels

a. Blocks	1 30psf	2 50psf	3 70psf	4 90psf	5 110psf	6 130psf	7 150psf	8 170psf	9 190psf	10 210psf
(a_1) Prototype specimen 3	1.23	2.23	3.40	4.20	5.4	6.10	7.30	8.30	9.60	10.4
(a_2) Prototype specimen 2	1.15	2.00	3.00	3.476	4.645	5.545	6.445	8.143	8.648	9.65
(a_3) Model Prediction	1.554	2.441	3.96	4.38	5.37	6.08	7.35	8.20	9.05	9.36

Data Cards - 1 3 10

2 Above Row-wise

3 -9. -7. -5. -3. -1. 1. 3. 5. 7. 9.

Table A.2. Data Matrix

Beam Central (Torsional) Rotation (10^{-4} Rad) RB-8 Design
b - Treatment Levels

a - Blocks	1 30psf	2 50psf	3 70psf	4 90psf	5 110psf	6 130psf	7 150psf	8 170psf
(a_1) Model Prediction for spec. 2	0.8472	1.412	1.412	2.824	3.760	4.547	5.334	6.120
(a_2) Prototype observed spec. 2	0.935	1.213	1.876	2.463	3.770	5.008	4.862	6.109
(a_3) Prototype spec.2 from experimental Central Deflection	0.771	1.575	2.555	2.660	3.784	4.651	5.372	7.058

Data Cards:			
	1	3	8
	2	Above	Row-wise
	3	-7. -5.	-3. -1. 1. 3. 5. 7.

A.3 Analysis

A.3.1 Preliminary Computations

The row means are computed by the formula $\overline{X}_{i.} = \sum_{j=1}^{k} X_{ij}/k.$

The values pointed out by the computer are as follows:

	Row 1	Row 2	Row 3
Deflection Data	5.815994	5.270196	5.774493
Rotation Data	3.282022	3.279499	3.553249

In general, column mean is given by $\overline{X}_{.j} = \sum_{i=1}^{n} X_{ij}/n.$

All the column means for both deflection and rotation data may be seen in the computer print-out of Appendix E.

$$\text{Grand mean} = \sum_{i=1}^{n} \sum_{j=1}^{k} X_{ij}/nk$$

Grand mean for deflection data = 5.620224 and for rotation data it is 3.371590. In general, i^{th} row variance = $\sum_{j=1}^{k} (X_{ij} - X_{i.})^2/(k - 1)$

$$j^{th} \text{ column variance} = \sum_{i=1}^{n} (X_{ij} - X_{.j})^2/(n - 1)$$

These variances as printed out by the computer are given in Appendix E.

A.3.2 Cochran's Test for Homogeneity of Column Variances

Observed value of 'C' is given by:

$$C_{obs} = (\hat{\sigma}^2 \text{largest}) / \sum_{j=1}^{k} \hat{\sigma}_j^2$$

For deflection data $C_{obs} = 0.1778764$

for rotation data $C_{obs} = 0.3933958$.

df for C are k and n - 1 i.e. 10 and 2 for deflection data;

8 and 2 for rotation data. Table values are respectively 0.4450 and 0.5157. $C_{obs} < C_{Table}$ for both data. Therefore, the column variances are homogeneous, i.e.

$$\sigma_{i1}^2 = \sigma_{i2}^2 = \text{------------------} \ \sigma_{ik}^2$$

A.3.3 Cochran's Test for Homogeneity of Row Variances

Observed value of C is given by:

$$C_{obs} = (\hat{\sigma}_j^2 \text{ largest}) / \sum_{j=1}^{k} \hat{\sigma}_j^2$$

For deflection data $C_{obs} = 0.376183$,

for rotation data $C_{obs} = 0.3621332$.

Table values of C for degrees of freedom 3, 9 and 3, 7 at $\alpha = 0.05$ are respectively 0.5017 and 0.5367.

$$C_{obs} < C_{Table}$$

Therefore, the variances are homogeneous and the basic condition of the analysis is satisfied.

A.3.4 ANOVA for RB-k Design

$$SS_{Total} = \sum_{1}^{n} \sum_{1}^{k} (X_{ij} - \bar{X}_{..})^2$$

Table A.3 ANOVA for the Rotation Data RB-8.

Source	SS	df	MS	F
1. Between b-treatment levels	82.38416	k-1=7	11.76917	128.56**
2. Between a-Blocks	0.3960256	n-1=2		2.1629
3. Residue		(k-1)(n-1) = 14		
4. Total	84.06183	n-1=23		

** Highly Significant $p < 0.01$

Table A.4 ANOVA for the Deflection Data RB-10

Source	SS	df	MS	F
1. Between b-treatment levels	228.0086	k-1=9	25.334	327.567**
2. Between a-Blocks	1.484644	n-1=2		11.937**
3. Residue	1.3922	(k-1)(n-1) = 18		
4. Total	231.2472	n-1=29		

SS between column treatment effects = SS_B

$$= SS_{Total} - \sum \sum (X_{ij} - \bar{X}_{.j})^2$$

SS between 'Blocks' = SS_A or SS_{Block}

$$= k \sum_{i=1}^{n} (X_{i.} - \bar{X}_{..})^2$$

$$SS_{residue} = SS_{Total} - SS_A - SS_B$$

MS = SS/df in general, etc. These analytical expressions are computerized. The results are given in the ANOVA tables numbered A.3 and A.4. Table A.3 shows that for the rotation data blocking is not significant. A conservative test would give the same result making the other follow-up procedures unnecessary. On the contrary, for the deflection data, the multivariate approach of conservative F-test followed by 'A Posteriori' T^2 test, is required.

Table A.5 ANOVA for Conservative F-test on the Deflection Data

Source	SS	df	MS	F
1. Between a-treatment levels	1.484644	1	1.484644	2.13
2. Residue	1.3922	(n-1)=2	0.6961	

$\therefore$F not significant.

The procedure for the T^2 test is summarized in the following steps.

(a) Construct the 'B' row matrix by

$$B = (\bar{X}_{.1} - \bar{X}_{.k}),\ (\bar{X}_{.2} - \bar{X}_{.k}) \text{ ---------------}$$
$$\text{-------} (\bar{X}_{.(k-1)} - \bar{X}_{.k})$$

Dimensions of 'B' matrix are 1 and (k - 1)

(b) Construct the 'C' matrix of dimensions (k - 1) x K by

$$C(i,\ i) = +1 \qquad i \longrightarrow 1 \text{ to } (k-1)$$

$$C(i,\ k) = -1 \qquad i \longrightarrow 1 \text{ to } (k-1)$$

All the remaining elements of 'C' matrix are zero.

(c) Construct a Variance-Covariance matrix (denoted by 'S') of dimensions k x k by using

$$S(i,\ i) = \hat{\sigma}_j^2 = \frac{1}{n-1} \sum_1^n \left[X_{ij}^2 - \left(\sum_1^n X_{ij} \right)^2 / n \right]$$

$$i \longrightarrow 1 \text{ to } k$$

All the other remaining elements of 'S' matrix are generated by

$$S(i,\ j) = \hat{\rho}\, \sigma_{jj'}^2 = \frac{1}{n-1} \left[\sum_1^n X_{ij} X_{ij'} - \left(\sum_1^n X_{ij} \right) \left(\sum_1^n X_{ij'} \right) / n \right]$$

$i \longrightarrow 1$ to k, $j \longrightarrow 1$ to k and $i \neq j$

(d) Calculate T^2 value by

$$T^2 = nB' S_y^{-1} B$$

where S_y^{-1} is an inverse of Sy which is given by: $Sy = CSC'$

B' and C' are respectively the transpose matrices of B and C.

(e) The calculated value of T^2 will be compared with the value given by

$$T_1^2 = \frac{(n-1)(k-1)}{n-k+1} \quad F_{\alpha},\ (k-1),\ (n-k+1)$$

For the deflection data, calculated value of T^2 is 39.888 as shown in the computer print-out of Appendix E. T_1^2 for the same data is 10.08 (at $\alpha = 0.05$) or 19.48 (at $\alpha = 0.01$)

$T^2 > T_1^2$ concluding that at least one contrast among means is significant. That contrast is obviously the one between the highest and the lowest means of row 1 and row 2 respectively. To check the probable existance of a significant difference between the means of row 2 and row 3, the procedure of "Analysis of Independent Samples when $\sigma_1 = \sigma_2$" is used. Accordingly

$$t = (\bar{X}_1 - \bar{X}_2) / \sqrt{\frac{S_p^2}{n_1} + \frac{S_p^2}{n_2}}$$

where S_p^2 is a pooled variance given by: $S_p^2 = \dfrac{S_1^2 + S_2^2}{2}$

When $n_1 = n_2 = n$, $t = \dfrac{\bar{X}_1 - \bar{X}_2}{\sqrt{\dfrac{2S_p^2}{n}}}$, df = (n - 1)

Using means and variances (of row 2 and row 3) printed out by the computer in Appendix E, the calculated value of t is 0.3999. The table value of t is $t_{9,\ 0.05} = 2.262$, which is higher than the calculated one. Thus, the "Analysis of Independent Samples when $\sigma_1 = \sigma_2$" suggests that the contrast among means of row 2 and row 3 is not significant.

A.3.5 Comparison of Row and Column Variances

In the deflection data, 'a' blocks have very small variation compared to the variation of 'b' treatment levels. $\hat{\sigma}_a^2 = 0.084$ and

$\hat{\sigma}_b^2 = 8.42$. The ratio of $\hat{\sigma}_b^2/\ \hat{\sigma}_a^2$ is very large. In the same way, in the rotation data the ratio of $\hat{\sigma}_b^2/\ \hat{\sigma}_a^2$ is also very large (3.89/0.013). These large ratios show that the 'blocking' effect is very small compared to the column effect (i.e. loading stage effect). These small row variances indicate that the individual differences are unusual amongst the rows[(23)].

Further, the correlation coefficient

$$\hat{w}^2 = \frac{SS_B - (k-1)MS_{res}}{SS_{Total} + MS_{res}} \times 100$$

is very large for both deflection and rotation data.

e.g. for deflection data $\hat{w}^2 = \frac{228.0086 - (10-1)0.0773}{231.2472 + 0.0073} \times 100$

$$= 98.2\%$$

Thus, more than 98 percent variation in the deflection data is explained by b-treatment effects, whereas only less than 2 percent variation is caused by blocking effect. This fact further indicates that the blocking effect is not very significant.

A.3.6 Nonadditivity Test

This test is carried out to see the presence, if any, of the interaction between the load stages and row effects. The following computations are computerized.

$$\text{DROW (I, 1)} = \sum_{i=1}^{n} (\bar{X}_{i.} - \bar{X}_{..})$$

$$\text{DCOL (1, J)} = \sum_{j=1}^{n} (\bar{X}_{.j} - \bar{X}_{..})$$

$$\text{Matrix } [D(I, J)] = [DROW (I, 1) * DCOL (1, J)]$$

Computer prints out this matrix which is a useful intermediate step to check the bulk of calculations involved so far.

$$SUM3 = \sum_{i=1}^{n} \sum_{j=1}^{k} D(I, J) * X(I, J)$$

$$SUM4 = \sum_{1}^{n} \sum_{1}^{k} [DROW (I, J)]^2$$

$$SUM5 = \sum_{1}^{n} \sum_{1}^{k} [DCOL (I, J)]^2$$

$$SS_{nonadd} = (SUM3)^2/(SUM4 * SUM5)$$

Computer prints all these quantities.

$$SS_{remainder} = SS_{residue} - SS_{nonadd}$$

$$F_{nonadd} = SS_{nonadd} * (kn-k-n)/SS_{remainder}$$

The calculated values of F_{nonadd}, given in Appendix E, for the deflection and rotation data are respectively 0.08 and 0.75. The tabled values $F_{1,\ kn-k-n}$ are as follows:

$$F_{1,\ 17} = 4.45 \text{ at } \alpha = 0.05$$

$$F_{1,\ 13} = 4.61 \text{ at } \alpha = 0.05$$

Thus in both cases $F_{nonadd} < F_{Table}$. The interaction effect is altogether absent and the models are 'Additive' type. This helps to generalize the load stage effect for all the observations irrespective of the row location.

A.3.7 Orthogonal Polynomial Coefficients to Test Linearity of the Data

The following procedure is computerized to find F_{ψ} to test the linear trend, if any, in the data.

(a) The computer reads the following orthogonal polynomial coefficients (C_j values):

Deflection Data -9. -7. -5. -3. -1. 1. 3. 5. 7. 9.

Rotation Data -7. -5. -3. -1. 1. 3. 5. 7.

(b) $\text{SUM7} = \sum_{j=1}^{k} (C_j)^2$, $SS_{B\psi} = (\bar{X}_{..} *n*k)^2/(n*\text{SUM7})$

$MS_{\psi} = SS_{B\psi}$, as df for $SS_{B\psi}$ is 1.

$MS_{res(lin)} = (SS_{res} + SS_{row} - SS_{B\psi})/(nk-n-1)$

$F_{\psi} = MS_{\psi}/MS_{res(lin)}$, the calculated values of F_{ψ} are:

Deflection Data $F_{\psi} = -29.30508$

Rotation Data $F_{\psi} = -22.96568$

The large negative values of F_{ψ} indicate the strong linear trend in the data.

A.4 Computer Program and Hints to Its Users

In connection of this statistical investigation a general computer program is written which can analyze an almost unlimited number of different experiments based on RB-k design. 'k' value may be of any magnitude large or small.

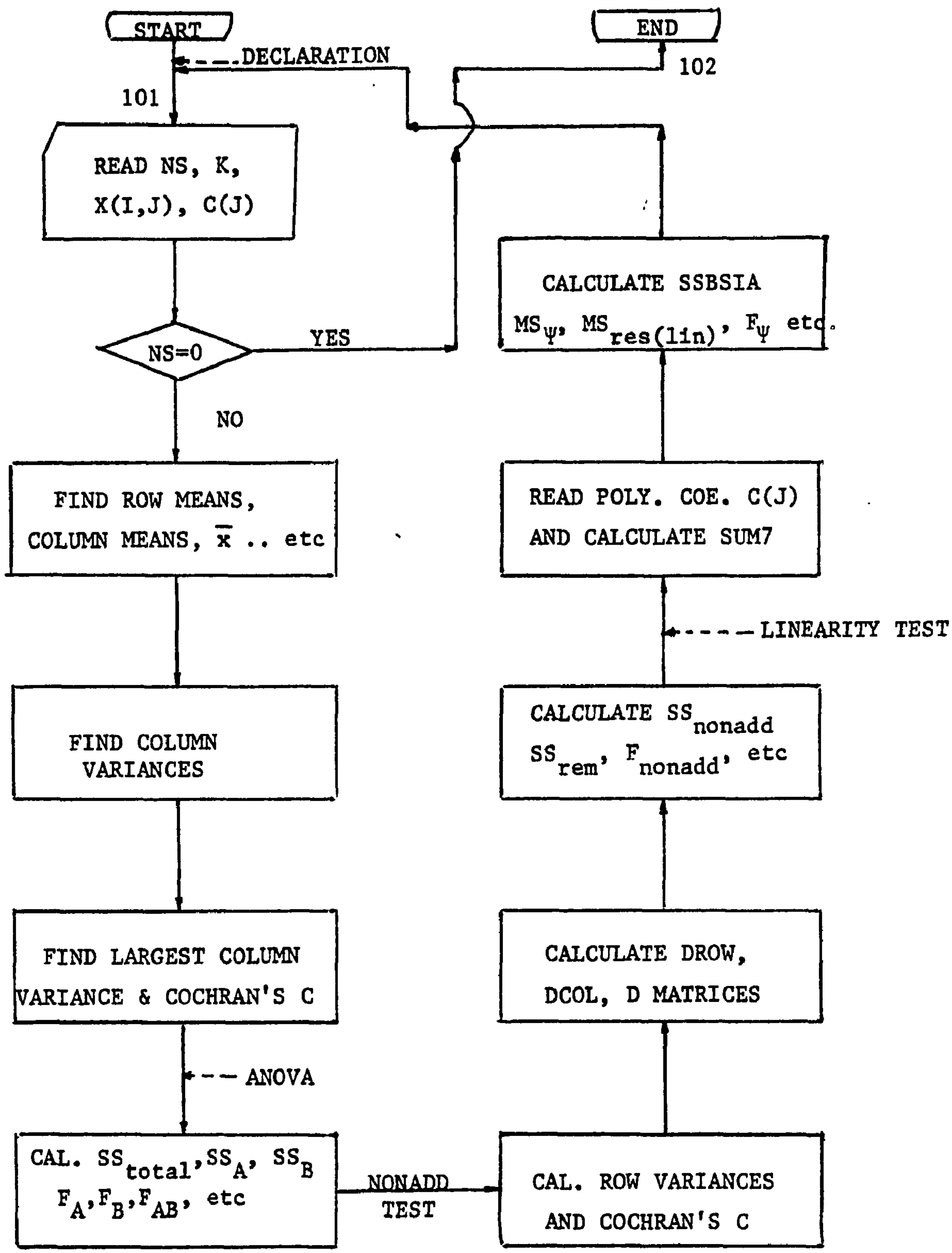

LOGIC DIAGRAM

This program was tested by the solved example of Reference (23). In one compilation, it can analyze an almost unlimited number of experiments. The compilation time is 0.73 seconds and the execution time per experiment is less than 1 second, the later time actually depends on n and k values. The program is written in the 'free format' system. The data cards are to be arranged as follows:

(i) NS, K

(ii) Data Matrix Row-wise

(iii) C_j Values

(iv) 0 0

For example the deflection data cards were-

(i) 3 10

(ii) 1.23 2.23 -----------9.05 9.36

(iii) -9. -7. -5. -3. -1. 1. 3. 5. 7. 9.

(iv) 0 0

The last card is used to terminate the program.

Another subprogram is written to calculate T^2 values to be used as a follow-up procedure of the conservative F-test. The program generates all the important matrices (including the variance-covariance matrix), does appropriate multiplication and inversion of matrices and prints the final T^2 value along with the important matrices.

A.5 Notations

Description	Computer Notation
Dependent variable X_{ij}	X(I, J)
Number of Rows (n)	NS
Number of Columns (k)	K
Column Sums $\sum_{i=1}^{n} X_{ij}$	XDT(J)
Row Sums $\sum_{j=1}^{k} X_{ij}$	XDTROW(I)
Column Means $X_{j.}$	XBARDT(J)
Row Means $X_{i.}$	XDTBAR(I)
Column Variances $\hat{\sigma}^2_{.j}$	VAR(J)
Row Variances $\hat{\sigma}^2_{i.}$	VARROW(I)
Grand Mean $\bar{X}_{..}$	XBDD
Largest Column Variance	VARLRG
Largest Row Variance	VARRLG
Cochran's 'C' for Row Variance	COCROW
Cochran's 'C' for Column Variance	CCOCRN
Orthogonal Polynomial Linear Coeff.	C(J)
In Nonadditivity Test-	
$d_i = \bar{X}_{i.} - \bar{X}_{..}$	DROW(I, J)
$d_j = \bar{X}_{.j} - \bar{X}_{..}$	DCOL(I, J)
$d_i * d_j$	D(I, J)
SS_{nonadd}	SSNOAD

Description	Computer Notation
F_{nonadd}	FNOADD
$MS_{res(lin)}$	MSRESL
MS_{ψ}	MSSIA
Variance-Covariance Matrix	S(I, J)
T^2 Value	TSQR

A.6 Structural Significance of the Statistical Analysis

The deflection data analyzed here is for the following experimental work.

(a) Prototype specimen 2

(b) Prototype specimen 3

(c) Prediction by model testing for specimen 2

The rotation data is for -

(a) Prediction by model testing for specimen 2

(b) Prototype specimen 2

(c) From the experimental central deflection of the slab of specimen 2

This statistical analysis has the following structural significance:

(i) All the data has a strong linear trend suggesting that the readings are in the elastic limit. (Analysis A.3.6 and A.3.7).

(ii) All the three sources listed above of the rotation data lead to the same results. It is expected because they are all related to the specimen 2 alone. (Analysis A.3.4, A.3.5, etc.).

(iii) The deflection data has a source-wise variation (conventional F-test), but this variation is not very significant (conservative F-test, large magnitudes of $\hat{\delta}_b^2$ / $\hat{\delta}_a^2$ and $\hat{w}^2$, insignificant 't' value, etc.). Part of this source-wise variation is due to the presence of nuisance variability which cannot be removed by this design procedure. The deflection data is for both specimens 2 and 3, which have different values of E and torsional stiffness (TS). The deflection depends upon (EI/aD) ratio and also on TS.

$$\frac{EI}{aD} = \frac{EI}{a\left[\frac{Eh^3}{12(1 - \nu^2)}\right]} = \frac{12(1 - \nu^2)I}{ah^3}$$, when both beam and slab have the same E. Thus, the specimens 2 and 3 have the same (EI/aD) value but different TS.

The effect of (EI/aD) on the slab central deflection is much more predominant compared to the torsional stiffness of the beam. Thus, we expect a little variation in deflection results as pointed out by this analysis. Such a difference is also seen in comparisons of other quantities associated with the slab center of specimen 2 and of 3. For example, the theoretical calculations have shown that for specimen 2, the slab central bending moment is given by $M = 0.0302683qa^2$, whereas for specimen 3, $M = 0.0302402qa^2$. Actually, these theoretical studies are the basis of grouping the deflections of specimen 2 and of 3 in one data matrix but under two separate blocks.

APPENDIX B

Condensed Tables of Deflections and Rotations

Table B.1 Experimental data of model specimen 1

Load Stage (psf)	Deflection (in.) 1	2	3	4	5	Rotation (Rad x 10^{-4}) 6	7	8
30	0.0055	0.0035	0.0025	0.0025	0.0020	1.20	0.80	0.50
50	0.0090	0.005	0.0065	0.0050	0.0035	2.00	1.25	0.90
70	0.0140	0.008	0.0090	0.0090	0.0050	2.00	-	1.10
90	0.0155	0.011	0.0135	0.0095	0.0065	4.00	2.35	-
110	0.0190	0.0135	0.0145	0.0125	0.0075	5.33	3.00	-
130	0.0220	0.0185	0.0190	0.0170	0.0090	-	-	2.10
150	0.0260	0.022	0.0210	0.0190	0.0115	-	3.90	2.65
170	0.0290	0.0245	0.0240	0.0220	0.0140	8.66	-	2.90
190	0.0320	0.0260	0.0285	0.0255	0.0175	-	4.50	-
210	0.0335	0.0305	0.0300	0.0265	0.0235	-	5.35	3.45
245	0.0455	0.041	0.0435	0.0340	0.0285	-	6.10	-

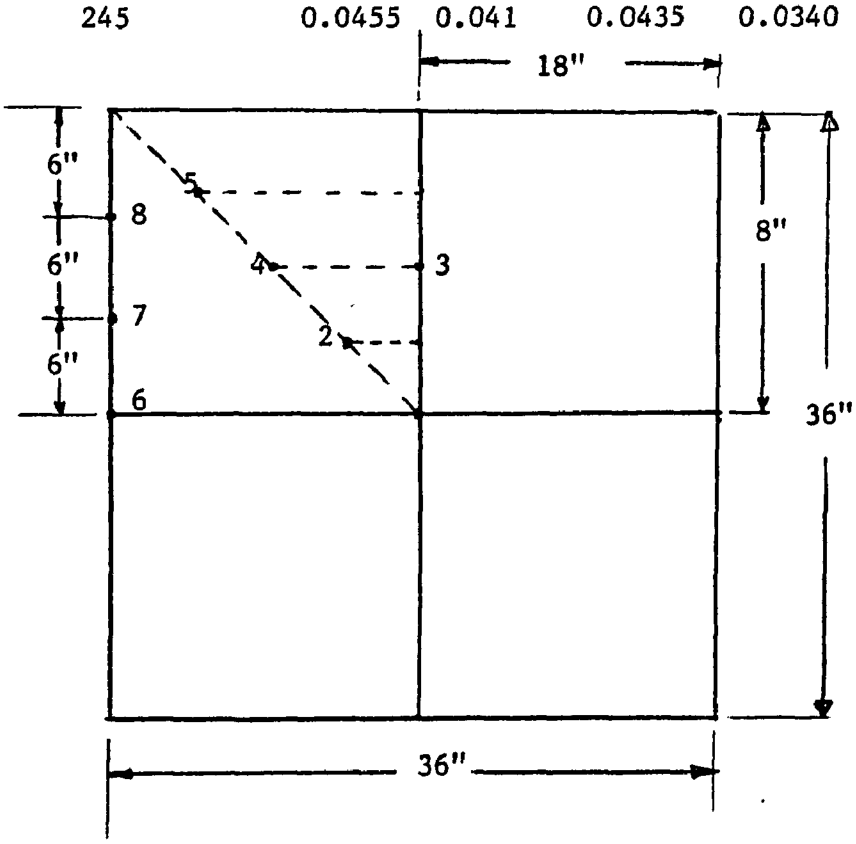

Scale:

1/11.43 Full size

(1 cm = 4.5 in)

Gage location diagram

Table B.2 Experimental data of model specimen 2

Load Stage (psf)	Deflections (in.) 1	2	3	4	5	Rotations (Rad x 10^{-4}) 6	7	8
100	0.004	0.0025	0.0020	0.0015	0.0025	1.787	1.110	-
210	0.008	0.0050	0.006	0.0045	0.0050	2.235	2.150	8.535
400	0.016	0.0155	0.0135	0.0115	0.0075	2.680	-	17.78
620	0.026	0.0225	0.0215	0.016	0.0125	5.381	4.952	26.33
800	0.0335	0.0310	0.028	0.022	0.0175	6.705	5.216	35.56
1000	0.0455	0.0415	0.039	0.028	0.0225	10.722	7.516	45.52
1200	0.0575	0.054	0.050	0.0365	0.027	11.620	8.220	56.18
1400	0.0745	0.0675	0.0635	0.044	0.032	18.78	10.163	69.00
1500	0.0800	0.0725	0.0685	0.047	0.036	19.66	10.341	74.67
1600	0.089	0.081	0.0760	0.0525	0.0385	25.02	12.335	74.66
1700	0.104	0.0925	0.089	0.062	0.0455	33.52	15.812	93.89
1800	0.126	0.109	0.1075	0.0715	0.0545	46.47	32.314	95.39

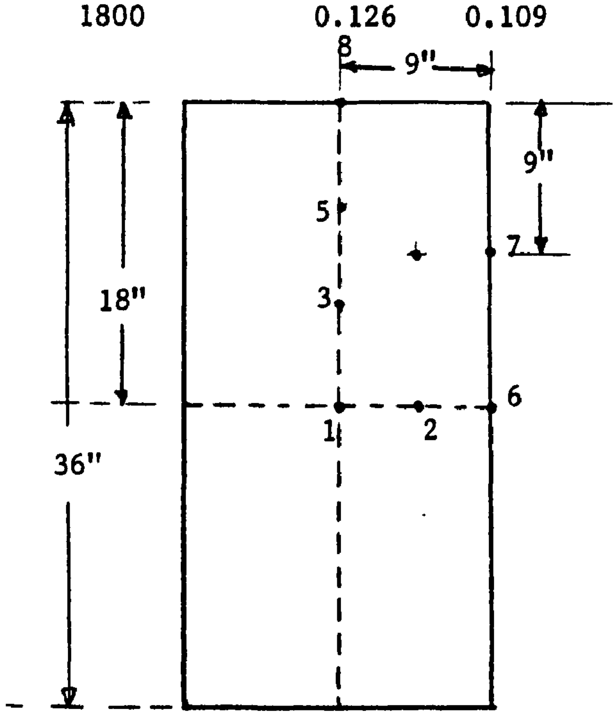

Scale:

1/11.43 Full size

(1 cm = 4.5 in)

Gage location diagram

Table B.3 Experimental data of model specimen 3

Load Stage (psf)	Deflections (in.) 1	2	3	4	5	Rotations (Rad x 10^{-4}) 6	7
50	0.005	0.0035	0.0015	0.0005	0.0005	2.238	1.101
70	-	0.055	0.0025	0.0015	0.0025	2.682	1.312
100	0.0085	0.0080	0.0045	-	0.004	4.467	2.189
132	0.011	-	-	0.0065	0.0035	-	-
170	0.014	0.0105	0.0085	0.0065	0.0065	-	4.288
200	0.015	0.0135	0.0085	0.0085	0.0075	8.50	4.616
270	0.0215	0.0155	0.0155	0.0120	0.0125	-	-
300	0.029	0.0195	0.0185	0.0155	0.0155	-	-
350	0.0325	0.0230	0.022	0.018	0.019	-	5.691
420	0.039	0.0305	0.0275	0.022	0.0225	11.63	5.599
470	0.044	0.0335	0.0325	0.0285	0.0255	15.80	6.18
500	0.0465	0.0360	0.035	0.0305	0.0285	21.95	7.732
570	0.053	0.0395	0.0405	0.0335	0.031	21.95	10.515
600	0.0575	0.0435	0.0430	0.0370	0.034	-	-
620	0.060	0.0475	0.0465	0.0395	0.036	22.34	10.541
680	0.069	0.0500	0.0535	0.0455	0.0425	26.40	12.639
730	0.079	0.0635	0.0635	0.0555	0.048	30.00	16.32
800	0.085	0.0675	0.0685	0.0585	0.053	31.3	16.56
880	0.1045	0.0815	0.083	0.072	0.0625	44.31	21.38
940	0.122	0.0930	0.097	0.088	0.075	46.50	23.99
1000	0.141	0.1060	0.1145	0.099	0.0855	61.20	32.11
1100	0.165	0.1280	0.1385	0.1165	0.1045	76.00	33.63
1170	0.234	0.1695	0.1975	0.160	0.143	165.0	70.62
1230	0.291	0.2115	0.243	0.197	0.1775	330.0	120.86

APPENDIX C

Main Computer Program of Elastic Analysis,

Printed Results for (1) Check for all the

Possible Edge Conditions (2) Prototype Specimen 2

(3) Prototype Specimen 3

```
      REAL NU,II,K
      REAL  AU(4,5),X(4),R(4)
      REAL  Y(4),ZU(4,5)
      REAL  COEA(7),COEC(7)
C TO SUPPLY DATA
C ALL QUANTITIES EXCEPT TS AND WEXPT ARE  KIP AND FT UNITS
C TS AND WEXPT ARE KIP AND INCH UNITS
C AU IS FINAL AUGMENTED MATRIX
      MCOUNT=0
 1001 CONTINUE
      MCOUNT=MCOUNT+1
      WRITE(6,551)MCOUNT
  551 FORMAT(////,10X,'ANALYSIS NUMBER',I3)
      READ (5,2) NU,E,D,II,A,TS
    2 FORMAT(F10.7,F10.1,F10.3,F20.5,F10.5,F20.2)
    3 FORMAT(2X,F10.7,F10.1,F10.3,F18.5,F10.5,F20.2)
      IF(D.EQ.C.)GO TO 1002
      WRITE(6,3)NU,E,D,II,A,TS
      TS=TS/144.
      READ(5,4)Q,WEXPT
    4 FORMAT(F10.7,F20.7)
C TO CONVERT WEXPT IN FT UNITS
      WEXPT=WEXPT/12.
C GRH1 EQUA.
      PI=22/7
      DO 101 I=1,3,2
      BETAI=I*PI/A
      ALPI=I*PI/2.
      J=(I+1)/2
      JJ=-1
      F2=(BETAI**2)*(1-NU)*COSH(ALPI)
      F3=2*BETAI*COSH(ALPI)+(A/2)*(BETAI**2)*(1-NU)*SINH(ALPI)
      F4=(JJ**J)*2*NU*Q*(A**2)/((PI**3)*(I**3)*D)
      F5=TS*(BETAI**3)*SINH(ALPI)/D
      FA=F2-F5
      F6=(TS/D)*((BETAI**2)*
     1                       SINH(ALPI)+(A*(BETAI**3)*COSH(ALPI))/2.)
      FB=F3-F6
      DO10 N=1,3,2
      BETAN=N*PI/A
      ALPN=N*PI/2
      K=BETAN**2+BETAI**2
      F1=-D*SIN(ALPN)*(BETAN**3)*(4*BETAI/(A*K))*SIN(ALPI)*COSH(ALPN)
      F7=(TS*4*I*PI*SIN(ALPI)*COSH(ALPN))/(D*K*(A**2))
      F8=(BETAN**3)*SIN(ALPN)
      F9=2*(BETAN**2)*SIN(ALPN)
      F12=F8*F7
      F13=F9*F7
      F10=(TS/D)*(BETAN**3)*SIN(ALPN)
      F11=(2/K) *BETAI*SIN(ALPI)*SINH(ALPN)-(8/(A*(K**2)))*
     1BETAN*BETAI*SIN(ALPI)*COSH(ALPN)
      F14=F10*F11
      FDN=F13+F14
C CONSTRUCTION OF TWO GRH1 EQUS.
      IF(I.EQ.1.AND.N.EQ.1)AU(1,1)=FA-F12
      IF(I.EQ.3.AND.N.EQ.3)AU(2,2)=FA-F12
      IF(I.EQ.1.AND.N.EQ.3)AU(1,2)=-F12
      IF(I.EQ.3.AND.N.EQ.1)AU(2,1)=-F12
      IF(I.EQ.1.AND.N.EQ.1)AU(1,3)=FB-FDN
      IF(I.EQ.3.AND.N.EQ.3)AU(2,4)=FB-FDN
      IF(I.EQ.1.AND.N.EQ.3)AU(1,4)=-FDN
      IF(I.EQ.3.AND.N.EQ.1)AU(2,3)=-FDN
      IF(I.EQ.1)AU(1,5)=-F4
      IF(I.EQ.3)AU(2,5)=-F4
   10 CONTINUE
  101 CONTINUE
C PROG FOR GRH2 EQUA.
      DO 102 I=1,3,2
      BETAI=I*PI/A
      ALPI=I*PI/2.
      F15=D*(BETAI**3)*COSH(ALPI)*((1-NU)*TANH(ALPI)+(E*II/D)*BETAI)
      F16=D*(BETAI**2)*SINH(ALPI)*(1+NU-(E*II*A*(BETAI**2)/(2*D))-
     1ALPI*(1-NU)/TANH(ALPI))
      F17=4*Q*SIN(ALPI)*(E*II/(2*D*A)-0.25)/BETAI
      DO 20N=1,3,2
      BETAN=N*PI/A
```

```
                  ALPN=N*PI/2
                  K=BETAN**2+BETAI**2
                  F1=-D*SIN(ALPN)*(BETAN**3)*(4*BETAI/(A*K))*SIN(ALPI)*COSH(ALPN)
                  F20=D*SIN(ALPN)*(BETAN**3)*4*I*PI*SIN(ALPI)*COSH(ALPN)/(K*A**2)
                  F21=F1*(1-NU)*(A*TANH(ALPN)/2-2*BETAN/K)
                  F22=(1-NU)*F20
                  F23=F21-2*(2-NU)*F20/BETAN
C CONSTRUCTION OF TWO GRH2 EQUAS.
                  IF(I.EQ.1.AND.N.EQ.1)AU(3,1)=-F15-F22
                  IF(I.EQ.3.AND.N.EQ.3)AU(4,2)=-F15-F22
                  IF(I.EQ.1.AND.N.EQ.3)AU(3,2)=-F22
                  IF(I.EQ.3.AND.N.EQ.1)AU(4,1)=-F22
                  IF(I.EQ.1.AND.N.EQ.1)AU(3,3)=F16+F23
                  IF(I.EQ.3.AND.N.EQ.3)AU(4,4)=F16+F23
                  IF(I.EQ.1.AND.N.EQ.3)AU(3,4)=F23
                  IF(I.EQ.3.AND.N.EQ.1)AU(4,3)=F23
                  IF(I.EQ.1)AU(3,5)=F17
                  IF(I.EQ.3)AU(4,5)=F17
               20 CONTINUE
              102 CONTINUE
                  N=4
                  CALL SIMQ(AU,X,N)
                  TSUMAN=X(1)+X(2)
                  ESUMAN=0.5*(WEXPT-(Q*(A**4)/(76.8*D)))
                  PERDIF=(TSUMAN-ESUMAN)*100.0/TSUMAN
                  WRITE(6,5)Q,TSUMAN,ESUMAN,PERDIF
                  R(1)=X(1)
                  R(2)=X(2)
                  R(3)=X(3)
                  R(4)=X(4)
                5 FORMAT(2X,'LOAD STAGE',2X,F6.4,2X,'THEORETICAL SUMAN=',
                 1F10.7,2X,'EXPERIMENTAL OR TABULATED SUMAN=',F10.7,2X,
                 1'PERCENTAGE DIFF=',F8.3)
                  WTHWCF=12*(Q*(A**4)/(76.8*D)+2*TSUMAN)
C CALCULATIONS FOR UCF START HERE
                  WRITE (6,7)
                7 FORMAT(2X,'CALCULATIONS BY UCF')
                  TS=0.
                  DO 107 I=1,3,2
                  BETAI=I*PI/A
                  ALPI=I*PI/2.
                  J=(I+1)/2
                  JJ=-1
                  F2=(BETAI**2)*(1-NU)*COSH(ALPI)
                  F3=2*BETAI*COSH(ALPI)+(A/2)*(BETAI**2)*(1-NU)*SINH(ALPI)
                  F4=(JJ**J)*2*NU*Q*(A**2)/((PI**3)*(I**3)*D)
                  F5=TS*(BETAI**3)*SINH(ALPI)/D
                  FA=F2-F5
                  F6=(TS/D)*((BETAI**2)*
                 1                          SINH(ALPI)+(A*(BETAI**3)*COSH(ALPI))/2.)
                  FB=F3-F6
                  DO 16 N=1,3,2
                  BETAN=N*PI/A
                  ALPN=N*PI/2
                  K=BETAN**2+BETAI**2
                  F1=-D*SIN(ALPN)*(BETAN**3)*(4*BETAI/(A*K))*SIN(ALPI)*COSH(ALPN)
                  F7=(TS*4*I*PI*SIN(ALPI)*COSH(ALPN))/(D*K*(A**2))
                  F8=(BETAN**3)*SIN(ALPN)
                  F9=2*(BETAN**2)*SIN(ALPN)
                  F12=F8*F7
                  F13=F9*F7
                  F10=(TS/D)*(BETAN**3)*SIN(ALPN)
                  F11=(2/K) *BETAI*SIN(ALPI)*SINH(ALPN)-(8/(A*(K**2)))*
                 1BETAN*BETAI*SIN(ALPI)*COSH(ALPN)
                  F14=F10*F11
                  FDN=F13+F14
C CONSTRUCTION OF TWO GRH1 EQUS.
                  IF(I.EQ.1.AND.N.EQ.1)AU(1,1)=FA-F12
                  IF(I.EQ.3.AND.N.EQ.3)AU(2,2)=FA-F12
                  IF(I.EQ.1.AND.N.EQ.3)AU(1,2)=-F12
                  IF(I.EQ.3.AND.N.EQ.1)AU(2,1)=-F12
                  IF(I.EQ.1.AND.N.EQ.1)AU(1,3)=FB-FDN
                  IF(I.EQ.3.AND.N.EQ.3)AU(2,4)=FB-FDN
                  IF(I.EQ.1.AND.N.EQ.3)AU(1,4)=-FDN
                  IF(I.EQ.3.AND.N.EQ.1)AU(2,3)=-FDN
                  IF(I.EQ.1)AU(1,5)=-F4
```

```
      IF(I.EQ.3)AU(2,5)=-F4
   16 CONTINUE
  107 CONTINUE
C PROG FOR GRH2 EQUA.
      DO 108 I=1,3,2
      BETAI=I*PI/A
      ALPI=I*PI/2.
      F15=D*(BETAI**3)*COSH(ALPI)*((1-NU)*TANH(ALPI)+(E*II/D)*BETAI)
      F16=D*(BETAI**2)*SINH(ALPI)*(1+NU-(E*II*A*(BETAI**2)/(2*D))-
     1ALPI*(1-NU)/TANH(ALPI))
      F17=4*Q*SIN(ALPI)*(E*II/(2*D*A)-0.25)/BETAI
      DO 26N=1,3,2
      BETAN=N*PI/A
      ALPN=N*PI/2
      K=BETAN**2+BETAI**2
      F1=-D*SIN(ALPN)*(BETAN**3)*(4*BETAI/(A*K))*SIN(ALPI)*COSH(ALPN)
      F20=D*SIN(ALPN)*(BETAN**3)*4*I*PI*SIN(ALPI)*COSH(ALPN)/(K*A**2)
      F21=F1*(1-NU)*(A*TANH(ALPN)/2-2*BETAN/K)
      F22=(1-NU)*F20
      F23=F21-2*(2-NU)*F20/BETAN
C CONSTRUCTION OF TWO GRH2 EQUAS.
      IF(I.EQ.1.AND.N.EQ.1)AU(3,1)=-F15-F22
      IF(I.EQ.3.AND.N.EQ.3)AU(4,2)=-F15-F22
      IF(I.EQ.1.AND.N.EQ.3)AU(3,2)=-F22
      IF(I.EQ.3.AND.N.EQ.1)AU(4,1)=-F22
      IF(I.EQ.1.AND.N.EQ.1)AU(3,3)=F16+F23
      IF(I.EQ.3.AND.N.EQ.3)AU(4,4)=F16+F23
      IF(I.EQ.1.AND.N.EQ.3)AU(3,4)=F23
      IF(I.EQ.3.AND.N.EQ.1)AU(4,3)=F23
      IF(I.EQ.1)AU(3,5)=F17
      IF(I.EQ.3)AU(4,5)=F17
   26 CONTINUE
  108 CONTINUE
      N=4
      CALL SIMQ(AU,X,N)
      ZSUMAN=X(1)+X(2)
C CALCULATIONS FOR COUPLED EQUA. CSUMAN
C CONSTRATION OF SIMULTATION EQUAS.
C FOR C1,C3,C5,C7.
      PI=22./7.
      DO 103 I=1,7,2
      JJ=(I-1)/2
      J=(-1)**JJ
      BETAI=I*PI/A
      ALPI=I*PI/2.
      F2=D*BETAI**2*SINH(ALPI)*(3+NU+(2*E*II/D)*(BETAI*(COSH(ALPI)/
     1SINH(ALPI))/(1-NU))+(1-NU)*I*PI*((SINH(ALPI)/COSH(ALPI))-
     1(COSH(ALPI)/SINH(ALPI)))/2.)
      F4=(4*Q/BETAI)*SIN(ALPI)*(E*II/(2*D*A)-0.25)
      F5=2*NU*Q*((1-NU)*SINH(ALPI)+E*II*BETAI*COSH(ALPI)/D)/
     1((1-NU)*A*(BETAI**2)*COSH(ALPI))*J
      SUMF6=0.
      DO 12 N=1,7,2
      NN=(N-1)/2
      NNN=(-1)**NN
      BETAN=N*PI/A
      ALPN=N*PI/2.
      K=BETAN**2+BETAI**2
      F1=-D*SIN(ALPN)*(BETAN**3)*(4*BETAI/(A*K))*SIN(ALPI)*COSH(ALPN)
      F3=F1*(2*(2-NU)*A/(N*PI)-2*A/(N*PI) -2*(1-NU)*N*PI/(A*K))
      F6=F1*2*NU*Q*A**4/(COSH(ALPN)*(
     1N**5)*(PI**5)*D)*NNN
      SUMF6=SUMF6+F6
      IF(I.EQ.1.AND.N.EQ.1)ZU(1,1)=F2+F3
      IF(I.EQ.1.AND.N.EQ.3)ZU(1,2)=F3
      IF(I.EQ.1.AND.N.EQ.5)ZU(1,3)=F3
      IF(I.EQ.1.AND.N.EQ.7)ZU(1,4)=F3
      IF(I.EQ.3.AND.N.EQ.1)ZU(2,1)=F3
      IF(I.EQ.3.AND.N.EQ.3)ZU(2,2)=F2+F3
      IF(I.EQ.3.AND.N.EQ.5)ZU(2,3)=F3
      IF(I.EQ.3.AND.N.EQ.7)ZU(2,4)=F3
      IF(I.EQ.5.AND.N.EQ.1)ZU(3,1)=F3
      IF(I.EQ.5.AND.N.EQ.3)ZU(3,2)=F3
      IF(I.EQ.5.AND.N.EQ.5)ZU(3,3)=F2+F3
      IF(I.EQ.5.AND.N.EQ.7)ZU(3,4)=F3
      IF(I.EQ.7.AND.N.EQ.1)ZU(4,1)=F3
```

```
      IF(I.EQ.7.AND.N.EQ.3)ZU(4,2)=F3
      IF(I.EQ.7.AND.N.EQ.5)ZU(4,3)=F3
      IF(I.EQ.7.AND.N.EQ.7)ZU(4,4)=F2+F3
   12 CONTINUE
      F7=F4+F5-SUMF6
      IF(I.EQ.1)ZU(1,5)=F7
      IF(I.EQ.3)ZU(2,5)=F7
      IF(I.EQ.5)ZU(3,5)=F7
      IF(I.EQ.7)ZU(4,5)=F7
  103 CONTINUE
      N=4
      CALL  SIMQ(ZU,Y,N)
      COEC(1)=Y(1)
      COEC(3)=Y(2)
      COEC(5)=Y(3)
      COEC(7)=Y(4)
C PROGRAM TO CALCULATE A COE FROM C COE ALSO TO FIND CENTRAL DEFLECTION
      PI=22./7.
      SUMA=0.
      DO1000 N=1,7,2
      ALPN=N*PI/2.
      COEA(N)=(2*NU*Q*(A**4)/((N**5)*(PI**5)*D)-COEC(N)*(2*A*
     1COSH(ALPN)/(N*PI)+(1-NU)*A*SINH(ALPN)/2.))
     1/((1-NU)*COSH(ALPN))
      SUMA=SUMA+2*COEA(N)
 1000 CONTINUE
      CSUMAN=COEA(1)+COEA(3)+COEA(5)+COEA(7)
      UCF=CSUMAN/ZSUMAN
      WRITE (6,8) UCF
    8 FORMAT(2X,'UNCOUPLING CORRECTION FACTOR=',F10.5)
      FSUMAN=TSUMAN*UCF
      PERDIV=((FSUMAN-ESUMAN)/FSUMAN)*100.
      WRITE(6,9)FSUMAN,ESUMAN,PERDIV
    9 FORMAT(2X,'SUMAN BY UCF=',F10.7,2X,'EXPERMENTAL OR TABULATED
     1SUMAN=',F10.7,
     12X,'PERCENTAGE DIFF=',F8.3)
      WTHUCF=12* (Q*(A**4)/(76.8*D)+2*FSUMAN)
      WEXPT=WEXPT*12.
      WRITE (6,18)WTHUCF,WEXPT
   18 FORMAT(2X,'THEORETICAL CENTRAL DEFLECTION=',F13.7,2X,'EXPERMENTAL
     1OR TABULATED CENTRAL DEFLECTION=',F13.7)
C NEW GIVEN BELOW COEA(1),COEA(3),COEC(1),COEC(3)
C ARE FINALLY REQUIRED VALUES.
      COEA(1)=R(1)*UCF
      COEA(3)=R(2)*UCF
      COEC(1)=R(3)*UCF
      COEC(3)=R(4)*UCF
      WRITE(6,552)
  552 FORMAT(2X,'COEA AND COEC AFTER MULT. BY UCF')
      WRITE(6,553)COEA(1),COEA(3),COEC(1),COEC(3)
  553 FORMAT(2X,4F10.7)
      SUMC=0.
      DO 1010 N=1,3,2
      CONST=(1+NU)*COEC(N)*2*PI*N*D/A
      SUMC=SUMC+CONST
 1010 CONTINUE
      BMCNTR=-Q*(A**2)*(1+NU)/16. +SUMC
      WRITE(6,554)BMCNTR
  554 FORMAT(2X,'B.M. AT CENTER=',F13.7)
      GO TO 1001
 1002 CONTINUE
      WRITE(6,59)
   59 FORMAT(2X,'BUT NO LOAD STAGE OR STRUCTURE TO ANALYSE.GOOD-BYE.')
      STOP
      END
```

```
      SUBROUTINE SIMQ(A,H,N)
      DIMENSION A(4,5),H(4),LOC(5),CK(5)
C READ SIZE OF MATRIX AND A SMALL NUMBER TO DETECT WHETHER
C DIAGONAL ELEMENT IS ZERO OR NOT
C B IS STORED IN N+1 COLUMN OF A
      EPS=0.0000001
      NP=N+1
      DO 1 I=1,N
C I IS PIVOT ROW
    1 CK(I)=0
      DO 100 I=1,N
      IP=I+1
C FIND MAXIMUM ELEMENT IN ITH ROW
      AMAX=0
      DO 2 K=1,N
      IF (AMAX-ABS(A(K,I)))3,2,2
C IS NEW MAX IN ROW PREVIOUSLY USED AS PIVOT
    3 IF (CK(K))4,4,2
    4 LOC(I)=K
      AMAX=ABS(A(K,I))
    2 CONTINUE
      IF (ABS(AMAX).LE.EPS)GOTO 99
C MAX ELEMENT IN ITH COLUMN IS A(L,I)
    5 L=LOC(I)
      CK(L)=1
C PERFORM ELEMINATION, L IS PIVOT ROW, A(L,I) IS PIVOT ELEMENT
      DO 50 J=1,N
      IF (L-J)6,50,6
    6 F=-A(J,I)/A(L,I)
      DO 40 K=IP,NP
   40 A(J,K)=A(J,K)+F*A(L,K)
   50 CONTINUE
  100 CONTINUE
      DO 200 I=1,N
      L=LOC(I)
  200 H(I)=A(L,N+1)/A(L,I)
   99 CONTINUE
      RETURN
      END
```

```
           ANALYSIS NUMBER   1
 0.2500000  530000.0  1000.000             0.0       10.00000                   0.0
LOAD STAGE   1.0000   THEORETICAL  SUMAN= 0.0809552  EXPERIMENTAL OR TABULATED SUMAN= 0.0633957  PERCENTAGE DIFF=  21.690
CALCULATIONS  BY UCF
UNCOUPLING CORRECTION FACTOR=    0.77956
SUMAN BY UCF= 0.0631096  EXPERMENTAL OR  TABULATED       SUMAN= 0.0633957  PERCENTAGE DIFF=  -0.453
THEORETICAL  CENTRAL  DEFLECTION=     3.0771322  EXPERMENTAL OR TABULATED CENTRAL DEFLECTION=     3.0839996
COEA AND COEC AFTER MULT. BY UCF
 0.0631872-0.0000775-0.0040326 0.0000095
B.M. AT CENTER=  -10.9585772

           ANALYSIS NUMBER   2
 0.2500000  500000.0  1200.000             0.0       10.00000                   0.0
LOAD STAGE   1.1000   THEORETICAL  SUMAN= 0.0742087  EXPERIMENTAL OR TABULATED SUMAN= 0.0581129  PERCENTAGE DIFF=  21.690
CALCULATIONS  BY UCF
UNCOUPLING CORRECTION FACTOR=    0.77957
SUMAN BY UCF= 0.0578506  EXPERMENTAL OR  TABULATED       SUMAN= 0.0581129  PERCENTAGE DIFF=  -0.453
THEORETICAL  CENTRAL  DEFLECTION=     2.8207054  EXPERMENTAL OR TABULATED CENTRAL DEFLECTION=     2.8269997
COEA AND COEC AFTER MULT. BY UCF
 0.0579217-0.0000711-0.0036565 0.0000087
B.M. AT CENTER=  -12.0544329

           ANALYSIS NUMBER   3
 0.2500000  504000.0  1660.000             0.14560   14.75000                   0.0
LOAD STAGE   0.2000   THEORETICAL  SUMAN=-0.0266169  EXPERIMENTAL OR TABULATED SUMAN=-0.0203615  PERCENTAGE DIFF=  23.502
CALCULATIONS  BY UCF
UNCOUPLING CORRECTION FACTOR=    0.76267
SUMAN BY UCF=-0.0202999  EXPERMENTAL OR  TABULATED       SUMAN=-0.0203615  PERCENTAGE DIFF=  -0.304
THEORETICAL  CENTRAL  DEFLECTION=     0.4038697  EXPERMENTAL OR TABULATED CENTRAL DEFLECTION=     0.4023909
COEA AND COEC AFTER MULT. BY UCF
-0.0203094 0.0000096 0.0012828-0.0000009
B.M. AT CENTER=   -2.2675104

           ANALYSIS NUMBER   4
 0.2500000  480000.0  1200.000             0.10000   10.00000                   0.0
LOAD STAGE   1.0000   THEORETICAL  SUMAN=-0.0412199  EXPERIMENTAL OR TABULATED SUMAN=-0.0315035  PERCENTAGE DIFF=  23.572
CALCULATIONS  BY UCF
UNCOUPLING CORRECTION FACTOR=    0.76272
SUMAN BY UCF=-0.0314394  EXPERMENTAL OR  TABULATED       SUMAN=-0.0315035  PERCENTAGE DIFF=  -0.204
THEORETICAL  CENTRAL  DEFLECTION=     0.5475390  EXPERMENTAL OR TABULATED CENTRAL DEFLECTION=     0.5459999
COEA AND COEC AFTER MULT. BY UCF
-0.0314537 0.0000143 0.0028573-0.0000020
B.M. AT CENTER=   -5.0864077

           ANALYSIS NUMBER   5
 0.3000000   53000.0  1200.000        999999.00000   10.00000                   0.0
LOAD STAGE   1.0000   THEORETICAL  SUMAN=-0.0488213  EXPERIMENTAL OR TABULATED SUMAN=-0.0373368  PERCENTAGE DIFF=  23.523
CALCULATIONS  BY UCF
UNCOUPLING CORRECTION FACTOR=    0.76268
SUMAN BY UCF=-0.0372349  EXPERMENTAL OR  TABULATED       SUMAN=-0.0373368  PERCENTAGE DIFF=  -0.274
THEORETICAL  CENTRAL  DEFLECTION=     0.4084454  EXPERMENTAL OR TABULATED CENTRAL DEFLECTION=     0.4059999
COEA AND COEC AFTER MULT. BY UCF
-0.0372502 0.0000153 0.0033297-0.0000021
B.M. AT CENTER=   -4.6662653

           ANALYSIS NUMBER   6
 0.3000000   53000.0  1000.000        999999.00000   10.00000                   0.0
LOAD STAGE   2.0000   THEORETICAL  SUMAN=-0.1171711  EXPERIMENTAL OR TABULATED SUMAN=-0.0896084  PERCENTAGE DIFF=  23.523
CALCULATIONS  BY UCF
UNCOUPLING CORRECTION FACTOR=    0.76268
SUMAN BY UCF=-0.0893636  EXPERMENTAL OR  TABULATED       SUMAN=-0.0896084  PERCENTAGE DIFF=  -0.274
THEORETICAL  CENTRAL  DEFLECTION=     0.9802752  EXPERMENTAL OR TABULATED CENTRAL DEFLECTION=     0.9743993
COEA AND COEC AFTER MULT. BY UCF
-0.0894003 0.0000366 0.0079512-0.0000051
```

```
B.M. AT CENTER=   -9.7325392


          ANALYSIS NUMBER   7
 0.3000000   530000.0  1000.000         999999.00000  10.00000            999999744.00
LOAD STAGE  0.1000  THEORETICAL  SUMAN=-0.0075734  EXPERIMENTAL OR TABULATED SUMAN=-0.0058804  PERCENTAGE DIFF=  22.355
CALCULATIONS BY UCF
UNCOUPLING CORRECTION FACTOR=    0.76268
SUMAN BY UCF=-0.0057761  EXPERMENTAL OR TABULATED        SUMAN=-0.0058804  PERCENTAGE DIFF=  -1.806
THEORETICAL CENTRAL DEFLECTION=    0.0176242  EXPERMENTAL OR TABULATED CENTRAL DEFLECTION=    0.0151200
COEA ANC COEC AFTER MULT. BY UCF
-0.0057751-0.0000010 0.0006879 0.0000003
B.M. AT CENTER=   -0.2495972


          ANALYSIS NUMBER   8
 0.3000000   500000.0  1200.000         999999.00000  10.00000            999999744.00
LOAD STAGE  0.1100  THEORETICAL  SUMAN=-0.0069425  EXPERIMENTAL OR TABULATED SUMAN=-0.0053904  PERCENTAGE DIFF=  22.356
CALCULATIONS BY UCF
UNCOUPLING CORRECTION FACTOR=    0.76268
SUMAN BY UCF=-0.0052949  EXPERMENTAL OR TABULATED        SUMAN=-0.0053904  PERCENTAGE DIFF=  -1.804
THEORETICAL CENTRAL DEFLECTION=    0.0161524  EXPERMENTAL OR TABULATED CENTRAL DEFLECTION=    0.0138600
COEA ANC COEC AFTER MULT. BY UCF
-0.0052939-0.0000009 0.0006306 0.0000003
B.M. AT CENTER=   -0.2745290


          ANALYSIS NUMBER   9
 0.1600000   530000.0  1675.000              0.14090  12.00000              60237840.00
LOAD STAGE  0.0300  THEORETICAL  SUMAN=-0.0023560  EXPERIMENTAL OR TABULATED SUMAN=-0.0019387  PERCENTAGE DIFF=  17.709
CALCULATIONS BY UCF
UNCOUPLING CORRECTION FACTOR=    0.76279
SUMAN BY UCF=-0.0017971  EXPERMENTAL OR TABULATED        SUMAN=-0.0019387  PERCENTAGE DIFF=  -7.881
THEORETICAL CENTRAL DEFLECTION=    0.0148993  EXPERMENTAL OR TABULATED CENTRAL DEFLECTION=    0.0115000
COEA ANC COEC AFTER MULT. BY UCF
-0.0017970-0.0000001 0.0001791 0.0000001
B.M. AT CENTER=   -0.1307523


          ANALYSIS NUMBER  10
 0.1600000   530000.0  1675.000              0.14090  12.00000              60237840.00
LOAD STAGE  0.0500  THEORETICAL  SUMAN=-0.0039266  EXPERIMENTAL OR TABULATED SUMAN=-0.0031965  PERCENTAGE DIFF=  18.593
CALCULATIONS BY UCF
UNCOUPLING CORRECTION FACTOR=    0.76279
SUMAN BY UCF=-0.0029952  EXPERMENTAL OR TABULATED        SUMAN=-0.0031965  PERCENTAGE DIFF=  -6.722
THEORETICAL CENTRAL DEFLECTION=    0.0248324  EXPERMENTAL OR TABULATED CENTRAL DEFLECTION=    0.0200000
COEA ANC COEC AFTER MULT. BY UCF
-0.0029950-0.0000002 0.0002985 0.0000001
B.M. AT CENTER=   -0.2179213


          ANALYSIS NUMBER  11
 0.1600000   530000.0  1675.000              0.14090  12.00000              60237840.00
LOAD STAGE  0.0700  THEORETICAL  SUMAN=-0.0054977  EXPERIMENTAL OR TABULATED SUMAN=-0.0043918  PERCENTAGE DIFF=  20.109
CALCULATIONS BY UCF
UNCOUPLING CORRECTION FACTOR=    0.76279
SUMAN BY UCF=-0.0041932  EXPERMENTAL OR TABULATED        SUMAN=-0.0043918  PERCENTAGE DIFF=  -4.735
THEORETICAL CENTRAL DEFLECTION=    0.0347653  EXPERMENTAL OR TABULATED CENTRAL DEFLECTION=    0.0300000
COEA ANC COEC AFTER MULT. BY UCF
-0.0041930-0.0000003 0.0004179 0.0000001
B.M. AT CENTER=   -0.3050896


          ANALYSIS NUMBER  12
 0.1600000   530000.0  1675.000              0.14090  12.00000              60237840.00
LOAD STAGE  0.0910  THEORETICAL  SUMAN=-0.0071464  EXPERIMENTAL OR TABULATED SUMAN=-0.0058760  PERCENTAGE DIFF=  17.777
CALCULATIONS BY UCF
UNCOUPLING CORRECTION FACTOR=    0.76279
SUMAN BY UCF=-0.0054512  EXPERMENTAL OR TABULATED        SUMAN=-0.0058760  PERCENTAGE DIFF=  -7.793
THEORETICAL CENTRAL DEFLECTION=    0.0451950  EXPERMENTAL OR TABULATED CENTRAL DEFLECTION=    0.0350000
COEA ANC COEC AFTER MULT. BY UCF
-0.0054508-0.0000004 0.0005433 0.0000002
```

```
B.M. AT CENTER=   -0.3966174

            ANALYSIS NUMBER 13
 0.1600000  530000.0  1675.000               0.14090  12.00000              60237840.00
LOAD STAGE  0.1110  THEORETICAL  SUMAN=-0.0087170  EXPERIMENTAL OR TABULATED SUMAN=-0.0070088  PERCENTAGE DIFF=  19.597
CALCULATIONS BY UCF
UNCOUPLING CORRECTION FACTOR=   0.76279
SUMAN BY UCF=-0.0066493  EXPERMENTAL OR TABULATED        SUMAN=-0.0070088  PERCENTAGE DIFF=  -5.406
THEORETICAL CENTRAL DEFLECTION=     0.0551278  EXPERMENTAL OR TABULATED CENTRAL DEFLECTION=     0.0465000
COEA AND COEC AFTER MULT. BY UCF
-0.0066488-0.0000004 0.0006626 0.0000002
B.M. AT CENTER=   -0.4837850

            ANALYSIS NUMBER 14
 0.1600000  530000.0  1675.000               0.14090  12.00000              60237840.00
LOAD STAGE  0.1310  THEORETICAL  SUMAN=-0.0102877  EXPERIMENTAL OR TABULATED SUMAN=-0.0082457  PERCENTAGE DIFF=  19.849
CALCULATIONS BY UCF
UNCOUPLING CORRECTION FACTOR=   0.76279
SUMAN BY UCF=-0.0078474  EXPERMENTAL OR TABULATED        SUMAN=-0.0082457  PERCENTAGE DIFF=  -5.076
THEORETICAL CENTRAL DEFLECTION=     0.0650605  EXPERMENTAL OR TABULATED CENTRAL DEFLECTION=     0.0555000
COEA AND COEC AFTER MULT. BY UCF
-0.0078468-0.0000005 0.0007820 0.0000002
B.M. AT CENTER=   -0.5709522

            ANALYSIS NUMBER 15
 0.1600000  530000.0  1675.000               0.14090  12.00000              60237840.00
LOAD STAGE  0.1510  THEORETICAL  SUMAN=-0.0118583  EXPERIMENTAL OR TABULATED SUMAN=-0.0094410  PERCENTAGE DIFF=  20.385
CALCULATIONS BY UCF
UNCOUPLING CORRECTION FACTOR=   0.76279
SUMAN BY UCF=-0.0090454  EXPERMENTAL OR TABULATED        SUMAN=-0.0094410  PERCENTAGE DIFF=  -4.373
THEORETICAL CENTRAL DEFLECTION=     0.0749937  EXPERMENTAL OR TABULATED CENTRAL DEFLECTION=     0.0654999
COEA AND COEC AFTER MULT. BY UCF
-0.0090448-0.0000006 0.0009014 0.0000003
B.M. AT CENTER=   -0.6581229

            ANALYSIS NUMBER 16
 0.1600000  530000.0  1675.000               0.14090  12.00000              60237840.00
LOAD STAGE  0.1715  THEORETICAL  SUMAN=-0.0134682  EXPERIMENTAL OR TABULATED SUMAN=-0.0104266  PERCENTAGE DIFF=  22.584
CALCULATIONS BY UCF
UNCOUPLING CORRECTION FACTOR=   0.76279
SUMAN BY UCF=-0.0102734  EXPERMENTAL OR TABULATED        SUMAN=-0.0104266  PERCENTAGE DIFF=  -1.490
THEORETICAL CENTRAL DEFLECTION=     0.0851746  EXPERMENTAL OR TABULATED CENTRAL DEFLECTION=     0.0815000
COEA AND COEC AFTER MULT. BY UCF
-0.0102728-0.0000007 0.0010238 0.0000003
B.M. AT CENTER=   -0.7474689

            ANALYSIS NUMBER 17
 0.1600000  530000.0  1675.000               0.14090  12.00000              60237840.00
LOAD STAGE  0.1915  THEORETICAL  SUMAN=-0.0150389  EXPERIMENTAL OR TABULATED SUMAN=-0.0118302  PERCENTAGE DIFF=  21.336
CALCULATIONS BY UCF
UNCOUPLING CORRECTION FACTOR=   0.76279
SUMAN BY UCF=-0.0114715  EXPERMENTAL OR TABULATED        SUMAN=-0.0118302  PERCENTAGE DIFF=  -3.127
THEORETICAL CENTRAL DEFLECTION=     0.0951079  EXPERMENTAL OR TABULATED CENTRAL DEFLECTION=     0.0865000
COEA AND COEC AFTER MULT. BY UCF
-0.0114707-0.0000008 0.0011432 0.0000004
B.M. AT CENTER=   -0.8346386

            ANALYSIS NUMBER 18
 0.1600000  530000.0  1675.000               0.14090  12.00000              60237840.00
LOAD STAGE  0.2110  THEORETICAL  SUMAN=-0.0165702  EXPERIMENTAL OR TABULATED SUMAN=-0.0129851  PERCENTAGE DIFF=  21.636
CALCULATIONS BY UCF
UNCOUPLING CORRECTION FACTOR=   0.76279
SUMAN BY UCF=-0.0126396  EXPERMENTAL OR TABULATED        SUMAN=-0.0129851  PERCENTAGE DIFF=  -2.733
THEORETICAL CENTRAL DEFLECTION=     0.1047920  EXPERMENTAL OR TABULATED CENTRAL DEFLECTION=     0.0965000
COEA AND COEC AFTER MULT. BY UCF
-0.0126388-0.0000009 0.0012596 0.0000004
```

```
B.M. AT CENTER=   -0.9196262


          ANALYSIS NUMBER 19
 0.1600000   530000.0  1675.000                0.14090  12.00000             63237840.00
LOAD STAGE  0.2205  THEORETICAL  SUMAN=-0.0173163  EXPERIMENTAL OR TABULATED SUMAN=-0.0133966  PERCENTAGE DIFF=  22.636
CALCULATIONS  BY UCF
UNCOUPLING CORRECTION FACTOR=    0.76279
SUMAN BY UCF=-0.0132087  EXPERMENTAL OR TABULATED        SUMAN=-0.0133966  PERCENTAGE DIFF=  -1.423
THEORETICAL CENTRAL DEFLECTION=      0.1095104  EXPERMENTAL OR TABULATED CENTRAL DEFLECTION=     0.1049999
COEA AND COEC AFTER MULT. BY UCF
-0.0132078-0.0000009 0.0013163 0.0000004
B.M. AT CENTER=   -0.9610348


          ANALYSIS NUMBER 20
 0.1600000   530000.0  1675.000                0.14090  12.00000             63237840.00
LOAD STAGE  0.2290  THEORETICAL  SUMAN=-0.0179838  EXPERIMENTAL OR TABULATED SUMAN=-0.0134567  PERCENTAGE DIFF=  25.173
CALCULATIONS  BY UCF
UNCOUPLING CORRECTION FACTOR=    0.76279
SUMAN BY UCF=-0.0137179  EXPERMENTAL OR TABULATED        SUMAN=-0.0134567  PERCENTAGE DIFF=   1.904
THEORETICAL CENTRAL DEFLECTION=      0.1137318  EXPERMENTAL OR TABULATED CENTRAL DEFLECTION=     0.1199999
COEA AND COEC AFTER MULT. BY UCF
-0.0137170-0.0000009 0.0013671 0.0000004
B.M. AT CENTER=   -0.9980783


          ANALYSIS NUMBER 21
 0.1600000   530000.0  1675.000                0.14090  12.00000             63237840.00
LOAD STAGE  0.2580  THEORETICAL  SUMAN=-0.0202612  EXPERIMENTAL OR TABULATED SUMAN=-0.0151690  PERCENTAGE DIFF=  25.133
CALCULATIONS  BY UCF
UNCOUPLING CORRECTION FACTOR=    0.76279
SUMAN BY UCF=-0.0154551  EXPERMENTAL OR TABULATED        SUMAN=-0.0151690  PERCENTAGE DIFF=   1.851
THEORETICAL CENTRAL DEFLECTION=      0.1281347  EXPERMENTAL OR TABULATED CENTRAL DEFLECTION=     0.1349999
COEA AND COEC AFTER MULT. BY UCF
-0.0154540-0.0000010 0.0015402 0.0000005
B.M. AT CENTER=   -1.1244736


          ANALYSIS NUMBER 22
 0.1600000   530000.0  1675.000                0.14090  12.00000             63237840.00
LOAD STAGE  0.2830  THEORETICAL  SUMAN=-0.0222245  EXPERIMENTAL OR TABULATED SUMAN=-0.0164340  PERCENTAGE DIFF=  26.055
CALCULATIONS  BY UCF
UNCOUPLING CORRECTION FACTOR=    0.76279
SUMAN BY UCF=-0.0169527  EXPERMENTAL OR TABULATED        SUMAN=-0.0164340  PERCENTAGE DIFF=   3.060
THEORETICAL CENTRAL DEFLECTION=      0.1405507  EXPERMENTAL OR TABULATED CENTRAL DEFLECTION=     0.1530000
COEA AND COEC AFTER MULT. BY UCF
-0.0169515-0.0000011 0.0016855 0.0000005
B.M. AT CENTER=   -1.2334347


          ANALYSIS NUMBER 23
 0.1600000   530000.0  1675.000                0.14090  12.00000             63237840.00
LOAD STAGE  0.3130  THEORETICAL  SUMAN=-0.0245805  EXPERIMENTAL OR TABULATED SUMAN=-0.0177685  PERCENTAGE DIFF=  27.713
CALCULATIONS  BY UCF
UNCOUPLING CORRECTION FACTOR=    0.76279
SUMAN BY UCF=-0.0187498  EXPERMENTAL OR TABULATED        SUMAN=-0.0177685  PERCENTAGE DIFF=   5.233
THEORETICAL CENTRAL DEFLECTION=      0.1554505  EXPERMENTAL OR TABULATED CENTRAL DEFLECTION=     0.1789999
COEA AND COEC AFTER MULT. BY UCF
-0.0187485-0.0000013 0.0018686 0.0000006
B.M. AT CENTER=   -1.3641582


          ANALYSIS NUMBER 24
 0.1600000   530000.0  1675.000                0.14090  12.00000             63237840.00
LOAD STAGE  0.3350  THEORETICAL  SUMAN=-0.0263082  EXPERIMENTAL OR TABULATED SUMAN=-0.0185208  PERCENTAGE DIFF=  29.600
CALCULATIONS  BY UCF
UNCOUPLING CORRECTION FACTOR=    0.76279
SUMAN BY UCF=-0.0200676  EXPERMENTAL OR TABULATED        SUMAN=-0.0185208  PERCENTAGE DIFF=   7.708
THEORETICAL CENTRAL DEFLECTION=      0.1663766  EXPERMENTAL OR TABULATED CENTRAL DEFLECTION=     0.2034999
COEA AND COEC AFTER MULT. BY UCF
-0.0200663-0.0000014 0.0019999 0.0000006
```

```
B.M. AT CENTER=   -1.4600716


            ANALYSIS NUMBER 25
 0.1600000  530000.0  1675.000          0.14090  12.00000          60237840.00
LOAD STAGE  0.3590  THEORETICAL  SUMAN=-0.0281930  EXPERIMENTAL OR TABULATED SUMAN=-0.0191427  PERCENTAGE DIFF=  32.101
CALCULATIONS BY UCF
UNCOUPLING CORRECTION FACTOR=    0.76279
SUMAN BY UCF=-0.0215054  EXPERMENTAL OR TABULATED        SUMAN=-0.0191427  PERCENTAGE DIFF=  10.987
THEORETICAL CENTRAL DEFLECTION=    0.1782955  EXPERMENTAL OR TABULATED CENTRAL DEFLECTION=     0.2350000
COEA AND COEC AFTER MULT. BY UCF
-0.0215039-0.0000015 0.0021432 0.0000007
B.M. AT CENTER=   -1.5646725


            ANALYSIS NUMBER 26
 0.1600000  530000.0  1675.000          0.14090  12.00000          60237840.00
LOAD STAGE  0.3940  THEORETICAL  SUMAN=-0.0309415  EXPERIMENTAL OR TABULATED SUMAN=-0.0197344  PERCENTAGE DIFF=  36.220
CALCULATIONS BY UCF
UNCOUPLING CORRECTION FACTOR=    0.76279
SUMAN BY UCF=-0.0236020  EXPERMENTAL OR TABULATED        SUMAN=-0.0197344  PERCENTAGE DIFF=  16.387
THEORETICAL CENTRAL DEFLECTION=    0.1956776  EXPERMENTAL OR TABULATED CENTRAL DEFLECTION=     0.2884999
COEA AND COEC AFTER MULT. BY UCF
-0.0236004-0.0000016 0.0023521 0.0000007
B.M. AT CENTER=   -1.7172165


            ANALYSIS NUMBER 27
 0.1600000  530000.0  1675.000          0.14090  12.00000          60237840.00
LOAD STAGE  0.4080  THEORETICAL  SUMAN=-0.0320410  EXPERIMENTAL OR TABULATED SUMAN=-0.0179878  PERCENTAGE DIFF=  43.860
CALCULATIONS BY UCF
UNCOUPLING CORRECTION FACTOR=    0.76279
SUMAN BY UCF=-0.0244406  EXPERMENTAL OR TABULATED        SUMAN=-0.0179878  PERCENTAGE DIFF=  26.402
THEORETICAL CENTRAL DEFLECTION=    0.2026309  EXPERMENTAL OR TABULATED CENTRAL DEFLECTION=     0.3574999
COEA AND COEC AFTER MULT. BY UCF
-0.0244390-0.0000016 0.0024357 0.0000008
B.M. AT CENTER=   -1.7782345


            ANALYSIS NUMBER 28
 0.1600000  530000.0  1675.000          0.14090  12.00000          60237840.00
LOAD STAGE  0.4140  THEORETICAL  SUMAN=-0.0325122  EXPERIMENTAL OR TABULATED SUMAN=-0.0091380  PERCENTAGE DIFF=  71.894
CALCULATIONS BY UCF
UNCOUPLING CORRECTION FACTOR=    0.76279
SUMAN BY UCF=-0.0248001  EXPERMENTAL OR TABULATED        SUMAN=-0.0091380  PERCENTAGE DIFF=  63.153
THEORETICAL CENTRAL DEFLECTION=    0.2056103  EXPERMENTAL OR TABULATED CENTRAL DEFLECTION=     0.5814999
COEA AND COEC AFTER MULT. BY UCF
-0.0247984-0.0000017 0.0024715 0.0000008
B.M. AT CENTER=   -1.8043833


            ANALYSIS NUMBER 29
 0.1600000  530000.0  1675.000          0.14090  12.00000          60237840.00
LOAD STAGE  0.4270  THEORETICAL  SUMAN=-0.0335331  EXPERIMENTAL OR TABULATED SUMAN=-0.0042899  PERCENTAGE DIFF=  87.207
CALCULATIONS BY UCF
UNCOUPLING CORRECTION FACTOR=    0.76279
SUMAN BY UCF=-0.0255782  EXPERMENTAL OR TABULATED        SUMAN=-0.0042899  PERCENTAGE DIFF=  83.229
THEORETICAL CENTRAL DEFLECTION=    0.2120673  EXPERMENTAL OR TABULATED CENTRAL DEFLECTION=     0.7230000
COEA AND COEC AFTER MULT. BY UCF
-0.0255771-0.0000017 0.0025451 0.0000008
B.M. AT CENTER=   -1.8610468


            ANALYSIS NUMBER 30
 0.1600000  530000.0  1675.000          0.14090  12.00000          60237840.00
LOAD STAGE  0.4500  THEORETICAL  SUMAN=-0.0353393  EXPERIMENTAL OR TABULATED SUMAN= 0.0011897  PERCENTAGE DIFF= 103.366
CALCULATIONS BY UCF
UNCOUPLING CORRECTION FACTOR=    0.76279
SUMAN BY UCF=-0.0269566  EXPERMENTAL OR TABULATED        SUMAN= 0.0011897  PERCENTAGE DIFF= 104.413
THEORETICAL CENTRAL DEFLECTION=    0.2234899  EXPERMENTAL OR TABULATED CENTRAL DEFLECTION=     0.8989999
COEA AND COEC AFTER MULT. BY UCF
-0.0269548-0.0000018 0.0026864 0.0000008
```

```
B.M. AT CENTER=   -1.5612894


          ANALYSIS NUMBER 31
 0.1600000  530000.0  1675.000              0.14090  12.00000            60237840.00
LOAD STAGE  0.4830  THEORETICAL  SUMAN=-0.0379309  EXPERIMENTAL OR TABULATED SUMAN= 0.0066966  PERCENTAGE DIFF= 117.655
CALCULATIONS BY UCF
UNCOUPLING CORRECTION FACTOR=    0.76279
SUMAN BY UCF=-0.0289334  EXPERMENTAL OR TABULATED        SUMAN= 0.0066966  PERCENTAGE DIFF= 123.145
THEORETICAL CENTRAL DEFLECTION=     0.2398791  EXPERMENTAL OR TABULATED CENTRAL DEFLECTION=     1.0949993
COEA ANC COEC AFTER MULT. BY UCF
-0.0289314-0.0000020 0.0028834 0.0000009
B.M. AT CENTER=   -2.1051130


          ANALYSIS NUMBER 32
 0.1600000  530000.0  1675.000              0.14090  12.00000            60237840.00
LOAD STAGE  0.5090  THEORETICAL  SUMAN=-0.0399727  EXPERIMENTAL OR TABULATED SUMAN= 0.0116219  PERCENTAGE DIFF= 129.075
CALCULATIONS BY UCF
UNCOUPLING CORRECTION FACTOR=    0.76279
SUMAN BY UCF=-0.0304909  EXPERMENTAL OR TABULATED        SUMAN= 0.0116219  PERCENTAGE DIFF= 138.116
THEORETICAL CENTRAL DEFLECTION=     0.2527918  EXPERMENTAL OR TABULATED CENTRAL DEFLECTION=     1.2634993
COEA ANC COEC AFTER MULT. BY UCF
-0.0304888-0.0000021 0.0030386 0.0000010
B.M. AT CENTER=   -2.2184343


          ANALYSIS NUMBER 33
 0.1600000  530000.0  1675.000              0.14090  12.00000            60237840.00
LOAD STAGE  0.5490  THEORETICAL  SUMAN=-0.0431140  EXPERIMENTAL OR TABULATED SUMAN= 0.0188147  PERCENTAGE DIFF= 143.639
CALCULATIONS BY UCF
UNCOUPLING CORRECTION FACTOR=    0.76279
SUMAN BY UCF=-0.0328869  EXPERMENTAL OR TABULATED        SUMAN= 0.0188147  PERCENTAGE DIFF= 157.210
THEORETICAL CENTRAL DEFLECTION=     0.2726605  EXPERMENTAL OR TABULATED CENTRAL DEFLECTION=     1.5134983
COEA ANC COEC AFTER MULT. BY UCF
-0.0328847-0.0000022 0.0032774 0.0000010
B.M. AT CENTER=   -2.3927813


          ANALYSIS NUMBER 34
 0.1600000  530000.0  1675.000              0.14090  12.00000            60237840.00
LOAD STAGE  0.5710  THEORETICAL  SUMAN=-0.0448417  EXPERIMENTAL OR TABULATED SUMAN= 0.0228332  PERCENTAGE DIFF= 150.920
CALCULATIONS BY UCF
UNCOUPLING CORRECTION FACTOR=    0.76279
SUMAN BY UCF=-0.0342048  EXPERMENTAL OR TABULATED        SUMAN= 0.0228332  PERCENTAGE DIFF= 166.754
THEORETICAL CENTRAL DEFLECTION=     0.2835867  EXPERMENTAL OR TABULATED CENTRAL DEFLECTION=     1.6524982
COEA ANC COEC AFTER MULT. BY UCF
-0.0342025-0.0000023 0.0034088 0.0000011
B.M. AT CENTER=   -2.4886684


          ANALYSIS NUMBER 35
 0.1600000  574000.0  1810.000              0.14090  12.00000            65393776.00
LOAD STAGE  0.0210  THEORETICAL  SUMAN=-0.0015268  EXPERIMENTAL OR TABULATED SUMAN=-0.0012121  PERCENTAGE DIFF=  20.609
CALCULATIONS BY UCF
UNCOUPLING CORRECTION FACTOR=    0.76279
SUMAN BY UCF=-0.0011646  EXPERMENTAL OR TABULATED        SUMAN=-0.0012121  PERCENTAGE DIFF=  -4.080
THEORETICAL CENTRAL DEFLECTION=     0.0096403  EXPERMENTAL OR TABULATED CENTRAL DEFLECTION=     0.0085000
COEA ANC COEC AFTER MULT. BY UCF
-0.0011645-0.0000001 0.0001161 0.0000000
B.M. AT CENTER=   -0.0914769


          ANALYSIS NUMBER 36
 0.1600000  574000.0  1810.000              0.14090  12.00000            65393776.00
LOAD STAGE  0.0400  THEORETICAL  SUMAN=-0.0029082  EXPERIMENTAL OR TABULATED SUMAN=-0.0023168  PERCENTAGE DIFF=  20.336
CALCULATIONS BY UCF
UNCOUPLING CORRECTION FACTOR=    0.76279
SUMAN BY UCF=-0.0022183  EXPERMENTAL OR TABULATED        SUMAN=-0.0023168  PERCENTAGE DIFF=  -4.437
THEORETICAL CENTRAL DEFLECTION=     0.0183674  EXPERMENTAL OR TABULATED CENTRAL DEFLECTION=     0.0160000
COEA ANC COEC AFTER MULT. BY UCF
-0.0022182-0.0000002 0.0002211 0.0000001
```

```
B.M. AT CENTER=   -0.1742419

          ANALYSIS NUMBER 37
 0.1600000  574000.0  1810.000              0.14090  12.00000           65393776.00
LOAD STAGE  0.1100  THEORETICAL  SUMAN=-0.0079974  EXPERIMENTAL OR TABULATED SUMAN=-0.0059544  PERCENTAGE DIFF=  25.546
CALCULATIONS BY UCF
UNCOUPLING CORRECTION FACTOR=    0.76279
SUMAN BY UCF=-0.0061004  EXPERMENTAL OR TABULATED        SUMAN=-0.0059544  PERCENTAGE DIFF=   2.393
THEORETICAL CENTRAL DEFLECTION=     0.0504967  EXPERMENTAL OR TABULATED CENTRAL DEFLECTION=     0.0540000
COEA AND COEC AFTER MULT. BY UCF
-0.0061000-0.0000004 0.0006079 0.0000002
B.M. AT CENTER=   -0.4791648

          ANALYSIS NUMBER 38
 0.1600000  574000.0  1810.000              0.14090  12.00000           65393776.00
LOAD STAGE  0.1795  THEORETICAL  SUMAN=-0.0130504  EXPERIMENTAL OR TABULATED SUMAN=-0.0096798  PERCENTAGE DIFF=  25.828
CALCULATIONS BY UCF
UNCOUPLING CORRECTION FACTOR=    0.76279
SUMAN BY UCF=-0.0099547  EXPERMENTAL OR TABULATED        SUMAN=-0.0096798  PERCENTAGE DIFF=   2.762
THEORETICAL CENTRAL DEFLECTION=     0.0824013  EXPERMENTAL OR TABULATED CENTRAL DEFLECTION=     0.0890000
COEA AND COEC AFTER MULT. BY UCF
-0.0099541-0.0000007 0.0009920 0.0000003
B.M. AT CENTER=   -0.7819099

          ANALYSIS NUMBER 39
 0.1600000  574000.0  1810.000              0.14090  12.00000           65393776.00
LOAD STAGE  0.2195  THEORETICAL  SUMAN=-0.0159585  EXPERIMENTAL OR TABULATED SUMAN=-0.0111215  PERCENTAGE DIFF=  30.310
CALCULATIONS BY UCF
UNCOUPLING CORRECTION FACTOR=    0.76279
SUMAN BY UCF=-0.0121731  EXPERMENTAL OR TABULATED        SUMAN=-0.0111215  PERCENTAGE DIFF=   8.638
THEORETICAL CENTRAL DEFLECTION=     0.1007639  EXPERMENTAL OR TABULATED CENTRAL DEFLECTION=     0.1260000
COEA AND COEC AFTER MULT. BY UCF
-0.0121722-0.0000008 0.0012131 0.0000004
B.M. AT CENTER=   -0.9561529

          ANALYSIS NUMBER 40
 0.1600000  574000.0  1810.000              0.14090  12.00000           65393776.00
LOAD STAGE  0.2500  THEORETICAL  SUMAN=-0.0181760  EXPERIMENTAL OR TABULATED SUMAN=-0.0116256  PERCENTAGE DIFF=  36.039
CALCULATIONS BY UCF
UNCOUPLING CORRECTION FACTOR=    0.76279
SUMAN BY UCF=-0.0138645  EXPERMENTAL OR TABULATED        SUMAN=-0.0116256  PERCENTAGE DIFF=  16.149
THEORETICAL CENTRAL DEFLECTION=     0.1147654  EXPERMENTAL OR TABULATED CENTRAL DEFLECTION=     0.1684999
COEA AND COEC AFTER MULT. BY UCF
-0.0138636-0.0000009 0.0013817 0.0000004
B.M. AT CENTER=   -1.0890131

          ANALYSIS NUMBER 41
 0.1600000  574000.0  1810.000              0.14090  12.00000           65393776.00
LOAD STAGE  0.3600  THEORETICAL  SUMAN=-0.0261735  EXPERIMENTAL OR TABULATED SUMAN=-0.0134967  PERCENTAGE DIFF=  48.434
CALCULATIONS BY UCF
UNCOUPLING CORRECTION FACTOR=    0.76279
SUMAN BY UCF=-0.0199649  EXPERMENTAL OR TABULATED        SUMAN=-0.0134967  PERCENTAGE DIFF=  32.398
THEORETICAL CENTRAL DEFLECTION=     0.1652616  EXPERMENTAL OR TABULATED CENTRAL DEFLECTION=     0.3204999
COEA AND COEC AFTER MULT. BY UCF
-0.0199636-0.0000014 0.0019896 0.0000006
B.M. AT CENTER=   -1.5681753

          ANALYSIS NUMBER 42
 0.1600000  574000.0  1810.000              0.14090  12.00000           65393776.00
LOAD STAGE  0.4470  THEORETICAL  SUMAN=-0.0324987  EXPERIMENTAL OR TABULATED SUMAN= 0.0071394  PERCENTAGE DIFF= 121.968
CALCULATIONS BY UCF
UNCOUPLING CORRECTION FACTOR=    0.76279
SUMAN BY UCF=-0.0247898  EXPERMENTAL OR TABULATED        SUMAN= 0.0071394  PERCENTAGE DIFF= 128.800
THEORETICAL CENTRAL DEFLECTION=     0.2051991  EXPERMENTAL OR TABULATED CENTRAL DEFLECTION=     0.9714997
COEA AND COEC AFTER MULT. BY UCF
-0.0247891-0.0000017 0.0024704 0.0000008
```

B.M. AT CENTER=   -1.9471493

ANALYSIS NUMBER 43
BUT NO LOAD STAGE OR STRUCTURE TO ANALYSE.GOOD-BYE.

APPENDIX D

Main Computer Program and Printed Results of Torsional Rotations

```
C PROGRAM TO COMPUTE TORSIONAL ROTATIONS
C OF THE BEAM CENTRAL SECTION.
C ALL DETA  IN KIP FT UNITS
      REAL COEA(3),COEC(3)
      NCOUNT=0
      PI=22/7
      A=12.
      D=1675.
      WRITE (6,551)
  551 FORMAT(2X,'LOAD STAGE',2X,'COEA(1)',4X,'COEA(3)',4X,'COEC(1)',
     14X,'COEC(3)',4X,'SMTH-RTN',4X,'EXPT-RTN')
  101 CONTINUE
      READ,Q,COEA(1),COEA(3),COEC(1),COEC(3),FSUMAN,ESUMAN,EROT
      IF (Q.EQ.0.) GO TO 102
      FT=ESUMAN/FSUMAN
      DO 10 I=1,3,2
      COEA(I)=COEA(I)*FT
      COEC(I)=COEC(I)*FT
   10 CONTINUE
      F1=Q*(A**3)/(48 *D)
      SUM1=0.
      SUM2=0.
      DO21 N=1,3,2
      ALPN=N*PI/2
      BETAN=N*PI/A
      F2=COEA(N)*(    BETAN*SINH(ALPN)-BETAN*SIN(ALPN))
      SUM1=SUM1+F2
      F3=COEC(N)*(SINH(ALPN)+ALPN*COSH(ALPN))
      SUM2=SUM2+F3
   21 CONTINUE
      STROT=F1-SUM1-SUM2
      WRITE(6,552) Q,COEA(1),COEA(3),COEC(1),COEC(3),STROT,EROT
  552 FORMAT(2X,F8.4,2X,F10.7,1X,F10.7,1X,
     1F10.7,1X,F10.7,1X,F10.7,2X,F10.7)
      GO TO 101
  102 CONTINUE
      STOP
      END
```

$ENTRY

LOAD STAGE	COEA(1)	COEA(3)	COEC(1)	COEC(3)	SMTH-RTN	EXPT-RTN
0.0300	-0.0019386	-0.0000001	0.0001932	0.0000001	0.0000771	0.0000935
0.0500	-0.0031963	-0.0000002	0.0003186	0.0000001	0.0001575	0.0001213
0.0700	-0.0043916	[illegible]	0.0004377	0.0000001	0.0002555	0.0001876
0.0910	-0.0058756	-0.0000004	0.0005856	0.0000002	0.0002663	0.0002493
0.1110	-0.0070083	-0.0000004	0.0006985	0.0000002	0.0003798	0.0003799
0.1310	-0.0082451	-0.0000005	0.0008217	0.0000002	0.0004655	0.0005037
0.1510	-0.0094404	-0.0000006	0.0009408	0.0000003	0.0005375	0.0004891
0.1715	-0.0104260	-0.0000007	0.0010391	0.0000003	0.0007052	0.0006139
0.1915	-0.0118295	-0.0000008	0.0011789	0.0000004	0.0007189	0.0006410
0.2110	-0.0129843	-0.0000009	0.0012940	0.0000004	0.0008174	0.0006776
0.2205	-0.0133957	-0.0000009	0.0013350	0.0000004	0.0009370	0.0008699
0.2290	-0.0134558	-0.0000009	0.0013411	0.0000004	0.0010747	0.0010160
0.2580	-0.015168C	-0.0000010	0.0015117	0.0000005	0.0011952	0.0011640
0.2830	-0.0164329	-0.0000011	0.0016378	0.0000005	0.0013823	0.0012905
0.3130	-0.0177673	-0.0000012	0.0017708	0.0000006	0.0015370	0.0014430
0.3350	-0.0185196	-0.0000013	0.0018457	0.0000006	0.0019045	0.0017310
0.3940	-0.0197331	-0.0000013	0.0019667	0.0000006	0.0028255	0.0027020
0.4080	-0.0179866	-0.0000012	0.0017926	0.0000006	0.0036105	0.0035700

CORE USAGE   OBJECT CODE=   1632 BYTES,ARRAY AREA=   24 BYTES,TOTAL AREA AVAILABLE=   80000 BYTES

COMPILE TIME=   0.18 SEC,EXECUTION TIME=   0.21 SEC, WATFIV - VERSION 1 LEVEL 2 AUGUST 1970   DATE= 74/352

$=EOF

APPENDIX E

General Computer Program for RB-k Design,
Printed Results for (1) Solved Example
in Reference (23) (2) Deflection Data
(3) Rotation Data

```
C STATISTICAL ANALYSIS,PROGRAM BY M.M.MOHARIR
C COCHRAN'S TEST FOR HOMOGENIETY OF VARIANCES,
C F-STATISTIC FOR RB-K DESIGN
C COMPARISON OF ROW AND COLUMN VARIANCES.
C COMPARISONS BETWEEN BLOCKS
C NONADDITIVITY TEST FOR GENERALISATION OF TREATMENT EFFECTS
C ORTHOGONAL POLYNOMIAL COEFFICIENTS FOR LINEARITY OF DATA
C DECLARATION
      REAL X(20,20),XDT(20),XBARDT(20),XDTROW(20), VAR(20),
     1XDTBAR(20),MSB,MSE,C(20),MSSIA
      REAL VARROW(20),MSBT,MSBB,MSRES,DROW(20,20),DCOL(20,20),D(20,20),
     1T(4,4),MSRESL,MSWG,CONST(4,4)
C TO READ THE DATA
  101 CONTINUE
      READ,NS,K
      IF(NS.EQ.0)GO TO 102
      READ,((X(I,J),J=1,K),I=1,NS)
      READ,(C(J),J=1,K)
C TO FIND COLUMN MEANS
      PRINT,'COLUMN MEANS'
      DO 10 I=1,K
   10 XDT(I)=0.
      DO 20 J=1,K
      DO 30 I=1,NS
      XDT(J)=XDT(J)+X(I,J)
   30 CONTINUE
      XBARDT(J)=XDT(J)/NS
      PRINT,XBARDT(J)
   20 CONTINUE
C TO FIND ROW MEANS
      PRINT,'ROW MEANS'
      DO 40 I=1,NS
   40 XDTROW(I)=0.
      DO 50 I=1,NS
      DO 60 J=1,K
      XDTROW(I)=XDTROW(I)+X(I,J)
   60 CONTINUE
      XDTBAR(I)=XDTROW(I)/K
      PRINT,XDTBAR(I)
   50 CONTINUE
C TO FIND GRAND MEAN XBDD
      SUMX=0.
      DO 70 I=1,NS
      SUMX=SUMX+XDTBAR(I)
   70 CONTINUE
      XBDD=SUMX/NS
      PRINT,'GRAND MEAN=',XBDD
C COCHRAN'S TEST FOR HOMOGENEITY OF VARIANCE
      PRINT,'COLUMN VARIANCES'
      DO 80 J=1,K
      VAR(J)=0.
      DO 90 I=1,NS
      VAR(J)=(X(I,J)-XBARDT(J))**2/(NS-1)+VAR(J)
   90 CONTINUE
      PRINT,VAR(J)
   80 CONTINUE
      IF(VAR(1).GE.VAR(2))VARLRG=VAR(1)
      IF(VAR(2).GE.VAR(1))VARLRG=VAR(2)
      DO 100 J=1,K
      IF(VAR(J).GE.VARLRG)VARLRG=VAR(J)
  100 CONTINUE
      PRINT,'LARGEST COLUMN VARIANCE =', VARLRG
      SUM1=0.
      DO 110 J=1,K
      SUM1=SUM1+VAR(J)
  110 CONTINUE
      CCOCRN=VARLRG/SUM1
      PRINT,'COCHRAN C FOR HOMOGENIETY OF VARIANCE=',CCOCRN
C ANALYSIS OF VARIANCE
      SSTOTL=0.
      SSEROR=0.
      DO 120 I=1,NS
      DO 130 J=1,K
      SSTOTL=SSTOTL+(X(I,J)-XBDD)**2
      SSEROR=SSEROR+(X(I,J)-XBARDT(J))**2
  130 CONTINUE
  120 CONTINUE
      PRINT,'TOTAL VARIABILITY=',SSTOTL
```

```
      PRINT,'SUM OF SQURES OF ERROR=',SSEROR
      SSBETN=SSTOTL-SSEROR
      PRINT,'SUM OF SQURES BETWEEN TREATMENTS=',SSBETN
      MSB=SSBETN/(K-1)
      MSE=SSEROR/(NS*K-K)
      FCAL=MSB/MSE
      PRINT,'MS FOR BETWEEN TREATMENTS=',MSB
C COCHRAN'S TEST FOR HOMOGENIETY OF ROW VARIANCES FOR PAIRED T TEST OF ROW MEANS
      WRITE(6,1)
    1 FORMAT(//,2X,'RANDOMIZED BLOCK DESIGN CONTINUED')
      PRINT,'ROW VARIANCES'
      DO 140 I=1,NS
      VARROW(I)=0.
      DO 150 J=1,K
      VARROW(I)=(X(I,J)-XDTBAR(I))**2/(K-1)+VARROW(I)
  150 CONTINUE
      PRINT,VARROW(I)
  140 CONTINUE
      IF(VARROW(1).GE.VARROW(2))VARRLR=VARROW(1)
      IF(VARROW(2).GE.VARROW(1))VARRLR=VARROW(2)
      DO 160 I=1,NS
      IF(VARROW(I).GE.VARRLR)VARRLR=VARROW(I)
  160 CONTINUE
      PRINT,'LARGEST ROW VARIANCE=',VARRLR
      SUM2=0.
      DO 170 I=1,NS
      SUM2=SUM2+VARROW(I)
  170 CONTINUE
      COCROW=VARRLR/SUM2
      PRINT,'COCHRAN C FOR HOMOGENIETY OF ROW VARIANCES=',COCROW
C TWO DIRECTIONAL ANOVA CONTINUES
      SSBLOK=0.
      DO 180 I=1,NS
      SSBLOK=SSBLOK+K*(XDTBAR(I)-XBDD)**2
  180 CONTINUE
      PRINT,'SUM OF SQUARES BETN BLOCKS=',SSBLOK
      SSRES=SSTOTL-SSBETN-SSBLOK
      MSBT=SSBETN/(K-1)
      MSBB=SSBLOK/(NS-1)
      MSRES=SSRES/((K-1)*(NS-1))
      FTREAT=MSBT/MSRES
      FBLOK=MSBB/MSRES
      PRINT,'FCAL FOR TREATMENT=',FTREAT
      PRINT,'FCAL FOR BLOCKS=',FBLOK
C TO FIND VARIANCE SIGBSQ OF THE TREATMANT MEANS
C TO FIND VARIANCE SIGPSQ OF THE BLOCK MEANS OR SEC TREAT LVL MEANS.
      SIGBSQ=(MSBT-MSRES)/NS
      SIGPSQ=(MSBB-MSRES)/K
      PRINT,'VARIANCE OF TREATMENT MEANS=',SIGBSQ
      PRINT,'VARIANCE OF BLOCK MEANS=',SIGPSQ
C TEST FOR NONADDITIVITY SIGNIFYING NO INTERACTOON BETWEEN
C BLOCK AND TREATMENT EFFECTS
C PRECONDITION FOR THE GENERALISATION OF TREATMENT EFFECTS
C FOR ALL BLOCKS
      DO 190 I=1,NS
      DO 200J=1,K
      DROW(I,J)=0.
      DCOL(I,J)=0.
  200 CONTINUE
  190 CONTINUE
      DO 210 I=1,NS
      DROW(I,1)=XDTBAR(I)-XBDD
  210 CONTINUE
      DO 220 J=1,K
      DCOL(1,J)=XBARDT(J)-XBDD
  220 CONTINUE
      PRINT,'D(I,J) MATRIX'
      DO 230 I=1,NS
      DO 240 J=1,K
      D(I,J)=DROW(I,1)*DCOL(1,J)
  240 CONTINUE
      PRINT,'ROW NUMBER=',I
      PRINT,(D(I,J),J=1,K)
  230 CONTINUE
      SUM3=0.
      SUM4=0.
      SUM5=0.
      DO 440 I=1,NS
      DO 250J=1,K
```

```
      SUM3=SUM3+D(I,J)*X(I,J)
      SUM4=SUM4+(ORDW(I,J))**2
      SUM5=SUM5+(OCOL(I,J))**2
  250 CONTINUE
  440 CONTINUE
      PRINT,'SUM3=',SUM3,'SUM4=',SUM4,'SUM5=',SUM5
      SSNOAD=SUM3**2/(SUM4*SUM5)
      PRINT,'SSNONADD=',SSNOAD
      SSRMDR=SSRES-SSNOAD
      FNOADD=SSNOAD*(K*NS-K-NS)/SSRMDR
      PRINT,'F FOR NONADDITIVITY TEST=',FNOADD
C ORTHOGONAL POLYNOMIAL COEFFICIENTS TO TEST
C LINEARITY OF TREATMENT EFFECTS.
      SUM7=0.
      DO260 J=1,K
      SUM7=SUM7+(C(J)**2)
  260 CONTINUE
      SSBSIA=(XBOD*NS*K)**2/(NS*SUM7)
      MSSIA=SSBSIA
      MSRESL=(SSRES+SSBLOK-SSBSIA)/(NS*K-NS-1)
      FSIA=MSSIA/MSRESL
      PRINT,'F FOR LINEARITY BY ORTHOGONAL POLYNOMIAL COEFF=',FSIA
      WRITE(6,2)
    2 FORMAT(////,2X,'ANALYSIS OF THE NEXT DATA STARTS HERE')
      GO TO 101
  102 CONTINUE
      PRINT,'BUT NO MORE DATA TO ANALYSE,GOOD-BYE.'
      STOP
      END
```

```
         $ENTRY
COLUMN MEANS
   0.2750000E 01
   0.6250000E 01
   0.3500000E 01
   0.9000000E 01
ROW MEANS
   0.5250000E 01
   0.6750000E 01
   0.5750000E 01
   0.5000000E 01
   0.4500000E 01
   0.5250000E 01
   0.5000000E 01
   0.5500000E 01
GRAND MEAN=     0.5375000E 01
COLUMN VARIANCES
   0.2214283E 01
   0.1071427E 01
   0.8571427E 00
   0.1714285E 01
LARGEST COLUMN VARIANCE=     0.2214283E 01
COCHRAN C FOR HOMOGENIETY OF VARIANCE=     0.3780486E 00
TOTAL VARIABILITY=     0.2355000E 03
SUM OF SQURES OF ERROR=     0.4100000E 02
SUM OF SQURES BETWEEN TREATMENTS=     0.1945000E 03
MS FOR BETWEEN TREATMENTS=     0.6483333E 02

 RANDOMIZED BLOCK DESIGN CONTINUED
ROW VARIANCES
   0.4249999E 01
   0.2249999E 01
   0.7583332E 01
   0.5999999E 01
   0.1633333E 02
   0.1291667E 02
   0.8666666E 01
   0.1633333E 02
LARGEST ROW VARIANCE=     0.1633333E 02
COCHRAN C FOR HOMOGENIETY OF ROW VARIANCES=     0.2197310E 00
SUM OF SQUARES BETN BLOCKS=     0.1250000E 02
FCAL FOR TREATMENT=     0.4777193E 02
FCAL FOR BLOCKS=     0.1315789E 01
VARIANCE OF TREATMENT MEANS=     0.7934523E 01
VARIANCE OF BLOCK MEANS=     0.1071429E 00
C(I,J) MATRIX
ROW NUMBER=           1
   0.3281250E 00   -0.1093750E 00    0.2343750E 00   -0.4531250E 00
```

```
ROW NUMBER=                 2
  -0.3609375E 01    0.1203125E 01   -0.2578125E 01    0.4984375E 01
ROW NUMBER=                 3
  -0.9843750E 00    0.3281250E 00   -0.7031250E 00    0.1359375E 01
ROW NUMBER=                 4
   0.9843750E 00   -0.3281250E 00    0.7031250E 00   -0.1359375E 01
ROW NUMBER=                 5
   0.2296875E 01   -0.7656250E 00    0.1640625E 01   -0.3171875E 01
ROW NUMBER=                 6
   0.3281250E 00   -0.1093750E 00    0.2343750E 00   -0.4531250E 00
ROW NUMBER=                 7
   0.9843750E 00   -0.3281250E 00    0.7031250E 00   -0.1359375E 01
ROW NUMBER=                 8
  -0.3281250E 00    0.1093750E 00   -0.2343750E 00    0.4531250E 00
SUM3=   -0.2468750E 02 SUM4=    0.3125000E 01 SUM5=    0.2431250E 02
SSNONADD=     0.8021851E 01
F FOR NONADDITIVITY TEST=     0.7834546E 01
F FOR LINEARITY BY ORTHOGONAL POLYNOMIAL COEFF=   -0.2955316E 02


 ANALYSIS OF THE NEXT DATA STARTS HERE
COLUMN MEANS
   0.1311333E 01
   0.2223666E 01
   0.3453333E 01
   0.4018666E 01
   0.5138333E 01
   0.5908330E 01
   0.7031662E 01
   0.8214330E 01
   0.9099324E 01
   0.9803324E 01
ROW MEANS
   0.5815994E 01
   0.5270196E 01
   0.5774493E 01
GRAND MEAN=    0.5620224E 01
COLUMN VARIANCES
   0.4576540E-01
   0.4865032E-01
   0.2325232E 00
   0.2289653E 00
   0.1827579E 00
   0.9910828E-01
   0.2587586E 00
   0.6316375E-02
   0.2284015E 00
   0.2880332E 00
LARGEST COLUMN VARIANCE=    0.2880332E 00
COCHRAN C FOR HOMOGENIETY OF VARIANCE=     0.1778764E 00
TOTAL VARIABILITY=    0.2312472E 03
SUM OF SQURES OF ERROR=    0.3238575E 01
SUM OF SQURES BETWEEN TREATMENTS=     0.2280086E 03
MS FOR BETWEEN TREATMENTS=     0.2533429E 02

 RANDOMIZED BLOCK DESIGN CONTINUED
ROW VARIANCES
   0.9588575E 01
   0.8526096E 01
   0.7374304E 01
LARGEST ROW VARIANCE=     0.9588575E 01
COCHRAN C FOR HOMOGENIETY OF ROW VARIANCES=     0.3761853E 00
SUM OF SQUARES BETN BLOCKS=     0.1846445E 01
FCAL FOR TREATMENT=     0.3275654E 03
FCAL FOR BLOCKS=    0.1193702E 02
VARIANCE OF TREATMENT MEANS=     0.8418981E 01
VARIANCE OF BLOCK MEANS=     0.9458811E-01
D(I,J) MATRIX
ROW NUMBER=                 1
  -0.8435528E 00   -0.6649450E 00   -0.4242128E 00   -0.3135374E 00   -0.9433985E-01    0.5640258E-01    0.2763175E 00
   0.5078487E 00    0.6811044E 00    0.8189265E 00
ROW NUMBER=                 2
   0.1508232E 01    0.1188890E 01    0.7534726E 00    0.5605901E 00    0.1686752E 00   -0.1008452E 00   -0.4940428E 00
  -0.9080097E 00   -0.1217782E 01   -0.1464202E 01
ROW NUMBER=                 3
  -0.6647292E 00   -0.5239843E 00   -0.3342845E 00   -0.2470710E 00   -0.7434088E-01    0.4444588E-01    0.2177414E 00
```

```
    0.4001907E 00      0.5367181E 00      0.6453235E 00
SUM3=    0.9688282E-01 SUM4=    0.1846445E 00 SUM5=    0.7500269E 02
SSNONADD=    0.4488489E-03
F FOR NONADDITIVITY TEST=    0.8171510E-02
F FOR LINEARITY BY ORTHOGONAL POLYNOMIAL COEFF=   -0.2930508E 02


 ANALYSIS OF THE NEXT DATA STARTS HERE
COLUMN MEANS
    0.8510666E 00
    0.1400000E 01
    0.1947666E 01
    0.2649000E 01
    0.3771334E 01
    0.4735333E 01
    0.5189333E 01
    0.6428995E 01
ROW MEANS
    0.3282022E 01
    0.3279499E 01
    0.3553249E 01
GRAND MEAN=    0.3371590E 01
COLUMN VARIANCES
    0.6735206E-02
    0.3286890E-01
    0.3304645E 00
    0.3267100E-01
    0.1453351E-03
    0.5846442E-01
    0.8072102E-01
    0.2967607E 00
LARGEST COLUMN VARIANCE=    0.3304645E 00
COCHRAN C FOR HOMOGENIETY OF VARIANCE=    0.3939584E 00
TOTAL VARIABILITY=    0.8406183E 02
SUM OF SQURES OF ERROR=    0.1677659E 01
SUM OF SQURES BETWEEN TREATMENTS=    0.8238416E 02
MS FOR BETWEEN TREATMENTS=    0.1176917E 02

 RANDOMIZED BLOCK DESIGN CONTINUED
ROW VARIANCES
    0.3889347E 01
    0.3734605E 01
    0.4328312E 01
LARGEST ROW VARIANCE=    0.4328312E 01
COCHRAN C FOR HOMOGENIETY OF ROW VARIANCES=    0.3621332E 00
SUM OF SQUARES BETN BLOCKS=    0.3960256E 00
FCAL FOR TREATMENT=    0.1285598E 03
FCAL FOR BLOCKS=    0.2162980E 01
VARIANCE OF TREATMENT MEANS=    0.3892539E 01
VARIANCE OF BLOCK MEANS=    0.1330832E-01
D(I,J) MATRIX
ROW NUMBER=              1
    0.2257561E 00    0.1765697E 00    0.1275368E 00    0.6472027E-01   -0.3580395E-01   -0.1221467E 00   -0.1628101E 00
   -0.2738432E 00
ROW NUMBER=              2
    0.2321165E 00    0.1815649E 00    0.1311299E 00    0.6654370E-01   -0.3681267E-01   -0.1255979E 00   -0.1673971E 00
   -0.2815583E 00
ROW NUMBER=              3
   -0.4578775E 00   -0.3581584E 00   -0.2586695E 00   -0.1312653E 00    0.7261735E-01    0.2477372E 00    0.3302107E 00
    0.5554073E 00
SUM3=    0.3083773E 00 SUM4=    0.4950320E-01 SUM5=    0.2745138E 02
SSNONADD=    0.6995344E-01
F FOR NONADDITIVITY TEST=    0.7505153E 00
F FOR LINEARITY BY ORTHOGONAL POLYNOMIAL COEFF=   -0.2296568E 02


 ANALYSIS OF THE NEXT DATA STARTS HERE
BUT NO MORE DATA TO ANALYSE.GOOD-BYE.
CORE USAGE       OBJECT CODE=    7432 BYTES,ARRAY AREA=    7088 BYTES,TOTAL AREA AVAILABLE=    80000  BYTES
COMPILE TIME=      0.69 SEC,EXECUTION TIME=      0.58 SEC,  WATFIV - VERSION 1 LEVEL 2 AUGUST  1970     DATE=  74/352
         $=EOF
```

```
      C SUBPROGRAM BY M.M.MOHARIR FOR CONSTRUCTION OF
      C VARIANCE-COVARIANCE MATRIX AND T-SQUARE TEST
      C
      C
      C DECLARATION
            REAL BS(20,20),B(20,20),BPRM(20,20),C(20,20),SY(20,20)
           1,S(20,20),XDT(20),XBARDT(20),XSQDT(20), MIXSUM(20,20),
           1CS(20,20),TSQR(20,20),CONST(20,20),
           1BSYBRM(20,20),BSY(20,20),CPRM(20,20)
      C
      C
      C TO READ DATA
        101 CONTINUE
            READ,N,K
            KK=K-1
            IF (N.EQ.0) GO TO 102
            PRINT,'ALL MATRICES ARE PRINTED ROW-WISE'
            READ,((BS(I,J),J=1,K),I=1,N)
      C
      C TO CONSTRUCT B,BPRM,C,CPRM MATRICES
            DO 10 J=1,K
         10 XDT(J)=0.
            DO 20 J=1,K
            DO 30 I=1,N
            XDT(J)=XDT(J)+BS(I,J)
         30 CONTINUE
            XBARDT(J)=XDT(J)/N
         20 CONTINUE
            DO 40 J=1,KK
            B(1,J)=XBARDT(J)-XBARDT(K)
         40 CONTINUE
            PRINT,'B MATRIX'
            PRINT,((B(I,J),J=1,KK),I=1,1)
**WARNING**  BECAUSE OF PARAMETER           1,THIS DO-LOOP WILL TERMINATE AFTER THE FIRST TIME THROUGH
            DO 50 I=1,KK
            DO 60 J=1,K
            C(I,J)=0.
         60 CONTINUE
         50 CONTINUE
            DO 70 I=1,KK
            C(I,I)=1.0
         70 CONTINUE
            DO 80 I=1,KK
            C(I,K)=-1.0
         80 CONTINUE
            DO 90 I=1,KK
            DO 100 J=1,K
            CPRM(J,I)=C(I,J)
        100 CONTINUE
         90 CONTINUE
            DO 110 J=1,KK
            BPRM(J,1)=B(1,J)
        110 CONTINUE
      C
      C
      C CONSTRUCT S,THE VARIANCE-COVARIANCE MATRIX
      C
            DO 1002 I=1,K
            DO 1001 J=1,K
            MIXSUM(I,J)=0.0
            DO 1000 II=1,N
            MIXSUM(I,J)=MIXSUM(I,J)+BS(II,I)*BS(II,J)
       1000 CONTINUE
       1001 CONTINUE
       1002 CONTINUE
            DO 1003 I=1,K
            DO 1004 J=1,K
            S(I,J)=(MIXSUM(I,J)-(XDT(I)*XDT(J))/N)/(N-1)
       1004 CONTINUE
       1003 CONTINUE
            PRINT,'S MATRIX'
            PRINT,((S(I,J),J=1,K),I=1,K)
      C
      C
      C MULTIPLICATION AND INVERSION OF MATRICES ,
      C
            LL=KK
            MM=K
```

```
      NN=K
      CALL LAJO(C,S,CS,LL,MM,NN)
      NN=KK
      CALL LAJO (CS,CPRM,SY,LL,MM,NN)
      CALL MUKUND(SY,NN)
      PRINT,'SY-INVERSE MATRIX'
      PRINT,((SY(I,J),J=1,KK),I=1,KK)
      LL=1
      MM=KK
      NN=KK
      CALL LAJO (B,SY,BSY,LL,MM,NN)
      LL=1
      MM=KK
      NN=1
      CALL LAJO (BSY,BPRM,BSYBRM,LL,MM,NN)
      CONST(1,1)=N
      LL=1
      MM=1
      NN=1
      CALL LAJO (BSYBRM,CONST,TSQR,LL,MM,NN)
      PRINT,'TSQR=',TSQR(1,1)
      WRITE(6,2)
    2 FORMAT(////,2X,'ANALYSIS OF NEXT DATA STARTS HERE')
      GO TO 101
  102 CONTINUE
      PRINT,'BUT NO MORE DATA TO ANALYZE,GOOD-BYE.'
      STOP
      END

      SUBROUTINE MUKUND(A,N)
      DIMENSION INDEX(20,20),A(20,20),B(20,20),C(20,20)
      DO 107 I=1,N
      DO 107 J=1,N
  107 B(I,J)=A(I,J)
      DO 108 I=1,N
  108 INDEX(I,1)=0
      II=0
  109 AMAX=-1
      DO 110 I=1,N
      IF (INDEX(I,1)) 110,111,110
  111 DO 112 J=1,N
      IF (INDEX(J,1))112,113,112
  113 TEMP=ABS(A(I,J))
      IF (TEMP-AMAX) 112,112,114
  114 IROW=I
      ICOL=J
      AMAX=TEMP
  112 CONTINUE
  110 CONTINUE
      IF (AMAX)225,115,116
  116 INDEX(ICOL,1)=IROW
      IF (IROW-ICOL) 119,118,119
  119 DO 120 J=1,N
      TEMP=A(IROW,J)
      A(IROW,J)=A(ICOL,J)
  120 A(ICOL,J)=TEMP
      II=II+1
      INDEX(II,2)=ICOL
  118 PIVOT=A(ICOL,ICOL)
      A(ICOL,ICOL)=1.
      PIVOT =1./PIVOT
      DO 121J=1,N
  121 A(ICOL,J)=A(ICOL,J)*PIVOT
      DO 122 I=1,N
      IF(I-ICOL)123,122,123
  123 TEMP=A(I,ICOL)
      A(I,ICOL)=0.
      DO 124 J=1,N
  124 A(I,J)=A(I,J)-A(ICOL,J)*TEMP
  122 CONTINUE
      GO TO 109
  125 ICOL=INDEX(II,2)
      IROW=INDEX(ICOL,1)
      DO 126 I=1,N
      TEMP=A(I,IROW)
      A(I,IROW)=A(I,ICOL)
  126 A(I,ICOL)=TEMP
      II=II-1
  225 IF(II)125,127,125
```

```
  127 CONTINUE
      DO 130 I=1,N
      DO 130 J=1,N
      C(I,J)=0.
      DO 130 K=1,N
  130 C(I,J)=C(I,J)+B(I,K)*A(K,J)
      GO TO 134
  115 CONTINUE
  134 CONTINUE
      RETURN
      END

      SUBROUTINE LAJO(A,B,C,L,M,N)
      DIMENSION A(20,20),B(20,20),C(20,20)
      DO 105 I=1,L
      DO 105 J=1,N
      C(I,J)=0
      DO 110 K=1,M
  110 C(I,J)=C(I,J)+A(I,K)*B(K,J)
  105 CONTINUE
      RETURN
      END
```

```
        $ENTRY
ALL MATRICES ARE PRINTED ROW-WISE
B MATRIX
 -0.6250000E 01  -0.2750000E 01  -0.5500000E 01
S MATRIX
  0.2214285E 01   0.1357142E 01   0.1142857E 01  -0.1142857E 01   0.1357142E 01   0.1071428E 01   0.7142857E 00
 -0.7142857E 00   0.1142857E 01   0.7142857E 00   0.8571428E 00  -0.7142857E 00  -0.1142857E 01  -0.7142857E 00
 -0.7142857E 00   0.1714285E 01
SY-INVERSE MATRIX
  0.2760155E 01  -0.2134145E 01  -0.1195114E 01  -0.2134145E 01   0.3670729E 01  -0.1024388E 01  -0.1195114E 01
 -0.1024388E 01   0.2646331E 01
TSQR=    0.2329347E 03


 ANALYSIS OF NEXT DATA STARTS HERE
ALL MATRICES ARE PRINTED ROW-WISE
B MATRIX
  0.4150105E-01  -0.5042973E 00
S MATRIX
  0.9588650E 01   0.9009223E 01   0.8377278E 01   0.9009223E 01   0.8526123E 01   0.7870632E 01   0.8377278E 01
  0.7670632E 01   0.7374375E 01
SY-INVERSE MATRIX
  0.1077063E 02  -0.9177957E 01  -0.9177957E 01   0.1410086E 02
TSQR=    0.3988786E 02


 ANALYSIS OF NEXT DATA STARTS HERE
BUT NO MORE DATA TO ANALYZE,GOOD-BYE.

CORE USAGE      OBJECT CODE=    6560 BYTES,ARRAY AREA=   25840 BYTES,TOTAL AREA AVAILABLE=   80000  BYTES

COMPILE TIME=     0.68 SEC,EXECUTION TIME=     0.21 SEC,  WATFIV - VERSION 1 LEVEL 2 AUGUST  1970     DATE=  74/352

        $=EOF
```

ABSTRACT

In this report a new method to design reinforced concrete floor slabs which terminate at edge beams is presented. The design procedure uses the Modified Yield Line Theory of Kemp and Wilhelm to account for the influence of torsional stiffness of edge beams on the load carrying capacity of slab and also to provide the economic reinforcement. Serviceability requirement of the structure is satisfied by using the "exact" elastic solution and the experimental and theoretical work of this investigation.

The necessary theoretical derivations of the "exact" elastic solution of square panels, design formulas to proportion the spandrels of both rectangular and square panels, ultimate equilibrium equation of the Modified Yield Line Theory, formulas for factor of safety against flexural cracking and combined effect of torsion and shear interaction on edge beams, etc. are first time successfully worked out and incorporated in this report. Also, two mathematical inequalities are developed which represent necessary conditions for the formation of torsional hinges in edge beams. Reasonableness of these inequalities is checked by the test data and observed behavior of the structure.

Three micro-concrete models of rectangular and square slabs of aspect ratios 1:1, 1:1.5 and 1:2 are fabricated and tested at the Concrete Research Laboratory of West Virginia University. The appropriate part of the test data is correlated with the previous

prototype test results and also with the elastic theory developed in this report, thus establishing the reliableness of these model tests. Statistical methods are used to analyze the test data.

Thus, the observed behavior, well established elastic solution, existing test data, statistical methods, sound concepts of the Modified Yield Line Theory, etc. contribute to the development of the simple and direct procedure to design reinforced concrete rectangular and square slabs which terminate at edge beams.

VITA

Mukund Moharir, son of Mr. and Mrs. M. A. Moharir, was born in Khamgaon (India) on January 16, 1941. He completed high school in April, 1957 (ranked within top two percent in the school) and his undergraduate education (Bachelor of Civil Engineering with Honors) in April, 1964 (ranked within top four percent in the University). He was a recipient of "Sinior Fellowship" of the government of India from October, 1964 to October, 1967, during which he obtained his Master's degree in Hydraulic Structures (with first division). Later he worked as a lecturer in the Government Engineering College Aurangabad (India) from December, 1967 to December, 1970.

In January, 1971 the author enrolled at West Virginia University in the Department of Civil Engineering and completed the work for Master of Science degree with a major in structural engineering in May, 1972. Since then he is pursuing the degree of Doctor of Philosophy in the same department.

The author married Miss V. W. Tamaskar in 1968, and they have a five year old son, Vikrant Moharir.

APPROVAL OF EXAMINING COMMITTEE

December 9, 1975
Date

Shirley Dowdy
Dr. Shirley Dowdy

Sunder Advani
Dr. Sunder Advani

Roger K. Seals
Dr. Roger K. Seals

E. L. Kemp
Dr. Emory L. Kemp, Co-Chairman

W. J. Wilhelm
Dr. William J. Wilhelm, Co-Chairman